



Universidade de Brasília
Instituto de Ciências Biológicas
Programa de Pós-Graduação em Biologia Microbiana

Genes de proteínas-chave para a montagem e a função da estrutura de esporos bacterianos

Danilo de Andrade Cavalcante

Tese apresentada ao Programa de Pós-Graduação em Biologia Microbiana da Universidade de Brasília como requisito parcial à obtenção do título de Doutor em Biologia Microbiana.

Orientadora: Prof^a. Dr^a. Marlene Teixeira De-Souza

Brasília, 2018

Agradecimentos

À minha esposa Thais Torres, por todo incentivo, paciência, dedicação e principalmente, por estar sempre presente. Obrigado por me ajudar a sempre seguir em frente e vencer cada obstáculo. Obrigado por não aceitar de mim nada menos que a excelência.

À minha mãe, Abigail e ao meu pai, Djalma, por todo o amparo, paciência e ensinamentos inestimáveis. Obrigado por todo o suporte, mesmo à distância. Tudo que sou e conquistei é devido a vocês.

Aos meus colegas de laboratório, Juliana, Paulo e Maria Inês por todas as horas de conversa, inúmeras contribuições com o trabalho, companheirismo e amizade. Dedico a vocês cada sorriso que dei em nosso laboratório.

À minha família americana, Monica and Joe Nordstrom. O coração de vocês é enorme. Acolheram um estranho desajustado e, com carinho e consideração imensuráveis, lhe deram um lar que deixou saudades eternas. Com vocês eu vivi 10 anos em 1. I still take your lessons with me; every day.

To Prof. Adam Driks, without whom this work would not be possible. You have set an example of excellence as a researcher, a mentor, a instructor, and role model. If I am in any way a better speaker, writer and scientist, or simply if I know the theories of everything, I have to dedicate it to you.

I'd like to thank the Post-docs, Dr. Dörthe Lehmann and Dr. Tyler Boone; the research technician, Mark Khemmani; my fellow graduate student, Ms. Justyna Kordzikowska; and the collaborators Dra. Gina Kuffel, Prof. José Castillo and Prof. Catherine Putonti; for all their guidance through this work. Your discussion, ideas, and feedback have been absolutely invaluable. I am very grateful to all of you.

Agradeço também ao Prof. Marcelo Brigido e à Dra. Tainá Raiol por todo auxílio e ensinamentos em bioinformática. Agradeço à Prof.^a Sônia Nair Bão por disponibilizar as instalações para elaboração de microscopia eletrônica de transmissão.

Agradeço, especialmente, à minha orientadora, Prof.^a Marlene Teixeira De-Souza, pelas “caixas” para carregar, pelas incontáveis horas de dedicação, palavras de incentivo, ideias para este trabalho como um todo. Obrigado por acreditar em mim todos estes anos, pela paciência, pelos conselhos sempre proveitosos e, sobretudo, pela amizade.

Sumário

Lista de abreviaturas	i
Lista de figuras	ii
Lista de tabelas	iii
Resumo	iv
Abstract	v
Introdução	1
I - Introdução	1
II – Revisão bibliográfica	1
1 - Filo Firmicutes	1
2 - Bactérias aeróbias formadoras de endósporos	3
3 – Endoesporulação e ultraestrutura de esporos bacterianos	4
4 – Morfogênese da capa do esporo	10
5 – Coleção de Bactérias aeróbias formadoras de esporos	14
III. Justificativa	16
IV. Objetivos	18
V. Referências bibliográficas	19-23
II. Capítulo 1. Ultrastructural analysis of spores from diverse Bacillales species isolated from Brazilian soil	23
I - Introdução	23
1. Introduction	26
2. Results and Discussion	28
3. Experimental procedures	35
4. Acknowledgements	35
4.1 Conflicts of interest	35
5. References	35-40
III. Capítulo 2. Inactivation of SpoVID protein gene in Lysinibacillus spp.	53

I - Introdução	53
II. Methods	55
III. Results and Discussion	64
III.1 – Construction of the mutant candidate <i>Lysinibacillus sphaericus</i> SDF0037 Ω pRP1028LysVID	75
V.3 –The ultrastructure of spores produced by <i>L. sphaericus</i> SDF0037, <i>L. fusiformis</i> CCGB 743, and mutant candidates <i>L. sphaericus</i> SDF0037 Δ spoVID and <i>L. fusiformis</i> CCGB 743 Δ spoVID	82
IV .Referências bibliográficas	88-91
IV. Capítulo 3. Distribution of spore outer layer proteins on the order Bacillales	94
I - Introdução	93
I.1 – <i>B. subtilis</i> outer layer protein genes	93
II. Methods	95
III. Results and Discussion	96
III.1 Frequently found proteins	97
III.2 Inconsistently found proteins	98
III.3 Exosporium and crust proteins	98
III.4 Relevant absent proteins	99
III.5 Core set of proteins and further experiments	99
IV .Referências bibliográficas	102-103
V . Supplementary information	104

Lista de abreviaturas

AA – Amino ácidos

Bafes – Bactérias aeróbias formadoras de endósporo

B. – *Bacillus*

Br. – *Brevibacillus*

DF – Distrito Federal

L. - *Lysinibacillus*

LaBafes – Laboratório de Bactérias aeróbias formadoras de endósporo

MCF – Microscopia de contraste de fase

MET – Microscopia eletrônica de transmissão

%G+C – Percentual de Guanina e Citosina no DNA

DPA-Ca²⁺ – Ácido piridina-2,6-dicarboxílico e cátions divalentes associados

SASPs – Pequenas proteínas ácido solúveis

P. - *Paenibacillus*

PC – Parede Celular

PG – Peptídeo Glicano

SDF – Solo do Distrito Federal

UV – Ultravioleta

mL – Mililitro

kDa – Kilodalton

UFC – Unidade formadora de colônia

MALDI-TOF – Ionização e dessorção a laser assistidos por matriz-tempo de voo

Lista de figuras

Figura 1. Ciclo celular de bactérias formadoras de endósporos.	7
Figura 2. Ultraestrutura do esporo bacteriano.	8
Figura 3. Arquitetura tipicamente observada em esporos bacterianos	9
Figura 4. Morfogênese da capa do esporo bacteriano.	11
Figura 5. Proteínas morfogenéticas de <i>B. subtilis</i> .	12
Figura 6. Fenótipo resultante da inativação do gene spoVID em <i>B. anthracis</i> .	13
Figure 1. Maximum likelihood phylogenetic tree based on 16S rRNA gene sequences, showing relationships between the 22 strains analysed in this study.	44
Figure 2. Thin-section TEM analysis of spores from SDF strains closely related to <i>B. subtilis</i> .	44
Figure 3. Thin-section TEM analysis of <i>B. clausii</i> SDF strains spores.	45
Figure 4. Thin-section TEM analysis of <i>B. amyloliquefaciens</i> SDF strains spores.	45
Figure 5. Thin-section TEM analysis of <i>Brevibacillus agri</i> SDF0020 spores	46
Figure 6. Thin-section TEM analysis of <i>Brevibacillus agri</i> SDF0020 spores harvested at various times during sporulation.	46
Figure 7. Thin-section TEM analysis of <i>P. alvei</i> SDF strains spores.	47
Figure 8. Thin-section TEM analysis of <i>Lysinibacillus</i> SDF strain spores.	48
Figure 9. Thin-section TEM analysis of <i>Lysinibacillus sphaericus</i> SDF0037	48
Figure 10. Thin-section TEM analysis of <i>B. megaterium</i> and <i>B.</i>	49
Figure 1. A model for spore encasement mediated by SpoVID.	54
Figure 2. pRP1028 map.	57
Figure 3. Thin-section TEM analysis of <i>Lysinibacillus sphaericus</i> SDF0037	65
Figure 4. Representation of the strategy used to disruption of the functional structure of morphogenetic protein genes	66
Figure 5. Analysis of transformation of strain SDF0037.	69
Figure 6. Conservation of morphogenetic protein genes intra-genus.	71
Figure 7. Representative model of the target fragment to be amplified by PCR.	72
Figure 8. spoVID gene from <i>Lysinibacillus sphaericus</i> SDF0037.	73
Figure 9. Analyzis of restricted plasmid pRP1028 Ω LysVID.	74
Figure 10. Homologous recombination event in SDF0037 Ω pRP1028LysVID	76

Figure 11. Analyzis of recombinant strain of <i>L. sphaericus</i> SDF0037 Ω pRP1028LysVID	77
Figure 12. Phenotypes and PCR results of the recombinant strain <i>L. sphaericus</i> SDF0037 Ω pRP1028LysVID	79
Figure 13. Phenotypes and PCR results of the recombinant strain <i>L. fusiformis</i> CCGB 743 Ω pRP1028LysVID.	81
Figure 14. Resultant phenotype from the inactivation of <i>spoVID</i> in <i>B. anthracis</i> .	82
Figure 15. Ultrastructure of the spore produced by <i>L. sphaericus</i> SDF0037 and <i>L. sphaericus</i> SDF0037 Δ <i>spoVID</i>	84
Figure 16. Ultrastructure of the spore produced by <i>L. fusiformis</i> CCGB 743 and <i>L. fusiformis</i> CCGB 743 Ω pRP1028LysVID	85
Figure 1. Core set of outer spore layer proteins across the order Bacillales.	100

Lista de tabelas

Tabela I. Proteínas morfogenéticas de esporo bacterianos	13
Table I. SDF strains selected for this work	41
Table I. SDF strains selected to this study	56
Table II. Plasmids used in this study	58
Table III. Primers used for the amplification of morphogenetic proteins and plasmids	59
Table IV. Resistance to antibiotics in SDF strains used in this study	66
Table V. Number of genomes present on NCBI database	70
Table S1. Assembled Bacillales genomes found on NCBI database and accession numbers.	104
Table S2. Alicyclobacillaceae , Paenibacillaceae , Sporolactobacillaceae , and Thermoactinomycetaceae genomes matches with outer layer AA database	109
Table S3. Bacillus genomes matches with outer layer AA database	110
Table S4. Non sporeformers, genomes matches with outer layer AA database	111

Resumo

Muitas espécies da ordem *Bacillales* formam um tipo celular especializado denominado esporo, que é resistente a diversos tipos de estresses ambientais. Estudos utilizando Microscopia Eletrônica de Transmissão (TEM) revelaram que o esporo é composto por uma série de conchas concêntricas, que englobam o compartimento que abriga o DNA. A parte mais externa destas conchas varia significativamente em morfologia entre espécies, o que provavelmente reflete adaptações aos altamente diversos nichos em que esporos são encontrados. Para melhor caracterizar variações na ultraestrutura de esporos entre as diversas espécies, nos empregamos experimentos de TEM, manipulação genética e detecção de genes e proteínas *in silico* para analisar a diversidade de esporos do banco de dados NCBI e da Coleção de Bactérias aeróbias formadoras de endósporos (CBafes), que engloba, dentre outros, espécies dos gêneros *Bacillus*, *Lysinibacillus*, *Paenibacillus*, e *Brevibacillus*, isoladas do solo do Distrito Federal. Neste estudo, nós descobrimos que as estruturas destes esporos variam consideravelmente, como esperado. Observamos, entretanto, que embora estes isolados sejam novos representantes destas espécies, existem muitas similaridades estruturais entre estes e espécies bem descritas na literatura. Como, na maioria dos casos, as espécies analisadas pertencem a ramos da árvore filogenética muito negligenciados e pouco caracterizados, nossos dados fornecem evidências importantes acerca de quais características estruturais tendem a ser constantes dentro de um *táxon* e quais tendem a variar.

Abstract

Many species in the order *Bacillales* form a specialized cell type called a spore that is resistant to a range of environmental stresses. Transmission electron microscopy (TEM) reveals that the spore is comprised of a series of concentric shells, surrounding an interior compartment harbouring the spore DNA. The outermost of these shells varies considerably in morphology among species, likely reflecting adaptations to the highly diverse niches in which spores are found. To better characterize the variation in spore ultrastructure among diverse species, we used TEM, genetic manipulation and *in silico* gene and protein detections to analyse spores from a collection of spore-forming bacteria spanning, among others, the genera *Bacillus*, *Lysinibacillus*, *Paenibacillus*, and *Brevibacillus*, isolated from soil from central Brazil, Distrito federal (SDFstrains). In this study, we found that the structures of these spores varied widely, as expected. Interestingly, even though these isolates are novel strains of each species, they were structurally very similar to the known examples of each species in the literature. Because in most cases, the species we analysed are poorly characterized, our data provide important evidence regarding which structural features are likely to be constant within a taxon and which are likely to vary

Introdução

I. Introdução

Esta tese foi dividida em três capítulos visando facilitar a compreensão do leitor. Inicialmente, uma revisão bibliográfica acerca da história da taxonomia do filo *Firmicutes* bem como do processo de formação do endósporo bacteriano fornecerão embasamento argumentativo para a justificativa deste trabalho bem como apresentará a Coleção de Bactérias aeróbias formadoras de endósporo (CBafes), repertório de onde buscamos as células utilizadas para este trabalho. Em seguida, o primeiro capítulo, apresentado em formato de artigo, expõe um atlas de imagens e tratará sobre análises de componentes ultra estruturais de diversos endósporos da CBafes por microscopia eletrônica de transmissão (MET). É importante ressaltar que, em maioria, as células utilizadas neste trabalho pertencem a espécies com pouca ou nenhuma descrição na literatura, em especial acerca de análises fenotípicas. O segundo capítulo trata, ainda, de análises ultra estruturais de endósporos, desta vez pela construção de linhagens mutantes de *Lysinibacillus spp.* com rompimento da sequência funcional de um gene que codifica uma proteína estrutural do esporo e a verificação de fenótipo resultante. Por fim, o terceiro capítulo trata de uma análise computacional da distribuição e evolução dos principais genes e proteínas relacionados com a formação da ultraestrutura de esporos bacterianos em diversas espécies com genoma disponível no banco de dados NCBI, bem como do sequenciamento de genomas e análise dos mesmos genes em 14 linhagens SDF selecionadas do acervo da CBafes. Os capítulos II e III servem como base para os artigos que estão em fase de escrita e construção respectivamente.

Parte das análises descritas foram realizadas no Department of Immunology and Microbiology da University of Loyola (Chicago, EUA) em colaboração com o professor Adam Driks (www.stitch.luc.edu/lumen/deptwebs/microbio/adriks.php), bem como no Department of Bioinformatics of the University of Loyola (Chicago, EUA) em colaboração com a professora Catherine Putonti (<https://www.luc.edu/biology/putonti.shtml>)

II. Revisão Bibliográfica

1 - Filo *Firmicutes*

O filo *Firmicutes* foi originalmente proposto para incorporar todas as bactérias Gram positivas (Gibbons e Murray, 1978), enquanto o filo *Proteobacteria* abrigaria as Gram negativas (Stackebrandt *et al.*, 1988). Posteriormente, o conteúdo de Guanina (G) e Citosina (C) ou Taxa de G+C, (%G+C), do DNA foi utilizado como ferramenta taxonômica para dividir o filo em três classes: i) *Clostridia* e ii) *Bacilli*, que se coram como Gram positivas e apresentam baixo %G+C (geralmente <50%) e iii) *Mollicutes*, que se coram como Gram positivas ou Gram negativas e apresentam alto %G+C (de Vos *et al.*, 2009; Schleifer, 2009).

Atualmente, a qualificação de *Firmicutes*, bem como a atribuição de novos isolados aos vários *taxa* dentro do filo, baseia-se, principalmente, em padrões de similaridade entre sequências de genes de rRNA 16S, na espessura da parede celular (PC; número de camadas de peptídeoglicana) e no baixo percentual de G+C, entre outras características adicionais (Logan *et al.*, 2009; Galperin, 2013). A classe *Mollicutes*, diversas vezes fenotípica e filogeneticamente diferenciada do paradigma de um *Firmicutes*, foi, portanto, realocada para o filo *Tenericutes* (de Vos *et al.*, 2009; Schleifer, 2009).

Até o momento, o filo *Firmicutes* consiste em, pelo menos, 26 famílias e 223 gêneros, distribuídos em cinco classes (Garrity, 2003; Fritze, 2004; de Vos *et al.*, 2009; Logan *et al.*, 2009; Galperin, 2013). Permanecem no filo *Firmicutes*, além das duas classes *Clostridia* e *Bacilli*, apenas alguns membros filogeneticamente relacionados aos *Mollicutes*, os *Erysipelotrichia* que compõem a terceira classe do filo. Por fim, as quarta e quinta classes restantes, respectivamente, *Negativicutes*, com membros filogeneticamente relacionados à classe *Clostridia* que, entretanto, se coram como Gram negativas e *Thermolithobacteria* (Sokolova, 2007).

Trata-se de um filo fenotipicamente diverso (Garrity, 2003; Fritze, 2004; de Vos *et al.*, 2009; Logan *et al.*, 2009; Galperin, 2013), que consiste em bactérias com PC rígida, podendo, também, apresentar ácido teicóico (de Vos *et al.*, 2009; Schleifer, 2009). Os representantes desse filo apresentam células nas formas esféricas, bastões, curvadas e helicoidais ou filamentosas, e podem ou não apresentar flagelo. Algumas linhagens são aeróbias, facultativas ou anaeróbias estritas e parte é termófila e/ou halófila. O crescimento ótimo *in vitro* da maioria das espécies, se dá em pH neutro, mas também já foram descritas espécies acidófilas ou alcalífilas.

A habilidade de formar endósporos tem sido uma característica definitiva para o filo *Firmicutes* desde as primeiras descrições de Ferdinand Cohn e Robert Koch em 1876 (Fritze, 2004; Logan e de Vos, 2009). Esta característica marcante, apesar de observada na maioria das linhagens, tanto aeróbias quanto anaeróbias, não constitui uma característica universal do filo, sendo que um mesmo gênero pode incluir espécies formadoras (esporulantes) e não formadoras (asporogênicas) de endósporos. Sem exceção, as linhagens pertencentes à classe *Thermolithobacteria* são asporogênicas (Sokolova, 2007). Contudo, todos os membros, esporulantes e asporogênicos, compartilham um conjunto de genes envolvidos na formação de um esporo (endoesporulação). Este alto índice de conservação sugere que um programa de diferenciação celular robusto e sofisticado provavelmente foi herdado de um último ancestral comum a todos os membros de *Firmicutes* (Galperin, 2013; Hutchison *et al.* 2014). É possível que a habilidade de formar esporos tenha sido perdida por algumas linhagens ao longo da evolução, sugerindo que a sobrevivência ambiental por produção de um esporo viável tem um custo elevado.

2 - Bactérias aeróbias formadoras de endósporos

Dentro do filo *Firmicutes*, as bactérias aeróbias formadoras de endósporos (deste ponto, referidas como Bafes) estão alocadas, principalmente, na classe *Bacilli*. Dentro dessa classe, a ordem *Bacillales* é constituída por nove famílias, das quais, sete incluem gêneros de Bafes: *Bacillaceae*, *Alycibacillaceae*, *Paenibacillaceae*, *Pasteuriaceae*, *Planococcaceae*, *Sporolactobacillaceae* e *Thermoactinomycetaceae* (de Vos *et al.*, 2009; Niall e Halket, 2011). O termo Bafes é utilizado para designar espécies aeróbias que possuem a capacidade de, após evento de diferenciação celular, produzir endósporos (quando internos à célula) ou esporos (quando livres no meio), células metabolicamente dormentes e extremamente resistentes.

O esporo bacteriano representa uma estratégia de conservação de informação genética altamente eficiente (Cano *et al.*, 1995; Vreeland *et al.*, 2000; Driks, 2002; La Duc *et al.*, 2004) e é o tipo celular mais resistente conhecido. Produzidos como último recurso em resposta a estresses ambientais e de agentes físicos e químicos, este tipo celular permite manter o genoma estável, até que as condições se tornem favoráveis. O esporo então retorna rapidamente ao ciclo celular por meio de um fenômeno denominado germinação (Setlow, 2003; Niall e Halket, 2011). Adicionalmente, apesar de diversos casos relatados, pouco se sabe sobre as vias metabólicas de esporulação que evoluíram para sistemas reprodutivos, recém-descobertos, e que resultaram na capacidade de formar uma ou mais células

descendentes, que permanecem no interior do citoplasma de diversas linhagens de *Firmicutes*, como em espécies de *Epulopiscium* e gêneros correlatos (Hutchison *et al.*, 2014).

Esporos podem ser encontrados em amostras isoladas de, praticamente, todas as partes da superfície e sub superfície terrestres (Priest, 1993; Nicholson *et al.*, 2000), ou ainda, associados a animais e plantas. Dessa forma, essas células são frequentemente isoladas de diversos ambientes, tais como, água doce e salgada, solo e ar (Pignatelli *et al.*, 2009). A diversidade fenotípica e metabólica permite que sejam, inclusive, isolados de ambientes peculiares, tais como aqueles que apresentam índices de salinidade extremas, condições ácidas ou alcalinas elevadas, entre outros (Holt, 1986; Setlow, 2006; Logan e de Vos, 2009). Esporos são ainda capazes de resistir a extremos de temperatura, radiações ionizantes e não ionizantes, agentes químicos e tempo (Driks, 1999; Driks, 2002; La Duc *et al.*, 2004). Essas propriedades são conferidas aos esporos graças às características de composição química e ultraestrutura.

O tamanho diminuto da maioria dos esporos (<1 µm), a ampla distribuição no ambiente, resistência extrema, quando comparado com células em estado vegetativo, além da habilidade em permanecerem dormentes e viáveis por milhares de anos, fazem com que essas células sejam singularmente bem preparadas para sobrevivência, sendo, ainda, patógenos eficientes (Davis, 1990; Cano *et al.*, 1995; Russel, 1990; Driks, 1999; Vreeland *et al.*, 2000; Driks, 2002; La Duc *et al.*, 2004). Relatos de esporos recuperados de amostras datadas de alguns poucos séculos ou milênios são frequentes. Em 1995, Cano *et al.*, relataram esporos viáveis de *Bacillus spp.*, isolados do intestino de uma abelha fossilizada em âmbar, datados de 25-40 milhões de anos. Em 2000 foi anunciada a descoberta de esporos viáveis de *L. sphaericus*, recuperados de cristais de sal da bacia sedimentar Permian Basin (Texas e Novo México, USA) e datados de 250 milhões de anos (Vreeland *et al.*, 2000; Ahmed *et al.*, 2007).

Vários fatores ambientais induzem a formação de esporos: temperatura, pH, aeração (Driks, 1999; Miller e Bassler, 2001; Hoon *et al.*, 2010; McKenney *et al.*, 2013). Entretanto, dois fatores ambientais são considerados determinantes: privação nutricional e alta densidade populacional.

Os esporos bacterianos são formados durante a fase estacionária (Driks, 1999; Miller e Bassler, 2001; McKenney *et al.*, 2013). Com o crescimento populacional e conseqüente redução na disponibilidade de nutrientes, há uma elevação dos níveis de moléculas secretadas, que atuam como autoindutores de *quorum sensing*. Quando as moléculas sinalizadoras atingem níveis intracelulares elevados induzem uma extensa cascata de fosforilação que resulta no

início do processo de esporulação (Hoon *et al.*, 2010; Narula *et al.*, 2015).

3 – Endoesporulação e ultraestrutura de esporos bacterianos

Ferdinand Cohn foi o primeiro a descrever o processo de endoesporulação (deste ponto referido como esporulação) bacteriana e iniciou a mudança da nomenclatura de algumas espécies, como é o caso do *Vibrio subtilis*, que passou a ser designado *Bacillus subtilis*, em 1872 (*apud* Verbaendert e de Vos, 2011), e se tornou, desde então, o paradigma da esporulação. A partir daí outras espécies esporulantes, tais como o *B. anthracis*, e asporogênicas foram alocadas no gênero *Bacillus* (Fritze, 2004; Logan *et al.*, 2009; Galperin, 2013). Taxonomicamente, com o passar do tempo, a capacidade de formar esporos bem como a arquitetura dos mesmos vieram a se tornar características muito importantes em nível de gênero dentro do filo *Firmicutes* (Logan e de Vos, 2009; Niall e Halket, 2011).

Em 1876, Koch observou que esporos de *B. anthracis* sobrevivem à ebulição, promovendo, assim, inúmeros estudos a cerca de como este tipo celular é estruturado para resistir aos diversos tipos de estresses (*apud* Verbaendert e de Vos, 2011). Graças a esse interesse e ao advento da microscopia eletrônica de transmissão (MET) observou-se que esporos são entidades estruturalmente complexas (Knaysi e Hillier, 1949), partilham uma arquitetura comum, consistindo em uma série de camadas concêntricas, que funcionam como barreiras protetoras e auxiliam na compressão do material genético em um estado dessecado, cristalino e estável (Moberly *et al.*, 1966; Holt e Leadbetter, 1969).

Também é notável como essas células são capazes de construir estruturas macromoleculares complexas com localização sub-celular exata, no tempo apropriado de desenvolvimento e com alta precisão na montagem (Driks, 1999; Waller *et al.* 2004; Driks, 2007; McKenney *et al.*, 2010). Sabemos que a disponibilidade correta de produtos proteicos, no tempo e em quantidades apropriadas, é garantida por mecanismos de regulação da expressão gênica altamente elaborados (King, 1980; Driks, 1999; Hoon *et al.*, 2010; McKenney *et al.*, 2010). Entretanto, a regulação da expressão gênica, por si só, não explica a forma que a estrutura do esporo é de fato construída. A habilidade em guiar componentes para formar uma estrutura complexa e com localização precisa requer que a informação estrutural esteja nas próprias proteínas do complexo macromolecular que se associam a ultraestrutura em construção.

O estudo da morfogênese e ultraestrutura do esporo são ferramentas fundamentais para entender como as espécies formadoras de endósporos constroem componentes sub

celulares, direcionam e alteram a organização dos mesmos em resposta aos eventos do ciclo celular e demais estímulos ambientais no tempo e compartimento celular exatos (Driks, 2007).

É importante ressaltar que, enquanto *B. subtilis* constitui um modelo consagrado para estudar a morfologia, bioquímica e os determinantes genéticos da esporulação, aspectos fundamentais deste evento permanecem desconhecidos para praticamente todos os outros gêneros (Fritze, 2004; de Vos *et al.*, 2009; Galperin, 2013; Hutchison *et al.*, 2014).

Quando, por estímulo ambiental, há a ativação de sensores histidina quinase (que incluem as proteínas KinA, KinB e KinC) que transportam fosfato por uma extensa cascata de fosforilação, estes resultam na ativação do regulador mestre da esporulação, Spo0A. Após a fosforilação de Spo0A (Spo0A-P), o padrão de expressão gênica da célula vegetativa é substituído pelo programa de regulação gênica especializado da esporulação, que garante uma rápida série de mudanças bioquímicas e morfológicas (McKenney *et al.*, 2013; Narula *et al.*, 2015). Este programa é composto por diversos fatores transcricionais, sendo mediado, principalmente, por fatores sigma (σ) associados ao núcleo da RNA polimerase (Losick e Stragier, 1992; Hoon *et al.*, 2010; McKenney *et al.*, 2013).

Os esporos bacterianos são tipos celulares completamente diferentes das células vegetativas: quando observados em microscopia de contraste de fase (MCF) são bem delineados e brilhosos (Giorno *et al.*, 2007). A morfologia de um esporo vista por microscopia óptica é, tipicamente, entre esférica, elipsoidal ou oval, raramente apresenta-se em forma cilíndrica ou em formato semelhante ao rim. A localização do esporo dentro do esporângio (célula em diferenciação) também é característica notável, variando entre posições central, subterminal e terminal (Logan e de Vos, 2009). Ainda que o formato do esporo possa variar dentre diversos gêneros, a morfologia do esporângio é característica de cada espécie e, portanto, de grande validade para classificação (Waller *et al.* 2004). O esporângio de algumas espécies, sendo *B. thuringiensis* e *L. sphaericus* (Priest *et al.* 2002) as mais notáveis neste caso, também é marcado pela presença de inclusões cristalinas de natureza proteica, conhecidas como δ -endotoxinas ou toxinas Cry e Cyt, frequentemente relacionadas à toxicidade em insetos e outros invertebrados (Aronson 2002; Brillard e Lereclus, 2004; Ohba *et al.*, 2009; Logan e de Vos, 2009; Reymond *et al.* 2010).

A esporulação, é um exemplo de diferenciação onde a célula replica o DNA, se divide assimetricamente e armazena uma cópia integral do genoma em cada um dos compartimentos (Driks, 2007; McKenney *et al.*, 2013), o maior, denominado célula mãe (esporângio) e o

menor denominado pré-esporo. O esporo maduro é formado após uma sequência de mudanças morfológicas governadas pela ativação sequencial dos fatores transcricionais especializados (Driks, 1999; Piggot e Losick, 2002; Kim *et al.*, 2006; McKenney *et al.*, 2013). Esta regulação temporal e espacial do programa de expressão gênica durante a formação do esporo garante a síntese de componentes requeridos no tempo e compartimento celular corretos. A formação do esporo pode ser dividida, didaticamente, em sete estágios (I a VII) morfolologicamente reconhecíveis. Os sucessivos estágios metabólicos da esporulação foram bem estabelecidos usando MCF e MET. Um resumo do processo de esporulação está descrito na figura 1.

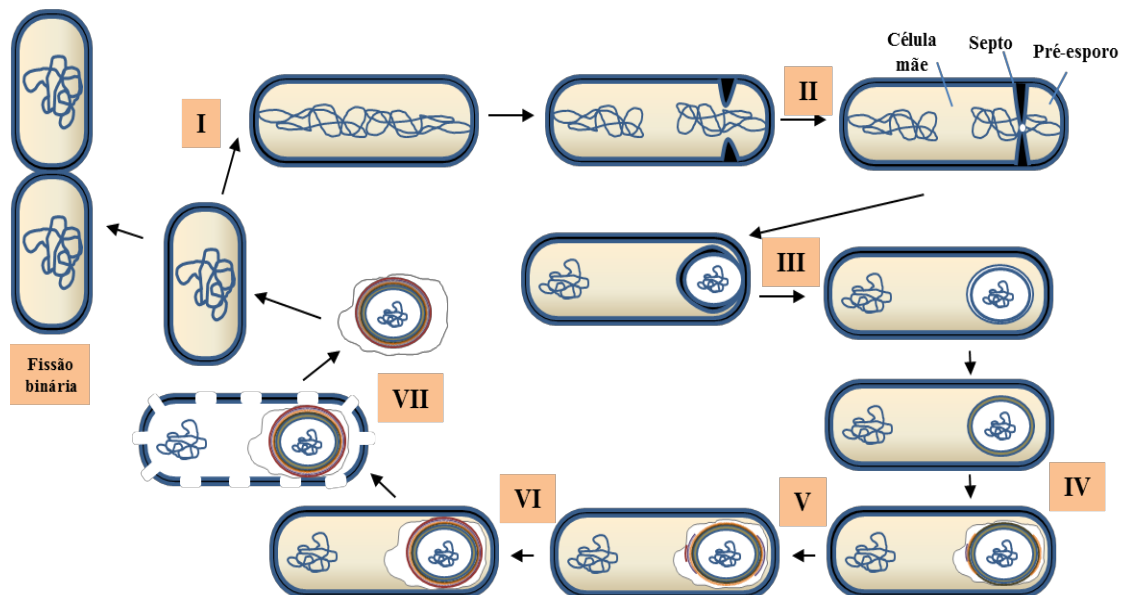


Figura 1. Ciclo celular de bactérias formadoras de endósporos. A esporulação é um processo dividido, didaticamente, em sete estágios (I à VII indicados na figura). No **estágio 0**, uma célula em final de fase logarítmica com genoma duplicado inicia o processo. A diferenciação se inicia com a formação do filamento axial (estágio I), seguido da formação do septo (estágio II) originando dois compartimentos, a célula mãe, o maior e o pré-esporo, o menor. A partir desse momento o processo torna-se irreversível. Em seguida, a célula mãe engolfa o pré-esporo (estágio III). Logo após o engolfamento inicia-se a formação e montagem das camadas que irão compor o esporo maduro, a deposição do córtex e possível formação do exósporo (estágio IV) e a estruturação da capa e outros possíveis componentes externos (estágio V e VI) como a crosta e apêndices externos ao exósporo. No estágio final (estágio VII), a parede celular do esporângio é lisada, liberando o esporo maduro no ambiente. Esporos são rapidamente capazes de germinar e continuar o ciclo vegetativo em resposta à presença de nutrientes.

Como mencionado anteriormente, os esporos bacterianos são entidades estruturalmente complexas (Knaysi e Hillier, 1949), que partilham uma arquitetura comum, consistindo em uma série de camadas concêntricas, que atuam como barreiras protetoras

(Driks, 1999; Driks, 2004; Priest *et al.*, 2004; McKenney *et al.*, 2013). A ultraestrutura mais comumente descrita para esporos é composta por três subestruturas básicas: cerne (ou citoplasma do espora), córtex e capas (Aronson e Fitz-James, 1976; Setlow, 1995; Driks, 1999; Meador-Parton e Popham 2000; Henriques e Moran, 2007; Driks, 2007, McKenney *et al.*, 2013), embora outras estruturas externas possam estar presentes, por exemplo, o exósporo (Beaman *et al.*, 1972; Driks, 1999; Driks, 2002; Waller *et al.* 2004; Driks, 2007; Traag *et al.*, 2010; McKenney *et al.*, 2013). Uma camada adicional de capa, designada crosta, foi descrita recentemente em *B. subtilis* (Waller *et al.*, 2004; McKenney *et al.*, 2010). A representação esquemática da ultraestrutura do espora é apresentada na figura 2.

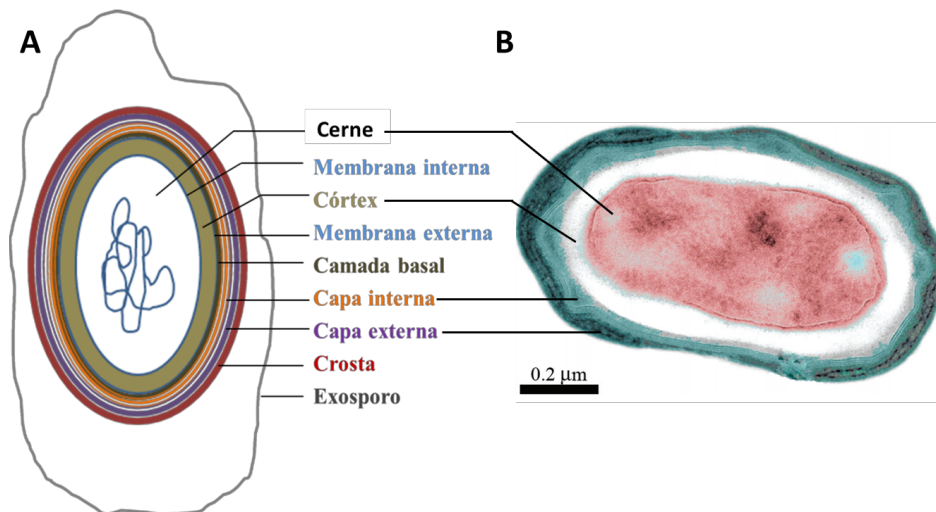


Figura 2. Ultraestrutura do espora bacteriano. Esporos bacterianos partilham uma arquitetura comum consistindo de uma série de membranas concêntricas (A). Apesar de apresentarem uma gigantesca diversidade no número de estruturas, espessura e complexidades de camadas, a ultraestrutura de esporos mais comumente descrita por MET consiste em três subunidades básicas: cerne, córtex e capas, nesta figura, apresentadas colorizadas (B). Outras estruturas externas frequentemente descritas em esporos são a crosta (*B. subtilis*) e o exósporo (*B. cereus*) vistos em (A).

O cerne, ou citoplasma do espora, é o compartimento mais interno e abriga o material genético, alto teor de dipicolinato de cálcio (5 a 15% do volume total do espora) e pequenas proteínas ácido-solúveis que contribuem enormemente para a resistência desta célula (Setlow, 2006). O estado de dormência e a resistência a altas temperaturas são características de resistência relacionadas à condição desidratada do cerne, sendo que durante a esporulação, em algumas espécies, até 96% do conteúdo inicial de água do cerne é substituído por dipicolinato de cálcio (Sunde *et al.*, 2009). O cerne é envolvido por uma membrana, denominada membrana interna, e uma camada (córtex) formada de peptídeoglicana (PG), contendo

menor número de ligações cruzadas entre as camadas adjacentes de PG, quando comparada à PC de células vegetativas típicas. O menor número de ligações cruzadas confere elasticidade a estrutura do esporo. Esta plasticidade mediada pelo córtex permite que o volume do esporo se expanda ou retraia, conforme o teor de umidade ambiental, até os respectivos limites que permitam a manutenção da viabilidade celular (Driks, 1999; Meador-Parton e Popham 2000; Driks, 2004; McKenney *et al.*, 2013).

Na espécie modelo *B. subtilis*, ao menos 70 proteínas diferentes são sintetizadas na célula mãe e arranjadas em torno do pré-esporo (Figura 1; estágios IV à VI) dando origem à complexa estrutura em multicamadas, comum a todos os esporos e denominada capa (Driks, 1999; Henriques e Moran, 2000; Driks, 2002; Kim *et al.*, 2006; McKenney *et al.*, 2013).

A capa apresenta morfogênese dinâmica e coordenada com o desenvolvimento do esporo e tem uma aparência marcante quando observada por MET. No caso de *B. subtilis* duas camadas principais da capa podem ser facilmente discernidas: a camada externa e a camada interna (Figuras 2 e 3). A camada interna, de aspecto lamelar delgado, é composta por duas a cinco lâminas e apresenta aproximadamente 75 nm de espessura (Driks, 1999). Circulando a camada interna, a camada externa, frequentemente, de maior espessura (80 a 200 nm), que vista por MET, se contrasta do restante da estrutura por pela aparência mais escura e irregular do que a camada interna (Driks, 1999).

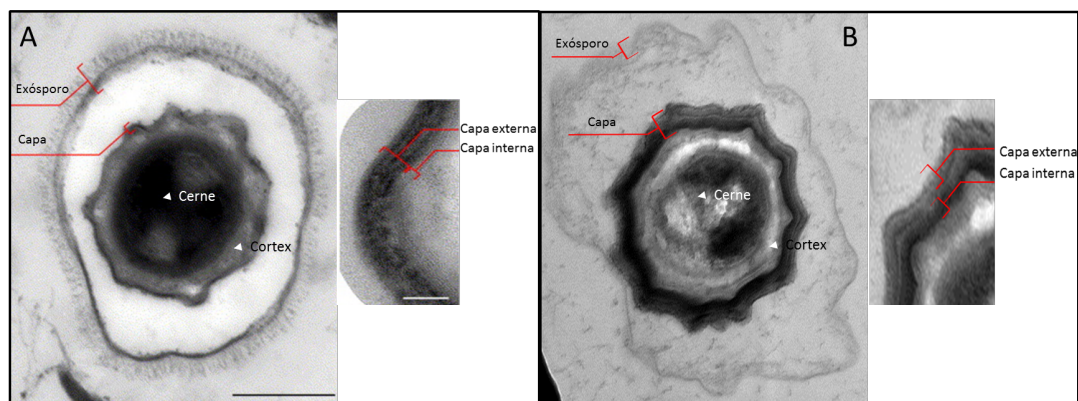


Figura 3. Arquitetura tipicamente observada em esporos bacterianos. A arquitetura do esporo de *B. anthracis* (A; adaptado de Driks, 2002), é bem conhecida e permite a identificação de vários componentes similares em outras espécies não modelo, por exemplo, o *Paenibacillus alvei* (B) representado pela linhagem SDF0028. Compartilhar estruturas similares, entretanto, não é garantia de uma estrutura final semelhante. O número de estruturas, a espessura e complexidade das camadas da capa diferem significativamente entre espécies.

O número de estruturas, a espessura e complexidade das camadas da capa diferem significativamente entre espécies de *Bacillus* (Giorno, 2007 – Figura 3). O *B. anthracis* apresenta uma estrutura delgada, quase única, enquanto em *L. sphaericus* uma estrutura mais complexa composta por várias lâminas é formada (Guinebrétiere e Sanchis, 2003; Galperin, 2013). A capa é um elemento crítico para as propriedades de resistência do esporo, agindo como uma barreira para enzimas degradativas e moléculas reativas, ao mesmo tempo em que permite a penetração de pequenas moléculas selecionadas e a interação com receptores de germinação localizados na camada basal do esporo (Driks, 1999; Driks, 2007).

Como mencionado anteriormente, os esporos de algumas espécies ainda apresentam outras estruturas externas a capa, de função e composição não muito bem estabelecidas (Figura 2), o exósporo (Driks, 2007; Traag *et al.*, 2010) e a crosta (McKenney *et al.*, 2013).

O exósporo é tipicamente descrito por MET como uma fina camada pouco eletrondensa que circula o esporo e é separada do mesmo por uma lacuna denominada inter espaço (Sousa *et al.*, 1978; Chen *et al.*, 2010; McKenney *et al.*, 2013). Encontrada em diversas espécies, notadamente aquelas do grupo do *B. cereus*, essa estrutura é inexistente, ou se apresenta em tamanho não detectável pelas técnicas usualmente empregadas, em outras espécies tais como a espécie modelo *B. subtilis* (Figura 2), *B. clausii* e *B. safensis*, sugerindo que o exósporo não é uma estrutura essencial para um esporo (Beaman *et al.*, 1972; Driks, 1999; Driks, 2002; Waller *et al.* 2004; Driks, 2007; Traag *et al.*, 2010; McKenney *et al.*, 2013).

Em adição ao exósporo, outros acessórios podem ser encontrados em alguns esporos, tais como, filamentos, estruturas semelhantes a fimbrias (Mizuki *et al.*, 1998; Driks, 1999), uma camada basal paracristalina cobrindo o exósporo de *B. anthracis* (Driks, 2002; Thompson *et al.*, 2012) ou outros componentes de tamanhos menores.

A recente incorporação de vermelho de rutênio no preparo da amostra a ser analisada por MET revelou em *B. subtilis*, uma camada adicional à camada mais externa da capa, e indetectável por MET com contrastação convencional (Waller *et al.*, 2004). Posteriormente, essa camada morfológicamente similar à capa externa, porém de aparência mais consistente e grosseira foi denominada crosta (McKenney *et al.*, 2010) embora a função permaneça indefinida.

Diversas variações entre componentes proteicos e açúcares nas camadas mais externas de esporos podem, ainda, serem críticas para definir nichos ecológicos (Redmond *et al.*, 2004) e propriedades químicas de superfície (McKenney *et al.*, 2010; Chen *et al.*, 2010), como adesão (Joshi, 2012).

4 – Morfogênese da capa do esporo

A morfogênese da capa do esporo envolve dois fenômenos coordenados, mas geneticamente desemparelhados: a concentração localizada de proteínas e o revestimento do esporo (Wang *et al.*, 2009). Tratando-se de uma série de estruturas concêntricas em formato esférico, seria intuitivo imaginar que a capa é construída em etapas, camada a camada, e de dentro para fora (Figura 1, estágios de IV à VI). Entretanto, em *B. subtilis* McKenney *et al.* (2010) relataram a presença de pelo menos duas proteínas de expressão tardia na camada interna da capa (CotD e CotT); três de expressão precoce na camada externa da capa (CotE, CotO, CotM) e duas na crosta (CotW e CotZ). Esses dados sugerem que a montagem da capa se inicia de forma assimétrica, com relação à superfície do pré-esporo (Figura 4).

Conforme os genes de capa são expressos, as proteínas se acumulam em uma cobertura de suporte localizada no polo proximal da célula mãe, em um estágio imediatamente após o engolfamento (Driks *et al.*, 1994; McKenney *et al.*, 2013). Em três ondas sucessivas, conjuntos coordenados de proteínas envolvem o esporo, estabelecendo as camadas da capa até a formação de estruturas laminares concêntricas. Ao longo do curso da esporulação, diversas proteínas de capa são expressas, alocadas na superfície do esporo e adicionadas à cobertura de suporte (Figura 4).

A montagem dessas proteínas nas estruturas da capa é mediada por interações entre as proteínas expressas e modificações pós-transcricionais, como, ligações covalentes cruzadas (Costa *et al.*, 2006; Ozin *et al.*, 2000; Ragkousi e Setlow, 2004; Ramamurthi *et al.*, 2006; Zilhao *et al.*, 2005).



Figura 4. Morfogênese da capa do esporo bacteriano. A montagem da capa do esporo envolve dois fenômenos coordenados, a expressão e concentração localizada de proteínas e o revestimento do esporo a partir de uma cobertura de suporte. Adaptado de McKenney *et al.*, 2013.

Um pequeno subgrupo de proteínas, conhecido como proteínas morfogenéticas da capa, possui papel fundamental na montagem das camadas dessa estrutura, direcionando as

demais proteínas para regiões específicas e apropriadas (Driks, 1999; Henriques e Moran, 2007; Piggot e Coote, 1976; Roels, 1992; Zheng, 1988). SpoIVA, SPoVM, SPoVID, SafA e CotE, além de CotO dependendo da espécie (por exemplo. *B. anthracis*) são denominadas proteínas morfogenéticas e são consideradas proteínas-chave ou de posição hierárquica máxima, pois têm papel relevante na morfogênese de capa, apesar de não interferirem na regulação da expressão gênica na célula mãe (Figura 5; Driks, 1999; Henriques e Moran, 2007).

A rede de interações de montagem de esporo é bem caracterizada na espécie modelo *B. subtilis* (Lai *et al.*, 2003; McKenney *et al.*, 2013). Constituída de três módulos (Figura 5), as interações são mediadas por três proteínas morfogenéticas, SpoIVA, SafA e CotE, primariamente envolvidas no direcionamento de proteínas de capa na superfície da célula em construção (Takamatsu *et al.*, 1999; Ozin *et al.*, 2000; Driks, 2002; McKenney *et al.*, 2013). SpoIVA forma a camada basal e é necessária para a ancoragem completa das demais camadas da capa (Ramamurthi *et al.*, 2006; Piggot e Coote, 1976; Roels, 1992). SafA é necessária para a montagem da camada interna da capa (McKenney *et al.*, 2010). CotE é fundamental para a montagem da camada externa da capa, influente sobre uma série de proteínas em ambas camadas basal e capa interna e, em conjunto com CotX, CotY e CotZ, pela montagem da crosta (Imamura *et al.*, 2011; McKenney *et al.*, 2010). As principais características dessas proteínas estão descritas na tabela I.

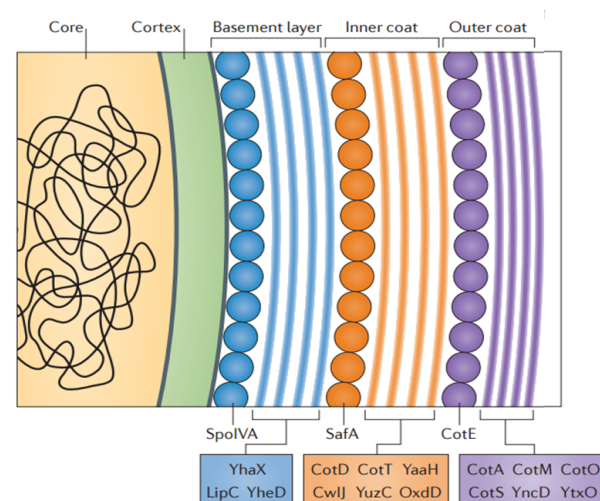


Figura 5. Proteínas morfogenéticas de *B. subtilis*. Quatro camadas estão representadas: a camada basal (azul), a porção interna da capa (laranja), a porção externa da capa (roxo). SpoIVA, SafA, CotE, SpoVID, CotH e CotO são proteínas que possuem papel crucial na montagem de capa de esporo. A perda de qualquer uma dessas causa efeitos significativos na arquitetura geral do esporo. Adaptado de McKenney *et al.*, 2013.

Tabela I. Proteínas morfogenéticas de esporo bacterianos

Proteína morfogenética	Localização	Função principal
CotE	Camada externa da capa	Montagem da camada externa da capa
SafA	Camada interna da capa	Montagem da camada interna da capa
SpoIVA	Camada basal	Formação da camada basal e ancoragem completa das demais camadas da capa
SpoVID	Camada basal	Direcionamento do revestimento do esporo

O modelo de montagem de capa em *B. subtilis* admite, ainda, a presença de outras proteínas essenciais para construção dessa estrutura (Figura 6). Este processo será discutido em detalhes no Capítulo II desta tese. SpoVM e SpoVID são responsáveis pelo agrupamento de proteínas e, conseqüente, formação do invólucro geral do esporo (Beall *et al.*, 1993; Ramamurthi, 2009; McKenney *et al.*, 2013). SpoVID é essencial para o direcionamento do revestimento do esporo, ou a transição de um aglomerado estrutural de proteínas em arranjos típicos, ou camadas concêntricas. Em casos de células com mutação nesse gene, ocorre o acúmulo de proteínas na cobertura de suporte no polo proximal da célula mãe, mas há falhas em revestir o esporo com as camadas resultantes (Figura 6B; Driks *et al.*, 1994; Wang *et al.*, 2009).

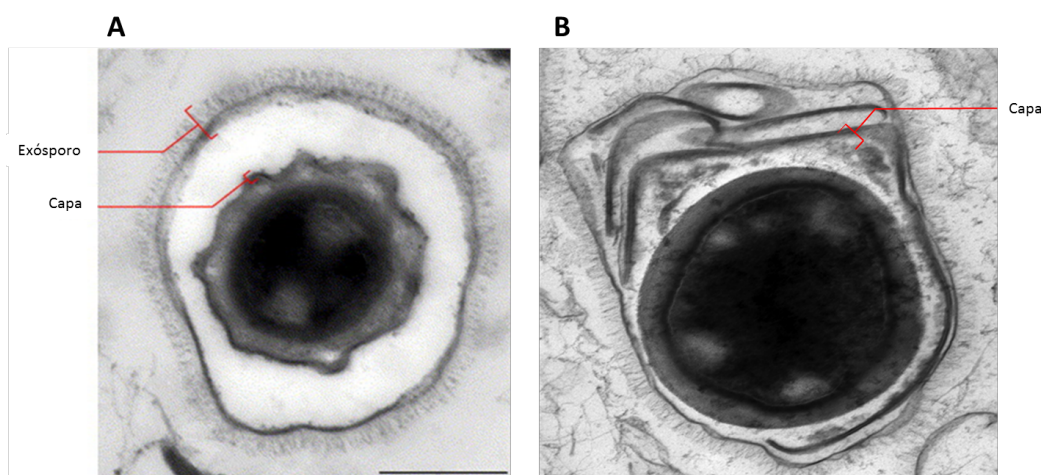


Figura 6. Fenótipo resultante da inativação do gene *spoVID* em *B. anthracis*. A arquitetura do esporo de *B. anthracis* (A; adaptado de Driks, 2002) é alterada drasticamente após deleção na sequência do gene que codifica a proteína morfogenética SpoVID. O mutante produz proteínas das camadas correspondentes às capas, mas falha em revestir o esporo com as camadas resultantes (B; cortesia de Tyler Boone).

Com raras exceções, individualmente, as proteínas de capa de esporo apresentam efeito fenotípico limitado ou não detectável (Driks, 2002; Lai *et al.*, 2003; Kim *et al.*, 2006). Consequentemente, as funções específicas de proteínas de capa, em quase totalidade, continuam desconhecidas. É importante nos perguntarmos até que nível as proteínas conservadas apresentam funções similares e até que ponto podemos continuar extrapolando o conhecimento sobre linhagens modelo para linhagens não modelo. É, ainda, muito provável que as funções da capa de esporos, como estrutura conservada entre espécies, sejam propriedades emergentes da interação entre múltiplas proteínas e que proteínas que participam dessas interações difiram entre as espécies.

Para montar uma rede de interações realista de proteínas de capa, compreender como essa estrutura é montada, bem como as respectivas funções, é crítico identificar os compostos proteicos-chave e determinar as respectivas funções nas diversas espécies.

5 – Coleção de Bactérias aeróbias formadoras de esporos

Espécies de Bafes são essenciais ao funcionamento de diversos ecossistemas. O solo é o principal *habitat*, onde observa-se a interação com a flora, outros microrganismos, insetos e nematoides (de Vos, 2011; Verbaendert e de Vos, 2011). No solo, as diversas espécies de Bafes participam dos ciclos de transformação de matéria e energia, como o ciclo do carbono e nitrogênio, e também na promoção do crescimento de plantas (Nicholson *et al.*, 2000; Driks, 2004; Santana *et al.*, 2008; Ohba *et al.*, 2009; Logan e Halket, 2011).

Um grande número de espécies de Bafes apresenta amplo potencial biotecnológico, podendo ser utilizadas na agricultura, indústria e área médica (humana e veterinária). Como exemplos de aplicação podemos destacar o *B. subtilis*, espécie produtora de diversas hidrolases, antibióticos, vitaminas e biosurfactantes, além de ser empregada na produção de vacinas, probióticos, dentre outras (Liu *et al.*, 2013; Eijlander *et al.*, 2014). *Geobacillus stearothermophilus* e *Paenibacillus polymyxa* são utilizados como agentes denitrificante em solos (Verbaendert e de Vos, 2011; Márquez *et al.*, 2011) e *B. licheniformis*, além de agente denitrificante ativo no solo, apresenta uso potencial em estações de tratamento de água (Verbaendert e de Vos, 2011). *B. thuringiensis* e *L. sphaericus*, espécies produtoras de cristais parasporais tóxicos para diversos invertebrados, vem sendo utilizadas a várias décadas na agricultura e no controle de vetores de doenças infecciosas (Jensen *et al.*, 2003; Ohba, 2009; Ehling-Schulz e Messelhäusser, 2013). *P. lentimorbus* e *P. popilliae* apresentam atividade larvicida contra besouros, pragas de gramíneas (de Vos *et al.*, 2009). A biorremediação de

solo também tem sido explorada utilizando espécies de Bafes, tais como, linhagens do gênero *Brevibacillus* (*Br.*), capazes de neutralizar metais tóxicos (Ruiz-Lozano e Azcón, 2011). Em adição, o *B. anthracis* é associado a atos de bioterrorismo e armas de guerra (Jenses *et al.*, 2003; Kølsto *et al.*, 2009; Mertens *et al.*, 2014), enquanto o *B. cereus* é um conhecido agente causador de intoxicação alimentar, constantemente encontrado em produtos alimentícios industrializados ou *in natura* (van der Auwera *et al.*, 2007).

Entender os modelos de diversidade de diferentes espécies de Bafes é essencial, considerando os padrões cosmopolitas em solo e o elevado potencial biotecnológico desses microrganismos (Logan e de Vos, 2009; Mandic-Mulec e Prosser, 2011). A natureza desses modelos e as respectivas funções são, entretanto, de difícil determinação (Mandic-Mulec e Prosser, 2011). Por estas razões, pesquisas que preservem e abordem a diversidade genética são fundamentais para gerar conhecimento básico e, conseqüentemente, aumentar a perspectiva de aplicação destas espécies altamente importantes para a saúde humana, conservação ambiental, a sustentabilidade agrícola e desenvolvimento industrial.

Dois fatores contribuíram para o crescimento rápido do conhecimento sobre o número de espécies de Bafes (Fritze, 2004; Logan e de Vos, 2009). Primeiramente, a diversificação e o aumento na eficiência do processo de isolamento, que repercute melhor a amplitude fisiológica e o requerimento nutricional para o cultivo destes organismos ubíquos. O segundo fator é o desenvolvimento de técnicas cada vez mais sofisticadas para a caracterização e identificação de linhagens bacterianas, em particular, no nível molecular, onde se destaca a análise de sequências de rDNA/rRNA 16S, outros marcadores, além de sequenciamento de genomas completos (Fritze, 2004; Galperin *et al.*, 2013).

A importância de estudos básicos abordando a diversidade e as potencialidades biotecnológicas de Bafes motivou o isolamento, a identificação e preservação de linhagens de solo do DF com diferentes características fenotípicas e genotípicas. A Coleção de Bafes (CBafes), da UnB/IB/Departamento de Biologia Celular, está localizada no Laboratório de Microbiologia/LaBafes é especializada em linhagens de interesse científico e com potencial tecnológico para os setores médicos (humano e veterinário) agropecuário, ambiental e industrial. Atualmente, a Coleção dispõe de um acervo que compreende 312 amostras, isoladas do solo do DF (SDF) e designadas SDF0001-SDF0312. É importante mencionar que esta estudos envolvendo as amostras desta Coleção não apresenta cunho ecológico, pois não tem como objetivo descrever as interações entre as comunidades microbianas ativas das amostras de solo isoladas ou de outra natureza.

As linhagens SDF0001 a SDF0154 foram selecionadas por choque térmico a 80 °C, enquanto as linhagens SDF0155 a SDF0312 foram selecionadas por choque térmico a 65 °C; 70 °C ou 80 °C e estão sendo inspecionadas por uma abordagem polifásica para fins taxonômicos. Os métodos microbiológicos e genéticos clássicos e moleculares utilizados incluem análises filogenética (rDNA 16S e genes de virulência); filoproteômica (espectrometria de massa MALDI-TOF), perfil plasmidial, termo resistência de esporos e ultraestrutura de células vegetativas, esporângios, esporos e cristais utilizando MET, dentre outros.

A ultraestrutura de esporos por MET (Cavalcante, 2014), além de perfil plasmidial (Orem, 2014) apontaram para uma considerável diversidade. Filogenia baseada em sequências de rDNA 16S (Orem, 2014) e filoproteômica por MALDI-TOF-MS (Bezerra, 2015) corroboram esses dados.

O acervo da CBafes ainda inclui a linhagem *B. cereus* FT9, isolada de uma fonte termal, com genoma sequenciado (Raiol *et al.*, 2014). Linhagens recombinantes expressando uma proteína de fluorescência verde (GFP), sendo oito de *B. thuringiensis* (Parente *et al.*, 2008) e mutantes derivados, além de uma de *B. circulans* (Sinott *et al.*, 2014), também estão incluídas. Ao menos vinte e uma células tipo e mutantes de *B. thuringiensis* totalmente curados de plasmídeos (Cry-; hospedeiras para expressão heteróloga) provenientes de centros de referência, dentre outras, completam a Coleção atual. As amostras depositadas na CBafes estão preservadas em forma de esporos, estocados à temperatura ambiente em tiras de papel.

A solicitação de Acesso a Amostra Componente do Patrimônio Genético foi autorizada pelo CNPq (010439/2015-3).

III. Justificativa

Atualmente apenas um número reduzido de Bafes modelos representa o ideal de conhecimento biológico detalhado (Binnewies *et al.*, 2006). Portanto, sem a caracterização celular e molecular aprofundada de novas linhagens, a ideia de diversidade bacteriana continuará simplista e limitada.

O potencial de utilização de espécies formadoras de esporos como fonte de novos bioprodutos bem como o aprendizado sobre a diversidade de Bafes de solo nos levou ao isolamento e identificação das linhagens SDF. Neste trabalho, nosso objetivo foi de analisar características ultraestruturais de espécies já bem conhecidas, assim como espécies pertencentes a regiões da árvore filogenética dos *Firmicutes* que apresentam pouca ou

nenhuma descrição na literatura. A análise dessas espécies pode revelar novas características estruturais de esporos e fornecer ideias sobre as relações filogenéticas e evolutivas destas espécies por similaridades ultraestruturais de esporos. Igualmente, este trabalho visa fornecer dados importantes sobre a questão da diversidade de composição proteica apresentada em espécies distintas e em que nível isso influencia em propriedades físico-químicas diversas.

IV. Objetivos

Caracterizar, *in vitro* e *in silico*, variações e similaridades na ultraestrutura do esporo de diversas linhagens de Bafes.

Objetivos específicos

1. Selecionar linhagens da CBafes para análise ultraestrutural;
2. Criar um atlas de imagens de esporos de diversas linhagens SDF selecionadas da CBafes por MET;
3. Acessar características morfológicas da ultraestrutura de esporângios, pré-esporos e esporos livres que tendem a serem preservadas dentro de um táxon;
4. Acessar características morfológicas da ultraestrutura de esporos que tendem a variar dentro de um táxon;
5. Criar um banco de dados de genes relacionados com a ultraestrutura das espécies modelo *B. subtilis* e *B. anthracis* presentes em genomas completos depositados em bancos de dados;
6. Identificar ortólogos de genes de proteínas morfogenéticas de *B. subtilis* em linhagens SDF selecionadas;
7. Comparar a relação molecular entre os genes ortólogos de diversas espécies e dos modelos;
8. Inativar o gene ortólogos da proteína SpoVID nas linhagens *Lysinibacillus sphaericus* SDF0037 e *Lysinibacillus fusiformis* 743;
9. Acessar o papel do gene ortólogo de *spoVID* na montagem da estrutura do esporo, por meio de análise do fenótipo resultante por MET;
10. Criar um banco de dados de genomas de Bafes presentes no banco de dados NCBI em nível completo ou *scaffold*;
11. Contrastar os bancos de dados de genes de proteínas relacionadas com ultraestrutura de esporos e genomas presentes no NCBI e gerar uma tabela de presença ou ausência de genes nestes genomas;
12. Utilizar a tabela contendo a anotação de genes relacionadas com ultraestrutura de esporos e genomas presentes no NCBI para orientar estudos de covariação e evolução de genes ultraestruturais na ordem *Bacillales*.

V. Referências bibliográficas

- Ahmed, Yokota, A., Yamazoe, A., and Fujiwara T. (2007). **Proposal of *Lysinibacillus boronitolerans* gen. nov.sp. nov., and transfer of *Bacillus fusiformis* to *Lysinibacillus fusiformis* comb. nov. and *Bacillus sphaericus* to *Lysinibacillus sphaericus*** Int Journal of Systematic and Evolutionary Microbiology.
- Armstrong K.A., Acosta R., Ledner E., Machida Y., Pancotto M., McCormick M.,(1984) **A 37 X 10(3) molecular weight plasmid-encoded protein is required for replication and copy number control in the plasmid pSC101 and its temperature-sensitive derivative pHS1.** J Mol Biol. 1984; 175(3):331–48.
- Aronson, A., 2002.**Sporulation and d-endotoxin synthesis by *Bacillus thuringiensis*.** Cell. Mol. Life Sci. 59, 417–425.
- Aronson, A., and Fitz-James, P., (1976).**Structure and morphogenesis of the bacterial spore coat.** Bacteriol Rev 40,360–402.
- Beaman,T.C., Pankratz H.S., and Gerhardt P.,(1972) **Ultrastructure of the exosporium and underlying inclusions in spores of *Bacillus megaterium* strains.** J. Bacteriol. 109:1198–1209.
- Binnewies, T.T., Motro, Y., Hallin, P.F., Lund, O., Dunn, D., La, T., *et al.* (2006) **Ten years of bacterial genome sequencing: comparative-genomics-based discoveries.** *Funct Integr Genomics* 6: 165–185.
- Brillard, J. e Lereclus, D. (2004). **Comparison of cytotoxin *cytK* promoters from *Bacillus cereus* strain ATCC 14579 and from a *B. cereus* food-poisoning strain.** *Microbiology-Sgm* 150, 2699-2705.
- Cano, R.J., Borucki, M.K. (1995). **Revival and identification of bacterial spores in 25- to 40-million-year-old Dominican amber.** *Science*, 268(5213):1060-4.
- Colleaux L., D'Auriol L., Galibert F., Dujon B. (1988) **Recognition and cleavage site of the intron-encoded omega transposase.** *Proc Natl Acad Sci U S A.*; 85(16):6022–6.
- Davis, B.D., Dulbecco, R., Eisen, H. and Ginsberg, (1990). **Bacterial architecture.** In **Microbiology**, Eds., p. 47. Philadelphia, PA: J.B. Lippincott.
- de Vos, P. (2011).**Studying the Bacterial Diversity of the Soil by Culture-independent approaches.** Endospore forming soil bacteria. Vol 27 1-7
- de Vos, P.; Garrity, G.; Jones, D.; Krieg, N.R.; Ludwig, W.; Rainey, F.A.; Schleifer, K.-H.; Whitman, W.B. (Eds.). (2009). **Bergey's Manual of Systematic Bacteriology. Volume 3: The Firmicutes.** Second Ed.
- Driks A, Roels S, Beall B, Moran CP, Jr, Losick R. (1994). **Subcellular localization of proteins involved in the assembly of the spore coat of *Bacillus subtilis*.** *Genes Dev.* 8:234–244
- Driks, A., (1999). **The *Bacillus subtilis* spore coat.** *Microbiol Mol Biol Rev* 63, 1–20.
- Driks, A., (2002). **Maximum shields:the assembly and function of the bacterial spore coat.** *TRENDS in Microbiology* Vol.10 No.6
- Driks, A., (2003). **The dynamic spore coat.** *Proc Natl Acad Sci USA* 100(6):3007–3009.
- Driks, A., (2007).**Surface appendages of bacterial spores.** *Molecular Microbiology* 63(3), 623–625.
- El-Bendary M., Priest F.G., Charles J.F., Mitchell W.J. (2005) **Crystal protein synthesis is dependent on early sporulation gene expression in *Bacillus sphaericus*.** 51-56 First published online: 1 November
- Fritze, D. (2004). **Taxonomy of the Genus *Bacillus* and related genera: the aerobic endospore-forming bacteria.** *Phytopatology*, 94(11). 1245-1248.
- Galperin, M.Y. (2013). **Genome diversity of spore-forming Firmicutes.** *Microbiology Spectrum*, 1(2): 1-15.

- Garrity, G.M.; Bell, J.A.; Lilburn, T.G. (2003). **Taxonomic outline of the prokaryotes**. In: Bergey's manual of systematic bacteriology.
- Gibbons, N.E., and Murray, R.G.E., (1978). **Proposals concerning the higher taxa of bacteria**. Int J Syst Bacteriol 28:1-6
- Giorno, R., Bozue. J., Cote, C., Wenzel, T., Sulayman, M., Krishna, M., Michael, R.M., Wang, R., Zielke, R.R., Maddock, J., Friedlander, A., Welkos, S., and Driks, A. (2007). **Morphogenesis of the *Bacillus anthracis* Spore**. Journal of bacteriology, p. 691–705 Vol. 189, No. 30021-9193.
- Guinebrétiere, M.H., and Sanchis, V., (2003). ***Bacillus cereussensu lato***. Bull Soc Fr Microbiol 18:95-103.
- Hannay Cl. 1957. **The parasporal body of *Bacillus laterosporus* Laubach**. J Biophys Biochem Cytol. Nov 25;3(6):1001-10.
- Henriques AO, Moran CP., Jr (2007). **Structure, assembly, and function of the spore surface layers**. Annu. Rev. Microbiol. 61:555–588
- Henriques, A.O., and Moran, C.P.Jr., (2007). **Structure, assembly, and function of the spore surface layers**. Annu. Rev. Microbiol. 61, 555–588. 16.
- Holt, SC. and Leadbetter, ER. (1969). **Comparative ultrastructure of selected aerobic spore-forming bacteria: a freeze-etching study**, Bacteriol Rev 33, 346-378.
- Holt S.C., Gauthier J.J., Tipper D.J. (1975). **Ultrastructural studies of sporulation in *Bacillus sphaericus***. J Bacteriol 122:1322–1338.
- Holt, J.G., (1986). **Bergey's Manual of Systematic Bacteriology gram-positive bacteria other than actinomycetes**. Williams & Williams, Baltimore, MD.
- Hoon M. J.L., Eichenberger P., and Vitkup D., (2010) **Hierarchical Evolution of the Bacterial Sporulation Network**. Current Biology20, R735–R745
- Hutchison E., Miller A., Angert D. (2014). **Sporulation in Bacteria: Beyond the Standard Model**. Microbiol spect. TBS-0013-2012.
- Imamura D, Kuwana R, Takamatsu H, Watabe K. (2011). **Proteins involved in formation of the outermost layer of *Bacillus subtilis* spores**. J. Bacteriol. 193:4075–4080
- Janes B.K. and Stibitz, S (2006). **Routine Markerless Gene Replacement in *Bacillus anthracis***. Infect. Immun. vol. 74 no. 3 1949-1953
- Joshi L.T., Phillips D.S., Williams C.F., Alyousef A., Baillie L. (2012) **Contribution of spores to the ability of *Clostridium difficile* to adhere to surfaces**. Appl Environ Microbiol Nov;78(21):7671-9.
- Kalfon A., Charles J.-F., Bourgin C. (1984) **Sporulation of *Bacillus sphaericus* 2297: an electron microscope study of crystal-like inclusion biogenesis and toxicity to mosquito larvae**. J. Gen. Microbiol. 130, 893–900.
- Kim, K.K., Lee K.C., Yu H., Ryoo S., Park Y. and Lee J.S., (2009). ***Paenibacillus sputi* sp. nov., isolated from the sputum of a patient with pulmonary disease**. *International Journal of Systematic and Evolutionary Microbiology* vol. 60, part 10, pp. 2371 - 2376
- King, J. (1980). **Regulation of structural protein interactions as revealed in phage morphogenesis regulation and development**. vol. 2. Plenum Press, New York, N.Y.
- Knaysi, G. and Hillier, J., (1949). **Preliminary observations on the germination of the endospore in *Bacillus megatherium* and the structure of the spore coat**. J Bacteriol 57, 23–29.
- La Duc, M.; Satomi, M.; Venkateswaran, K. (2004). ***Bacillus odyseyi* sp. nov., a round-spore-forming bacillus isolated from the Mars Odyssey spacecraft**. International Journal of Systematic and Evolutionary Microbiology, 54: 195-201.
- Lai E.M., Phadke N.D., Kachman M.T., Giorno R., Vazquez S., Vazquez J.A., Maddock J.R., Driks A., (2003). **Proteomic analysis of the spore coats of *Bacillus subtilis* and *Bacillus anthracis***. J Bacteriol. Feb;185(4):1443-54.

- Logan N.A., Berge O., Bishop A.H., Busse H.J., De Vos P., Fritze D., Heyndrickx M., Kämpfer P., Salkinoja-Salonen M.S., Seldin L., Rabinovitch L., Ventosa A., (2009). **Proposed minimal standards for describing new taxa of aerobic, endospore-forming bacteria.** *Int J Syst Evol Microbiol* 59:2114–2121
- Logan, N.A. and De Vos, P. (2009). **Genus I. *Bacillus* Cohn 1872, Bergey's Manual of Systematic Bacteriology.** 174AL. Vol3. *The firmicutes* 2nd Edition.
- Losick, R., and P. Stragier. (1992). **Crisscross regulation of cell-type-specific gene expression during development in *Bacillus subtilis*.** *Nature* 355:601– 604.
- Maguin E., Duwat P., Hege T., Ehrlich D., Gruss A. (1992) **New thermosensitive plasmid for gram-positive bacteria.** *J Bacteriol.* 174(17):5633–8.
- Mandic-Mulec I., Prosser J.I.; 2011. **Diversity of Endospore forming Bacteria in soil: characterization and driving mechanisms.** *Endospore forming soil bacteria.* Vol 27 31-57
- McKenney P.T., Driks A., Eichenberger P. ,(2013). **The *Bacillus subtilis* endospore: assembly and functions of the multilayered coat.** *Nat Rev Microbiol.* 33-44. December.
- McKenney PT, Eichenberger P. (2012). **Dynamics of spore coat morphogenesis in *Bacillus subtilis*.** *Mol. Microbiol.* 83:245–260
- McKenney PT, et al. (2010). **A distance-weighted interaction map reveals a previously uncharacterized layer of the *Bacillus subtilis* spore coat.** *Curr. Biol.* 20:934–938
- Meador-Parton, J. and Popham, D. (2000). **Structural analysis of *Bacillus subtilis* spore peptidoglycan during sporulation.** *J Bacteriol* 182, 4491–4499.
- Merzlyak EM, Goedhart J, Shcherbo D, Bulina ME, Shcheglov AS, Fradkov AF, (2007). **Bright monomeric red fluorescent protein with an extended fluorescence lifetime.** *Nat Methods.*; 4(7):555–7.
- Miller M.B. and Bassler B.L..(2001). **Quorum sensing in bacteria.** *Annu Rev Microbiol.*;55:165-99.
- Moberly, B.J., Shafa, F. and Gerhardt, P., (1966). **Structural details of *anthrax* spores during stages of transformation into vegetative cells.** *J Bacteriol* 92, 220–228.
- Montaldi F.A., Roth I.L. (1990) **Parasporal bodies of *Bacillus laterosporus* sporangia.** *J. Bacteriol.*;172:2168–2171.
- Narula J., Kuchina A., Dong-yeon D., Fujita M., Gurol M., Oleg A. (2015) **Chromosomal Arrangement of Phosphorelay Genes Couples Sporulation and DNA Replication,** *Cell* 162, 328–337 Elsevier Inc.
- Niall, A.L.,and Halket, G., (2011). **Developments in the taxonomy of aerobic, endospore forming Bacteria.** *Endospore forming soil bacteria.* Vol 27 1-7
- Nicholson, W.L., Munakata, N., Horneck, G., Melosh, H.J. and Setlow, P. (2000). **Resistance of *Bacillus* endospores to extreme terrestrial and extraterrestrial environments.** *Microbiol Mol Biol Rev* 64, 548–572.
- Ohba M, Mizuki E, and Uemori, A., (2009). **Parasporin, a New Anticancer Protein Group from *Bacillus thuringiensis*.** *Anticancer Research,* 29: 427-434,
- Ozin AJ, Henriques AO, Yi H, Moran CP., Jr (2000). **Morphogenetic proteins SpoVID and SafA form a complex during assembly of the *Bacillus subtilis* spore coat.** *J. Bacteriol.* 182:1828–1833
- Piggot, P.J., and Coote, J.G., (1976). **Genetic aspects of bacterial endospore formation.** *Bacteriol. Rev.* 40, 908–962.
- Piggot, P.J., and Losick, R., (2002). **Sporulation genes and intercompartmental regulation. In *Bacillus subtilis* and Its Closest Relatives: From Genes to Cells,** A.L. Sonenshein, J.A. Hoch, and R. Losick, eds. (Washington, DC: American Society for Microbiology), pp. 483–518.

- Pignatelli, M., Moya, A., Tamames, J., (2009). **EnvDB, a database for describing the environmental distribution of prokaryotic taxa.** *Environ. Microbiol. Rep.* 1, 191–197.
- Plaut R.D., Stibitz S. (2015) **Improvements to a Markerless Allelic Exchange System for *Bacillus anthracis*.** *PLoS ONE* 10(12): e0142758.
- Priest F. G., (1993). **Systematics and ecology of *Bacillus*.** In: *Bacillus subtilis and Other Gram-Positive Bacteria: Biochemistry, Physiology and Molecular genetics.* American Society for Microbiology. pp. 3–16.
- Ragkousi K, Setlow P. (2004). **Transglutaminase-mediated cross-linking of GerQ in the coats of *Bacillus subtilis* spores.** *J. Bacteriol.* 186:5567–5575
- Raiol, T., De-Souza, M. T., Oliveira, J. V. A., Silva, H. S. da I. L., Orem, J. C., Cavalcante, D. A., Moraes, L. M. P. (2014). **Draft Genome Sequence of FT9, a Novel *Bacillus cereus* Strain Isolated from a Brazilian Thermal Spring.** *Genome Announcements*, 2(5), e01027–14.
- Ramamurthi KS, Clapham KR, Losick R. (2006). **Peptide anchoring spore coat assembly to the outer forespore membrane in *Bacillus subtilis*.** *Mol. Microbiol.* 62:1547–1557
- Raymond B., Johnston P.R., Nielsen L.C., Lereclus D. and Crickmore N., (2010). ***Bacillus thuringiensis*: an impotent pathogen?**, Cell press.Elsevier Ltd.0966-842X, 2010.
- Redmond, C., Baillie, L.W., Hibbs, S., Moir, A.J. and Moir, A., (2004). **Identification of proteins in the exosporium of *Bacillus anthracis*.** *Microbiology* 150, 355–363.
- Roels S, Driks A, Losick R. (1992). **Characterization of *spoIVA*, a sporulation gene involved in coat morphogenesis in *Bacillus subtilis*.** *J. Bacteriol.* 174:575–585
- Ruiu L., (2013). ***Brevibacillus laterosporus*, a Pathogen of Invertebrates and a Broad-Spectrum Antimicrobial Species** *Insects.* Sep; 4(3): 476–492
- Russell, A., 1990.**Bacterial spores and chemical sporocidal agents.** *Clin Microbiol Rev* 3, 99–119.
- Schleifer, K. (2009) **Phylum XIII. Firmicutes** Gibbons and Murray 1978, 5 (Firmacutes [sic] Gibbons and Murray 1978, 5) **Bergey's Manual of Systematic Bacteriology.** Vol3. *The firmicutes* 2nd Edition
- Setlow P. 2006. **Spores of *Bacillus subtilis*: Their resistance to and killing by radiation, heat and chemicals.** *J Appl Microbiol* 101(3):514– 525.
- Setlow P., 2003. **Spore germination.** *Curr Opin Microbiol* 6:550–556.
- Setlow, P. 1995. **Mechanisms for the prevention of damage to DNA in spores of *Bacillus* species.** *Ann Rev Microbiol* 49, 29–54.
- Sokolova, T.; Hanel, J.; Onyenwoke, R.U.; Reysenbach, A.L.; Banta, A.; Geyer, R.; Gonzalez, J.M.; Whitman, W.B.; Wiegel, J. (2007). **Novel chemolithotrophic, thermophilic, anaerobic bacteria *Thermolithobacter ferrireducens* gen. nov., sp. nov. and *Thermolithobacter carboxydvorans* sp. nov.** *Extremophiles.* 11 (1): 145–157.
- Stackebrandt, E., Murray, R.G.E and Trüper, H.G., (1988). ***Proteobacteria* classis nov., a name for the phylogenetic taxon that includes the "purple bacteria and their relatives.** *Int. J. Syst. Bacteriol*38, 321-325.
- Stewart G.C. (2015). **The exosporium layer of bacterial spores: a connection to the environment and the infected host.** October. *Microbiol Mol Biol Rev*
- Stibitz, S. and Carbonetti, N.H. (1994) **Hfr mapping of mutations in *Bordetella pertussis* that define a genetic locus involved in virulence gene regulation.** *J Bacteriol.* Dec; 176(23): 7260–7266.
- Sundea E. P., Setlow P., Hederstedt L., and Hallea B. (2009) **The physical state of water in bacterial spores.** *PNAS*, November 17, vol. 106 no. 46 Edited by Richard M. Losick
- Traag B.A., Driks, A., Stragier, P., Bitter W., Broussard, G., Hatfull, G., Chu, F., Adams, 22

- K.N., Losick, R., (2010). **Do *mycobacteria* produce endospores?** Proc. Natl. Acad. Sci. U.S.A 107, 878-881.
- Trieu-Cuot P., Carlier C., Poyart-Salmeron C., Courvalin P. (1991) **Shuttle vectors containing a multiple cloning site and a lacZ alpha gene for conjugal transfer of DNA from *Escherichia coli* to gram-positive bacteria.** Gene.; 102(1):99–104.
- Verbaendert, I.; de Vos, P. (2011). **Studying Denitrification by Aerobic Endospore-forming Bacteria in Soil.** Em: **Endospore-Forming Soil Bacteria.** Springer, 1^a Ed.
- Villafane, R., Bechhofer, D.H. Narayanan, C.S., and Dubnau, D. (1987) **Replication control genes of plasmids pE194.** J Bacteriol 169: 4822-4829
- Vreeland, R.H., Rosenzweig, W.D., Powers, D.W. (2000). **Isolation of a 250 million-year-old halotolerant bacterium from a primary salt crystal.** Nature, 407(6806):897-900.
- Waller, L.N., Fox, N., Fox, K.F., Fox, A. and Price, R.L., (2004). **Ruthenium red staining for ultrastructural visualization of a glycoprotein layer surrounding the spore of *Bacillus anthracis* and *Bacillus subtilis*.** J Microbiol Methods 58, 23–30. Costa T, Isidro AL, Moran CP, Jr, Henriques AO. (2006). **Interaction between coat morphogenetic proteins SafA and SpoVID.** J. Bacteriol. 188:7731–7741
- Wang D-B, Yang R, Zhang Z-P, Bi L-J, You X-Y, Wei H-P, et al. (2009) **Detection of *B. anthracis* Spores and Vegetative Cells with the Same Monoclonal Antibodies.** PLoS ONE 4(11): e7810.
- Wang KH, et al. (2009). **The coat morphogenetic protein SpoVID is necessary for spore encasement in *Bacillus subtilis*.** Mol. Microbiol. 74:634–649
- Wang KH, et al. (2009). **The coat morphogenetic protein SpoVID is necessary for spore encasement in *Bacillus subtilis*.** Mol. Microbiol. 74:634–649
- Yousten A.A., Davidson E.A. (1982) **Ultrastructural analysis of spores and parasporal crystals formed in *Bacillus sphaericus*.** Appl. Environ. Microbiol. 44, 1449–1455
- Zheng LB, Donovan WP, Fitz-James PC, Losick R. (1988). **Gene encoding a morphogenic protein required in the assembly of the outer coat of the *Bacillus subtilis* endospore.** Genes Dev. 2:1047–1054
- Zilhao R, et al. (2005). **Assembly and function of a spore coat-associated transglutaminase of *Bacillus subtilis*.** J. Bacteriol. 187:7753–7764

II. Capítulo 1. Ultrastructural analysis of spores from diverse *Bacillales* species isolated from Brazilian soil

I. Introdução

O capítulo a seguir é referente ao artigo publicado na revista *Environmental Microbiology Reports* (EMIR), na data 06 de Novembro de 2018. (doi:10.1111/1758-2229.12713).

Partes das análises descritas abaixo foram realizadas no Departamento de Microbiologia e Imunologia da Universidade Loyola (Chicago, EUA), em colaboração com o prof. Adam Driks (www.stitch.luc.edu/lumen/deptwebs/microbio/adriks.php).

Ultrastructural analysis of spores from diverse *Bacillales* species isolated from Brazilian soil

Spore ultrastructure of diverse *Bacillales*

Danilo de Andrade Cavalcante¹; Marlene Teixeira De-Souza^{1*}; Juliana Capela de Orem¹;
Maria Inês André de Magalhães¹; Paulo Henrique Martins¹; Tyler J Boone^{2,3}, José A.
Castillo⁴ and Adam Driks²

¹University of Brasilia
Department of Cell Biology
Brasilia, DF, Brazil

²Loyola University Chicago
Stritch School of Medicine, Department of Microbiology and Immunology
IL, USA

⁴Yachay Tech University
School of Biological Sciences and Engineering
Urucuquí, Ecuador

***Corresponding author** Address: Universidade de Brasília; IB/Departamento de Biologia
Celular; Campus Universitário Darcy Ribeiro; 70.910-900 - Brasília - DF Brazil. Telephone:
+55 61 3107-3047. e-mail: marlts@unb.br

Abstract

Many species in the order *Bacillales* form a specialized cell type called a spore that is resistant to a range of environmental stresses. Transmission electron microscopy (TEM) reveals that the spore is comprised of a series of concentric shells, surrounding an interior compartment harbouring the spore DNA. The outermost of these shells varies considerably in morphology among species, likely reflecting adaptations to the highly diverse niches in which

³ Present address: Innovotech, Inc., Edmonton, Alberta, Canada.

spores are found. To better characterize the variation in spore ultrastructure among diverse species, we used TEM to analyse spores from a collection of 23 aerobic spore-forming bacteria from the *Solo do Distrito Federal* (SDF strains), spanning the genera *Bacillus*, *Lysinibacillus*, *Paenibacillus*, and *Brevibacillus*, isolated from soil from central Brazil. We found that the structures of these spores varied widely, as expected. Interestingly, even though these isolates are novel strains of each species, they were structurally very similar to the known examples of each species in the literature. Because in most cases, the species we analysed are poorly characterized, our data provide important evidence regarding which structural features are likely to be constant within a taxon and which are likely to vary.

1. Introduction

Electron microscopy is widely used to characterize bacterial spore ultrastructure. Thin-section and freeze-fracture transmission electron microscopy studies performed in the late 1960s and early 1970s revealed structural features and, in a few cases, surface appendages, on spores produced by diverse species in the genera *Bacillus* and *Clostridium* (Warth *et al.*, 1963; Roth & Williams, 1963; Gerhardt & Ribi, 1964; Hachisuka *et al.*, 1966; Yolton *et al.*, 1968; Hoeniger and Headley, 1969; Walker *et al.*, 1976). A number of species within these genera have been characterized, and the model species *Bacillus subtilis* and *Bacillus anthracis* have been studied in some depth (Holt and Leadbeater, 1969; Santo and Doi, 1974; Aronson and Fitz-James, 1976; Driks, 1999; Driks, 2009; Mckenney *et al.*, 2013; Bozue *et al.*, 2015; Stewart, 2015; Driks and Eichenberger 2016). Nonetheless, the spore formation remains incompletely understood in these species, and almost entirely unstudied in the other spore forming bacteria within these genera and the order *Bacillales*, which encompasses several families with spore-forming species (Galperin, 2013; Driks and Eichenberger 2016).

Bacterial endospores share a common architecture, consisting of layers that act as protective barriers (Knaysi and Hillier, 1949; Pandey and Aronson 1979; Driks, 1999; Driks, 2004; Priest *et al.*, 2004; Ghosh *et al.*, 2008; McKenney and Eichenberger 2012; McKenney *et al.*, 2013). A series of concentric shells surround the core (the inner most compartment, housing the spore chromosome): an inner membrane, a thin peptidoglycan layer called the germ cell wall, a thick peptidoglycan layer (the cortex) and additional outer layers that vary in number and structure among species (Driks and Eichenberger, 2016). At a minimum, these outer layers include those of the coat, a protein shell that provides protection to the spore and participates in germination, the process of breaking dormancy and returning to active metabolism (Aronson and Fitz-James, 1976; Setlow, 1995; Driks, 1999; Meador-Parton and Popham 2000; Henriques and Moran, 2007; Driks, 2007, McKenney *et al.*, 2013; Driks and Eichenberger, 2016). For many species, including *B. subtilis*, the coat is the outer-most spore layer. In other species, however, including *B. anthracis* and *B. megaterium*, there are two additional layers, an interspace and, surrounding that, an exosporium (Beaman *et al.*, 1972; Waller *et al.* 2004; Driks, 2007; Traag *et al.*, 2010; McKenney *et al.*, 2013; Bozue *et al.*, 2015; Stewart, 2015). The interspace has a variable width, such that the exosporium does not follow the contours of the coat. Soon after, the spore begins forming inside the rod-shaped cell (now called the “mother cell”). After a period of time (about 8-10 hours for these two species), the mother cell lyses, releasing the spore into the environment.

In general, there is significant variability in spore outer layer structure across species, suggesting that these outer layers are assembled in a range of ways that can vary significantly from the model organisms *B. subtilis* and *B. anthracis* (Driks and Eichenberger 2016). However, among closely related species examined so far, there are significant similarities, as there are among many close relatives of *B. subtilis* (which all lack an interspace and exosporium, and have similar coat structures) and among members of the so-called *B. cereus*

group (which includes *B. anthracis*), which possess structurally related exosporia. These conserved structural features likely identify functionally important components of the spore that provide adaptive value to members of each group. A better understanding of which structural features are conserved within a given taxon, and which features vary, could provide critical insights into the evolutionary forces driving structural diversification among bacterial spores.

The potential utility of spore-forming strains as sources of novel bioproducts and gaining insight into the diversity of spore formers in the soil, led us to isolate and identify strains from Brazilian soil that we designated SDF (*Solo do Distrito Federal*) strains. We previously isolated 312 SDF strains by heat-shocking soil samples collected at random areas of the Federal District, Midwest region of Brazil. These environmental strains, designated SDF0001-SDF0312, are deposited at the *Coleção de Bactérias aeróbias formadoras de endósporos* (CBafes, or AEFB Collection - AEFBC). The CBafes is hosted at the University of Brasilia and is being analysed for taxonomic classification. CBafes' strains are preserved as dry spores in filter paper, stored at room temperature.

In this study, we show the results of analyses of spores of 22 selected SDF strains by transmission electron microscopy (TEM). We were interested in analysing strains related to well-studied species, as well as strains from regions of the phylogenetic tree where few species have been imaged by TEM. Images of spores of these species could reveal novel structural features and give insight into the relationship between phylogenetic relatedness and spore structural similarity. Specifically, we are interested in better understanding the degree to which spores from closely related species share structural features.

2. Results and Discussion

In the present work, we used TEM to analyse spores from 22 SDF strains. The species were identified by means of partial 16S rRNA gene sequencing and significant identity to sequences in the database (GenBank). This taxonomic identification is preliminary since, in few cases, we found alternative possible species identities (Table I). Nonetheless, our assignments are useful because they clearly identify the genera and restrict the identity of SDF strains to one or two possible species in the *Bacillales*. Using the 16S rRNA gene sequences, we reconstructed the phylogeny of the SDF strains. The inferred tree (Figure 1) shows the relationship among these strains, which is consistent with the known organization of *Bacillales*. We note that the exact location in the current phylogeny of the two families in this order present in our data set (*Bacillaceae* and *Paenibacillaceae*) is under debate (Zhang & Lu, 2015; DeMaayer *et al.*, 2018).

TABLE I

FIGURE 1

We first used TEM to analyse spores from SDF strains that, based on partial 16S rDNA consensus sequences, are close relatives of *B. subtilis*. Figure 2 shows TEM data of *B. pumilus*, *B. safensis*, and *B. simplex*. As expected, these spores lack the interspace and exosporium, and clearly show inner and outer coat layers, a defining characteristic of the *B. subtilis* spore (Warth *et al.*, 1963; Driks, 1999; Driks and Eicheberger, 2016). *B. subtilis* possesses a third coat layer, the crust, that is only detected using Ruthenium red staining (Waller *et al.*, 2004; McKenney *et al.*, 2010). Because we did not employ this method, we do not know whether these species possess this layer.

FIGURE 2

We next analysed two strains, SDF0010 and SDF0012, which we classified as *B. clausii* based on their 16S rDNA sequences. Spores of both strains lack the interspace and exosporium, and possess a multi-layered coat (Figure 3). The outer coat is thin in comparison to the *B. subtilis* outer coat, and does not form a contiguous layer, appearing instead to possess breaks. These spores lack the long spike-like structures reported previously for *B. clausii* spores (Traag and Driks *et al.* 2010; Driks and Eichenberger, 2016). This could be due to morphological variation within the species.

FIGURE 3

TEM images found on the literature are not sufficient to argue that this dotted outer coat (Figure 3) is actually a species-specific feature, as they are not observed, or at least not frequently observed in TEM images of *B. clausii* spores (Driks and Eichenberger, 2016). *Bacillus amyloliquefaciens* strains, SDF00141 and SDF0151 produced spores possessing readily distinguished inner and outer coat layers and lacked an interspace and exosporium (Figure 4), as previously reported for this species and which is also expected for a close relative of *B. subtilis* (Traag and Driks *et al.* 2010; Driks and Eichenberger, 2016). Our data also showed a previously observed distinctive feature of this species; the outer coat is consistently and significantly thicker at the poles than along the rest of the spore. We do not know the basis for this difference between this species and *B. subtilis*. However, we speculate is that coat assembly is more abundant in this species at early and intermediate times in coat assembly, when these regions of the coat are deposited (Wang *et al.*, 2009; McKenney *et al.*, 2013). Possibly, the timing of coat protein gene expression varies from that in *B. subtilis* such that expression is higher at these early times.

FIGURE 4

SDF0020 was identified by partial 16S rDNA consensus sequence as *Brevibacillus agri*. As previously documented, spores of *Br. laterosporus* possess a distinctive layered structure that extends from the coat, called the canoe-shaped body (csb) (Hannay, 1957; Ruiu, 2013; Driks and Eichenberger, 2016; Marche *et al.*, 2017). We found that *Br. agri* presents the same structure, suggesting that the canoe-shaped body might be a common feature of the genus (Figure 5). This structure does not usually encircle the entire spore, but rather is attached only along a small portion of the coat surface area. Interestingly, the attachment surface is larger in other images in the literature, raising the possibility that this feature varies with the strain or the sporulation conditions. In contrast to previous observations, however, we also identified a structure consistent with an exosporium that was not previously reported in the literature. We suggest that it might be a species-specific feature of *Br. agri*.

FIGURE 5

To document the progression of events during formation of the canoe-shaped body, we harvested spores at various times after the initiation of sporulation (t_0) but before completion and analysed them by TEM (Figure 6). Here we show selected images that might represent the steps of assembly of the distinctive *Brevibacillus* structure, based on the time when the spores were harvested. We infer that this structure is deposited during coat formation.

FIGURE 6

We found that SDF strains of *Paenibacillus alvei* (SDF0008, SDF0028, and SDF0080) possess a multilayered coat and a lightly staining exosporium apparently free of the hair-like

projections or other appendages (Figure 7). As expected, these spores also possess an interspace. *P. alvei* spores possess a thick, dark coat, with distinct inner and outer layers. The outer coat layer is lighter than the inner coat, in contrast to the coat in *B. subtilis* and its close relatives. Most spores had multiple folds in the coat that are sharper than the coats of most other species (Lida, 2007; SooKim, 2016; Driks and Eichenberger, 2016). A notable feature of these spores is their distinctive exosporium. The exosporium has a clear outer boundary but its thickness varies significantly around its circumference. The interspace possesses amorphous material that does not obviously connect the exosporium to the coat.

FIGURE 7

We identified three SDF strains as members of the genus *Lysinibacillus*: SDF0005, *Lysinibacillus fusiformis*; SDF0037, *Lysinibacillus sphaericus*; and SDF0063, *Lysinibacillus xylanilyticus*. Spores of strains SDF0005 and SDF0037 possess a lightly stained, irregularly folded coat (Figure 8). It is difficult to discern distinct layers within the coats in many cases in both SDF0005 and SDF0037 strains. Intriguingly the exosporia in these spores appear to have two layers. The inner layer surrounds the spore and has an interspace of varying width, as is seen in exosporia of other species. The outer layer surrounds this inner layer, and there is also a variable width between it and the inner layer. The only distinguishing difference observed between these two *Ly. sphaericus* strains and what is reported on the literature is the presence of a parasporal crystal in the interspace of *Ly. sphaericus* (Priest *et al.* 2002; Berry, 2012) which, in turn, was not observed for either SDF0005 or SDF0037. However, it is known that crystals are not present in all *Ly. sphaericus* strains (Cokmus, and Yousten, 1993; Berry, 2012). SDF0063, *Ly. xylanilyticus*, possesses a more structurally complex coat the other two members of this genus. The *Ly. xylanilyticus* exosporium is also different, in that apparently it has only a single layer (Figure 8). It is possible that more layers would be observable if the

spore was released from the surrounding mother cell. However, we were unable to obtain free spores in our experiments.

FIGURE 8

To gain insight into the formation of the *Ly. sphaericus* spore (Kalfon *et al.*, 1986), we used TEM to analyse sporulating cells at several time points during sporulation. Consistent with previous work (Kalfon *et. al.*, 1984), we found that the forespore-pole of the cell is swollen, and that forespore septation and engulfment, and coat formation, occur at roughly the times as in other species (Figure 9). We did not detect discreet stages within coat assembly. We visualized a single exosporium layer at hour 6 (t_6), which is, at least, several hours prior to the time we would expect the release of the spore from the mother cell.

FIGURE 9

We identified three *Bacillus megaterium* strains in the SDF collection (SDF0047, SDF0049, and SDF0051). As expected for this species (Figure 10), all the spores were larger than typical *Bacillus* spores, being about 2 μm along their long axis and possessing a lightly stained coat. Spores of these strains all possessed the distinctive morphology previously reported (Rode *et al.*, 1962; Manetsberger *et al.*, 2010; Traag *et al.*, 2010; Manetsberger *et al.*, 2015; Driks and Eichenberger, 2016); a walnut-like exosporium with a small number of folds (often but not always at the poles). One or two openings are often seen in the exosporium.

FIGURE 10

We also identified a strain of *Bacillus aryabbathay* (Figure 10), a very close relative of *B. megaterium* (Shivaji *et al.*, 2009; Ramos-Silva *et al.*, 2015). SDF0096, is quite different from the usual morphology described to *B. megaterium*. Spores of this strain lack the exosporium and have a distinct, more darkly staining, coat with numerous folds. Like *B. megaterium*, however, SDF0096 spores are larger than most other species, being about 2 μm along the long axis. These differences are readily detected and may point to a functionally relevant variation within strains of this species. While this level of variation has not been observed within *B. megaterium*, we note that at least one *B. megaterium* strain lacks an exosporium (Beaman *et al.*, 1972).

As we see in the results presented above, in some species, TEM reveals structurally novel coat layers. These include, for example, the non-contiguous outermost layer that encircles the *B. clausii* coat (Figure 3), the canoe-shaped body that projects from the coat on *Brevibacillus* (Figure 4 and 5) or the thick caps of coat on *B. amyloliquefaciens* (Figure 4). We speculate that at least some of these structural differences might be species-specific. This could be better validated with images from more strains and species.

Taken together, these and previous findings raise an important question: what are the benefits of such significant diversity in coat and outer layers structure? It is reasonable to propose that much of this diversity is driven by adaptation to varying environments, and their niche-specific stresses. However, any model of this type needs to account for observations made by us and in previous studies that a large number of highly diverse spore-forming species can be found in many different soil samples (Fritze, 2004; Mandic-Mulec *et al.*, 2015; Driks and Eichenberger, 2016). The roles of the diverse challenges in each niche, and in sub-compartments in these niches, need to be much better understood to dissect the manner in which environmental differences influence phenotypic variation.

3. Experimental procedures

Available as Supplementary Information (Supplementary Methods).

4. Acknowledgements

This work was financially supported by the Brazilian program Ciências sem fronteiras of National Council for Scientific and Technological Development (CNPq). We are grateful for the expert technical assistance of Mark Khemmani.

4.1 Conflicts of interest

The authors declare that there are no conflicts of interest.

5. References

Altschul, S.F., Gish, W., Miller, W., Myers, E.W., and Lipman, D.J. (1990) Basic local alignment search tool. *J Mol Biol* 215:403-410.

Aronson A.I., Fitz-James P.C. (1971) Reconstitution of bacterial spore coat layers *in vitro*. *J Bacteriol* 108:571-578.

Aronson A.I., Fitz-James P. C. (1976) Structure and morphogenesis of the bacterial spore coat. *J Bacteriol Rev* 40:360-402.

Bagyan I, Setlow P. (2002) Localization of the cortex lytic enzyme CwlJ in spores of *Bacillus subtilis*. *J Bacteriol* 184:1219-1224.

Barbosa T. M., Serra C.R., La Ragione R.M., Woodward M.J., and Henriques A.O. (2005) Screening for *Bacillus* Isolates in the Broiler Gastrointestinal Tract. *Appl Environ Microbiol* 71(2):968-978.

- Bauer T, Little S, Stöver AG, Driks A. (1999) Functional regions of the *Bacillus subtilis* spore coat morphogenetic protein CotE. *J Bacteriol* 181(22):7043-51.
- Beaman T.C., Pankratz H.S., and Gerhardt P. (1972) Ultrastructure of the Exosporium and Underlying Inclusions in Spores of *Bacillus megaterium* strains. *J Bacteriol* 1198-1209.
- Berry C. (2012) The bacterium, *Lysinibacillus sphaericus*, as an insect pathogen. *J Invertebr Pathol* 109:1-10.
- Bozue J.A., Welkos S., Cote C.K. (2015) The *Bacillus anthracis* exosporium: what's the big "hairy" deal? *Microbiol Spectr* 3(5):0021-2015.
- Chada V.G., Sanstad E.A., Wang R., Driks A. (2003) Morphogenesis of *Bacillus* spore surfaces. *J Bacteriol* 185:6255-6261.
- Chen G., Driks A., Tawfiq K., Mallozzi M., Patil S. (2010) *Bacillus anthracis* and *Bacillus subtilis* spore surface properties and transport. *Colloids Surf B Biointerfaces* 76:512-518.
- Chen X., Mahadevan L., Driks A. and Sahin O. (2014) *Bacillus* spores as building blocks for stimuli-responsive materials and nanogenerators. *Nat Nanotechnol* 9:137-141.
- Cokmus, C., Yousten, A. A. (1993) Bacteriocin production by *Bacillus sphaericus*. *J. Invertebr Pathol* 61:323-325.
- DeMaayer P., Aliyu H. Cowan D.A. (2018) Reorganising the order Bacillales through phylogenomics. *Syst. Appl. Microbiol.* In press.
- Donovan W., Zheng L.B., Sandman K., Losick R. (1987) Genes encoding spore coat polypeptides from *Bacillus subtilis*. *J Mol Biol* 196:1-10.
- Driks A. (1999) *Bacillus subtilis* spore coat. *Microbiol Mol Biol Rev* 63:1-20.
- Driks A. (2007) Surface appendages of bacterial spores. *Mol Microbiol* 63:623-625.
- Driks A. (2009) The *Bacillus anthracis* spore. *Mol Aspects Med* 30:368-373.

- Eichenberger P., Fujita M., Jensen S.T., Conlon E.M., Rudner D.Z., Wang S.T., Ferguson C., Haga K., Sato T, Losick R. (2004) The program of gene transcription for a single differentiating cell type during sporulation in *Bacillus subtilis*. PLoS Biol 2(10):e328.
- Fritze D. (2004) Taxonomy of the Genus *Bacillus* and Related Genera: The Aerobic Endospore-Forming Bacteria. Phytopathology 94:1245-1248.
- Galperin M.Y., Mekhedov S.L., Puigbo P., Smirnov S., Wolf Y.I., Rigden D.J. (2012) Genomic determinants of sporulation in *Bacilli* and *Clostridia*: towards the minimal set of sporulation-specific genes. Environ Microbiol 14:2870-2890.
- Galperin M.Y. (2013) Genome diversity of spore-forming *Firmicutes*. Microbiol Spectr 1(2): 0015-2012.
- Ghosh S., Setlow B., Wahome P.G., Cowan A.E., Plomp M., Malkin A.J., Setlow P. (2008) Characterization of spores of *Bacillus subtilis* that lack most coat layers. J Bacteriol 190:6741-6748.
- Giorno R., Bozue J., Cote C., Wenzel T., Moody K.S., Mallozzi M., Ryan M., Wang R., Zielke R., Maddock J.R., Friedlander A., Welkos S., Driks A. (2007) Morphogenesis of the *Bacillus anthracis* spore. J Bacteriol 189:691-705.
- Hannay C.L. (1957) The parasporal body of *Bacillus laterosporus* Laubach. J Biophys Biochem Cytol 253:1001-10.
- Henriques A.O., Moran C.P. Jr. (2007) Structure, assembly, and function of the spore surface layers. Annu Rev Microbiol 61:555-588.
- Holt S.C., Leadbeter E.R. (1969) Comparative ultrastructure of selected aerobic spore-forming bacteria: a freezeetching study. Bacteriol Rev 33:346-378.
- Kalfon A., Charles J.F., Bourgoign C. and de Barjac H. (1984) Sporulation of *Bacillus sphaericus* 2297: an Electron Microscope Study of Crystal-like Inclusion Biogenesis and Toxicity to Mosquito Larvae. J Gen Microbiol 130:893-900.

- Lida K., Amako K., Takade A., Ueda Y., Yoshida S. (2007) Electron Microscopic Examination of the Dormant Spore and the Sporulation of *Paenibacillus motobuensis* Strain MC10. *Microbiol Immunol* 51:643-648.
- Liu J.S., Losick R. (2004) The program of gene transcription for a single differentiating cell type during sporulation in *Bacillus subtilis*. *PLoS Biol* 2:328.
- Manetsberger J., Hall E.h and Christie G. (2015) Plasmid-encoded genes influence exosporium assembly and morphology in *Bacillus megaterium* QM B1551 spores. *FEMS Microbiol Letters* 362.
- Manetsberger J., Manton J. D., Erdelyi M., Lin H., Rees D., Christie G. and Rees E.J. (2015) Ellipsoid Localization Microscopy Infers the Size and Order of Protein Layers in *Bacillus* Spore Coats *Biophysical J* 109:2058-2066.
- Marche M. G., Mura M.E., Falchi G., Ruiu L. (2017) Spore surface proteins of *Brevibacillus laterosporus* are involved in insect pathogenesis. *Sci Rep* 7:43805.
- McKenney P.T., Driks A., Eskandarian H.A., Grabowski P., Guberman J., Wang K.H., Gitai Z., Eichenberger P. (2010). A distance-weighted interaction map reveals a previously uncharacterized layer of the *Bacillus subtilis* spore coat. *Curr Biol* 20:934-938.
- McKenney P.T., Eichenberger P. (2012) Dynamics of spore coat morphogenesis in *Bacillus subtilis*. *Mol Microbiol* 83:245-260.
- McKenney P.T., Driks A., Eichenberger P. (2013) The *Bacillus subtilis* endospore: assembly and functions of the multilayered coat. *Nat Rev Microbiol* 11:33-44.
- Milhaud P. and Balassa G. (1973) Biochemical genetics of bacterial sporulation. IV. Sequential development of resistances to chemical and physical agents during sporulation of *Bacillus subtilis*. *Mol Gen Genet* 25:241-250.
- Moir A. (1981) Germination properties of a spore coat defective mutant of *Bacillus subtilis*. *J Bacteriol* 146:1106-1116.

NCBI Resource Coordinators. (2016) Database Resources of the National Center for Biotechnology Information. *Nucleic Acids Res* 44:7-19.

Nicholson W.L., Munakata N., Horneck G., Melosh H.J., Setlow P. (2000) Resistance of *Bacillus* endospores to extreme terrestrial and extraterrestrial environments. *Microbiol Mol Biol Rev* 64:548-572.

Paidhungat M., Ragkousi K., Setlow P. (2001) Genetic requirements for induction of germination of spores of *Bacillus subtilis* by Ca(2+)-dipicolinate. *J Bacteriol* 183: 4886–4893.

Piggot P.J, Coote J.G. (1976) Genetic aspects of bacterial endospore formation. *Bacteriol Rev* 40:908-962.

Ramos-Silva P., Brito P.H., Serrano M., Henriques A.O., Pereira-Leal J.B. (2015) Rethinking the Niche of Upper-Atmosphere Bacteria: Draft Genome Sequences of *Bacillus aryabhatai* C765 and *Bacillus aerophilus* C772, Isolated from Rice Fields. Ramos-Silva P, *et al.* *Genome Announc* 3:e00094-15.

Ruiu L. (2013) *Brevibacillus laterosporus*, a Pathogen of Invertebrates and a Broad-Spectrum Antimicrobial Species. *Insects* 4:476-492.

Ryu, E. (1939) On the gram-differentiation of bacteria by the simplest method. II. The caustic potash method. *Jpn J Vet Sci* 1:209-210.

Ryu, E. (1940) A simple method of differentiation between gram-positive and gram-negative organisms without staining. *Kitasato Arch Exp Med* 17:58-63.

Sahin O., Yong E.H., Driks A., Mahadevan L. (2012) Physical basis for the adaptive flexibility of *Bacillus* spore coats. *J R Soc Interface* 9:3156-3160.

Santo L.Y., Doi R.H. (1974) Ultrastructural analysis during germination and outgrowth of *Bacillus subtilis* spores. *J Bacteriol* 120:475-481.

Setlow P. (2014) Germination of spores of *Bacillus* species: what we know and do not know. *J Bacteriol* 196:1297-1305.

- Setlow P. (2014) Spore resistance properties. *Microbiol Spectr* 2:0003-2012.
- Shivaji S., Chaturvedi P., Begum Z., Pindi P.K., Manorama R., Padmanaban D.A., Shouche Y.S, Pawar S., Vaishampayan P., Dutt C.B., Datta G.N., Manchanda R.K., Rao U.R., Bhargava P.M., Narlikar J.V. (2009) *Janibacter hoylei* sp. nov., *Bacillus isronensis* sp. nov. and *Bacillus aryabhatai* sp. nov., isolated from cryotubes used for collecting air from the upper atmosphere. *Int J Syst Evol Microbiol* 59:2977-86.
- SooKim Y., Kotnala B., HoKim Y., Jeon Y. (2016) Biological characteristics of *Paenibacillus polymyxa* GBR-1 involved in root rot of stored Korean ginseng. *J Ginseng Res* 40:453-461
- Stewart G.C. (2015) The Exosporium Layer of Bacterial Spores: a Connection to the Environment and the Infected Host. *Microbiol Mol Biol Rev* 4:437-57.
- Traag B.A., Driks A., Stragier P., Bitter W., Broussard G., Hatfull G., Chu F., Adams K.N., Ramakrishnan L., Losick R. (2010) Do *mycobacteria* produce endospores? *Proc Natl Acad Sci USA* 107:878-881.
- Waller L.N., Fox N., Fox K.F., Fox A., Price R.L. (2004) Ruthenium red staining for ultrastructural visualization of a glycoprotein layer surrounding the spore of *Bacillus anthracis* and *Bacillus subtilis*. *J Microbiol Methods* 58:23-30.
- Wang K.H., Isidro A.L., Domingues L., Eskandarian H.A., McKenney P.T., Drew K., Grabowski P., Chua M.H., Barry S.N., Guan M., Bonneau R., Henriques A.O., Eichenberger P.(2009) The coat morphogenetic protein SpoVID is necessary for spore encasement in *Bacillus subtilis*. *Mol Microbiol* 74:634-49.
- Warth A.D., Ohye D.F., Murrell W.G. (1963) The composition and structure of bacterial spores. *J Cell Biol* 16:579-592.
- Zhang W, Lu Z. (2015) Phylogenomic evaluation of members above the species level within the phylum Firmicutes based on conserved proteins. *Environ Microbiol Rep.* 7(2):273–81.

Table I. SDF strains selected for this work

Strain	Species (ID%)*	Accession number**
SDF0001	<i>Bacillus pumilus</i> (99%)	MH356287
SDF0002	<i>Bacillus safensis</i> (99%)	MH356288
SDF0005	<i>Lysinibacillus fusiformis</i> (98%)	MH356291
SDF0008	<i>Paenibacillus alvei</i> (99%)	MH356294
SDF0009	<i>Bacillus simplex</i> (99%)	MH356295
SDF0010	<i>Bacillus clausii</i> (99%)	MH356296
SDF0011	<i>Bacillus pumilus</i> (100%)	MH356297
SDF0012	<i>Bacillus clausii</i> (99%)	MH569343
SDF0013	<i>Bacillus safensis</i> (99%) ^a	MH356298
SDF0018	<i>Bacillus clausii</i> (100%)	MH356303
SDF0020	<i>Brevibacillus agri</i> (100%)	MH356305
SDF0027	<i>Bacillus safensis</i> (100%)	MH356308
SDF0028	<i>Paenibacillus alvei</i> (100%)	MH356309
SDF0037	<i>Lysinibacillus sphaericus</i> (99%)	MH356316
SDF0047	<i>Bacillus megaterium</i> (98%)	MH356320
SDF0049	<i>Bacillus megaterium</i> (99%)	MH356321
SDF0051	<i>Bacillus megaterium</i> (99%)	MH356323
SDF0063	<i>Lysinibacillus xylanilyticus</i> (99%)	MH356333
SDF0080	<i>Paenibacillus alvei</i> (99%)	MH356346
SDF0096	<i>Bacillus aryabhatay</i> (100%) ^b	MH356357
SDF0141	<i>Bacillus amyloliquefaciens</i> (99%)	MH356389
SDF0151	<i>Bacillus amyloliquefaciens</i> (99%)	MH356399

*As determined by partial 16S rDNA sequences. ** NCBI GenBank.
Alternative identity: ^a*B. pumilus* or ^b*B. megaterium*.

Figure captions

Figure 1. Maximum likelihood phylogenetic tree based on 16S rRNA gene sequences, showing relationships between the 22 strains analysed in this study.

Numbers at nodes are bootstrap values (>50 %) based on 1000 replications. Bar represents the scale of the branch lengths in nucleotide substitutions per site.

Figure 2. Thin-section TEM analysis of spores from SDF strains closely related to *B. subtilis*. SDF strain numbers, species, and 200 nm bars are indicated.

Figure 3. Thin-section TEM analysis of *B. clausii* SDF strains spores. Brackets indicate the presence of an inconsistent outer coat layer. SDF strain numbers, species, and 200 nm bars are indicated.

Figure 4. Thin-section TEM analysis of *B. amyloliquefaciens* SDF strains spores. Brackets labelled IC indicate the inner coat and brackets labelled OC indicate the thick caps of outer coat at the poles. SDF strain numbers, species, and 500 nm bars are indicated.

Figure 5. Thin-section TEM analysis of *Brevibacillus agri* SDF0020 spores. Csb indicates the distinctive structure associated with the coat described previously as the canoe shaped body. Exo indicates the exosporium. SDF strain numbers, species, and 200 nm bars are indicated.

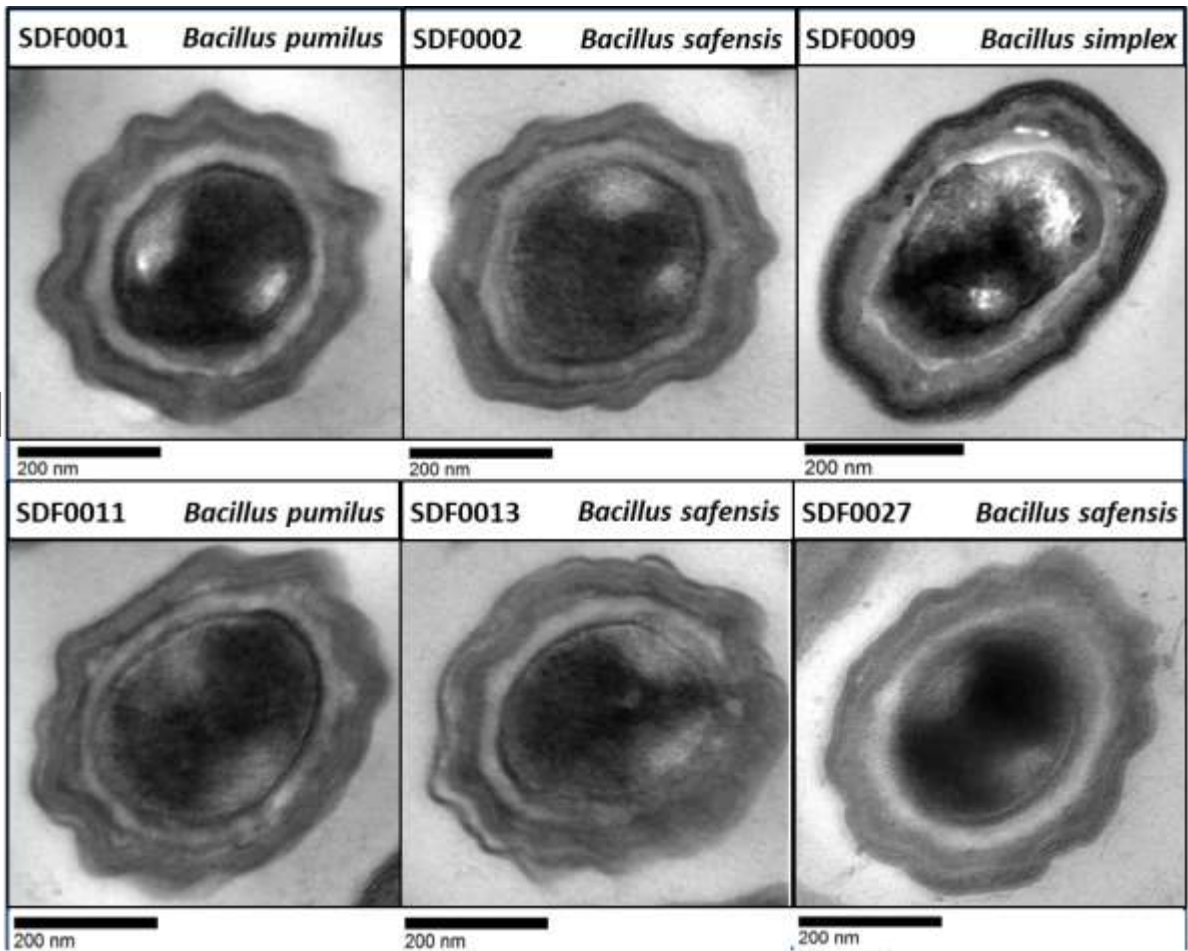
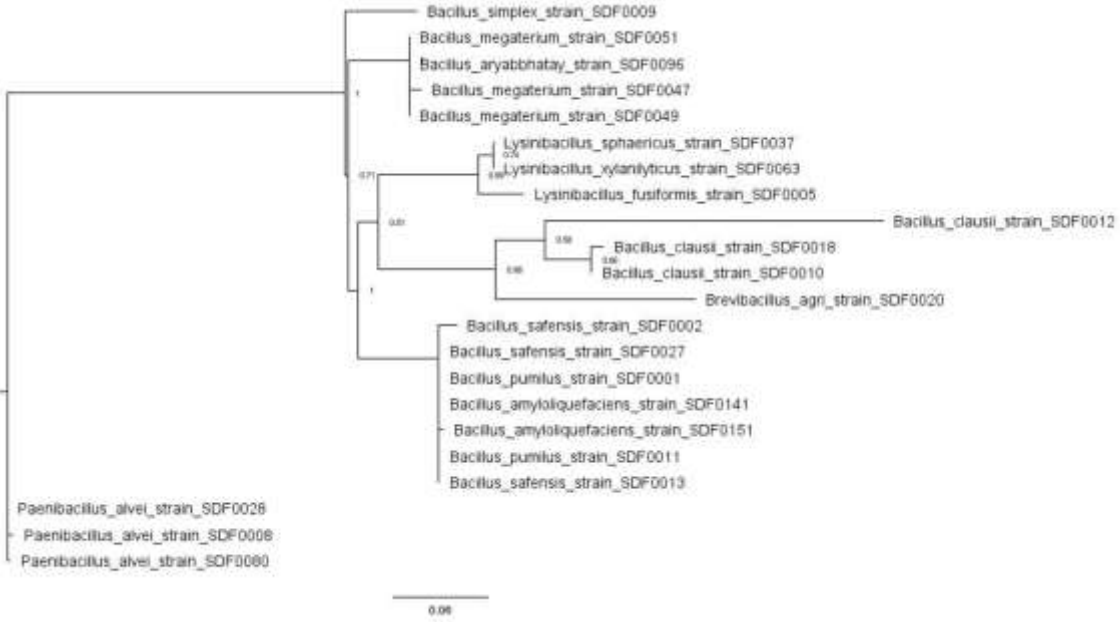
Figure 6. Thin-section TEM analysis of *Brevibacillus agri* SDF0020 spores harvested at various times during sporulation. Sporulating cells were harvested for fixation at (A) 3 hours and (B) 4 to (C) 5 hours after the start of sporulation. 200 nm and 500 nm bars are indicated.

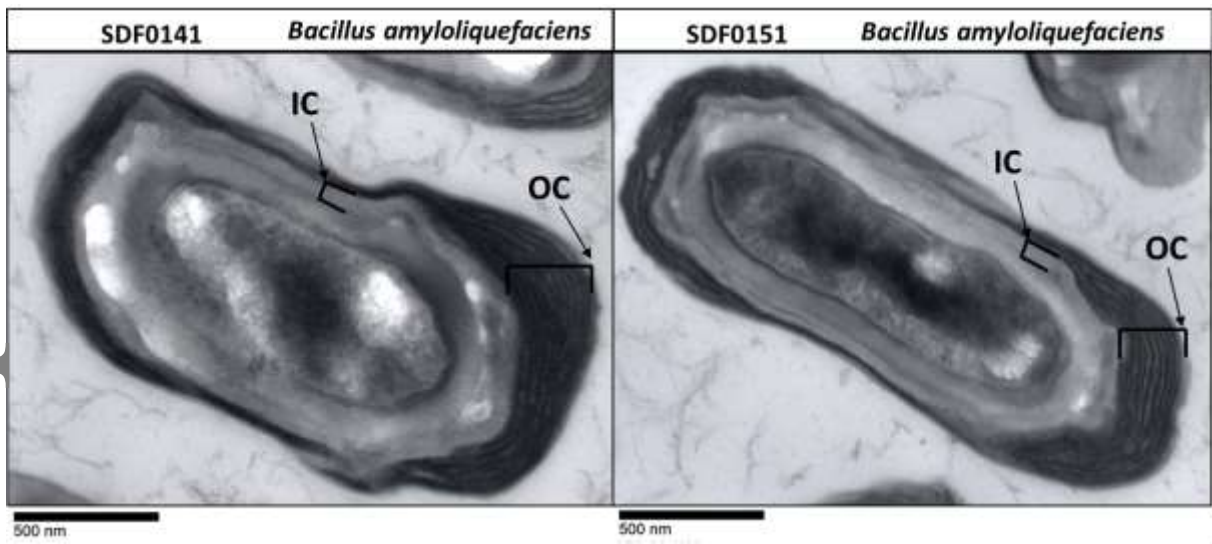
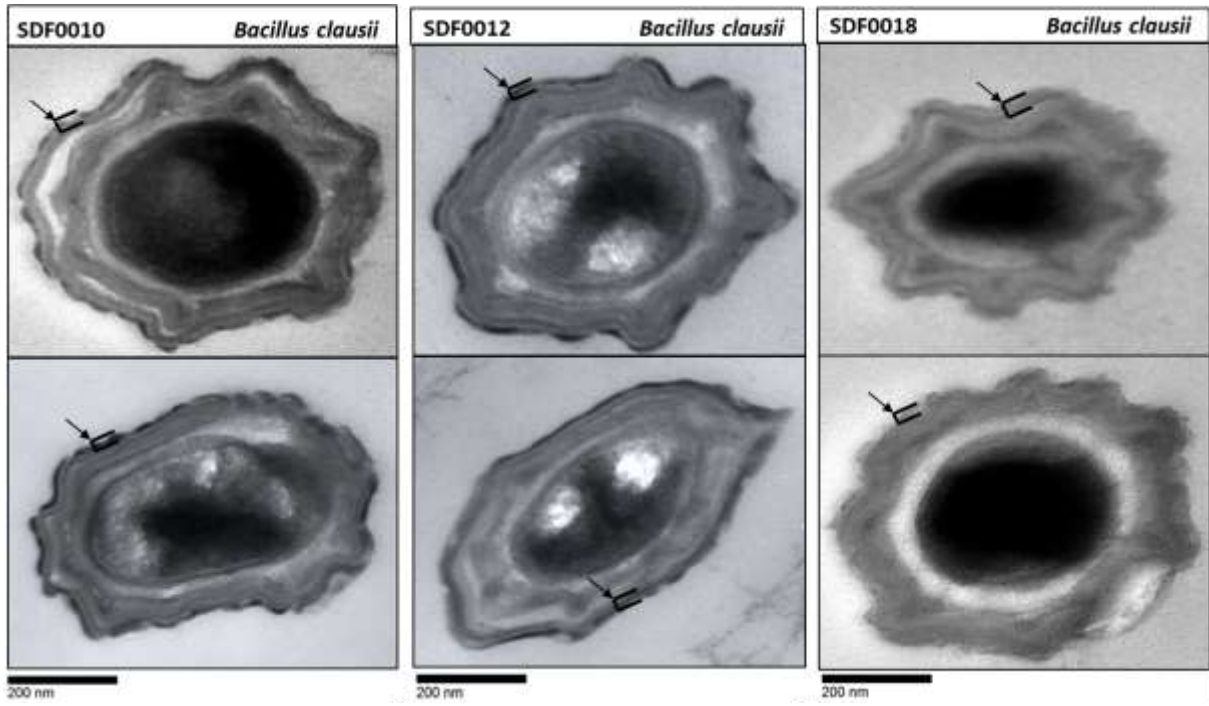
Figure 7. Thin-section TEM analysis of *P. alvei* SDF strains spores. Ct indicates the coat and Exo the exosporium. SDF strain numbers, species, 200 nm, and 500 nm bars are indicated.

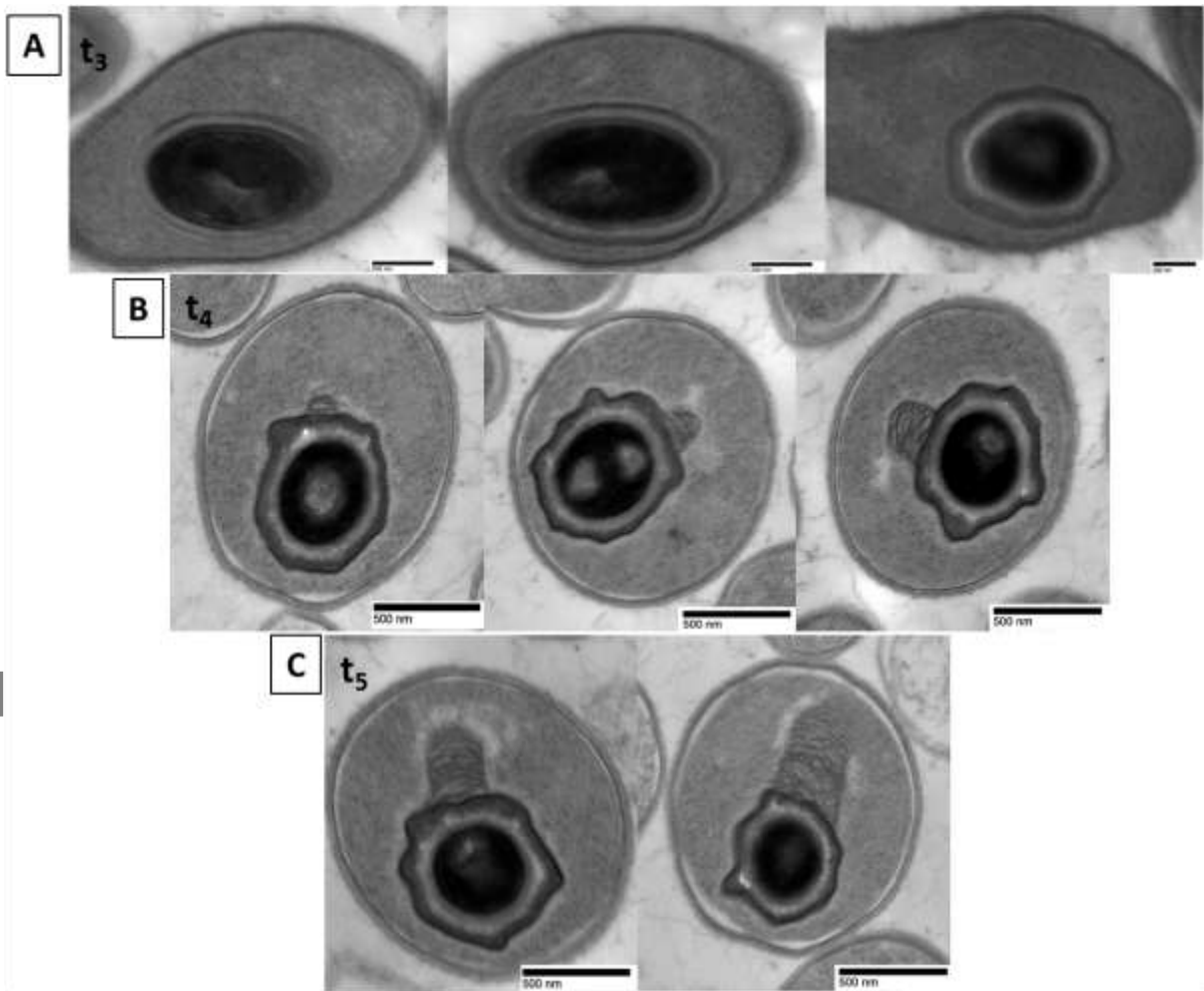
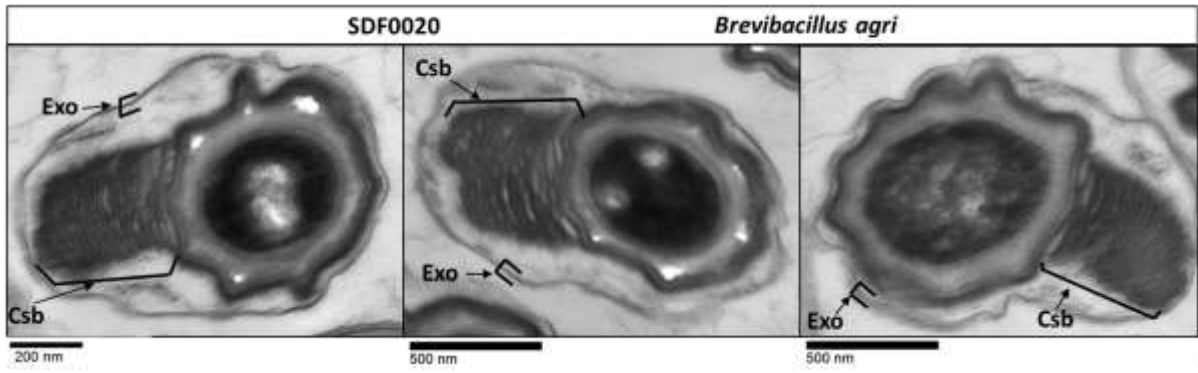
Figure 8. Thin-section TEM analysis of *Lysinibacillus* SDF strain spores. Brackets labelled In Exo indicate the inner exosporium and those labelled Out Exo (the outer exosporium). C.env indicates the cell envelope. SDF strain numbers, species and 200 nm bars are indicated.

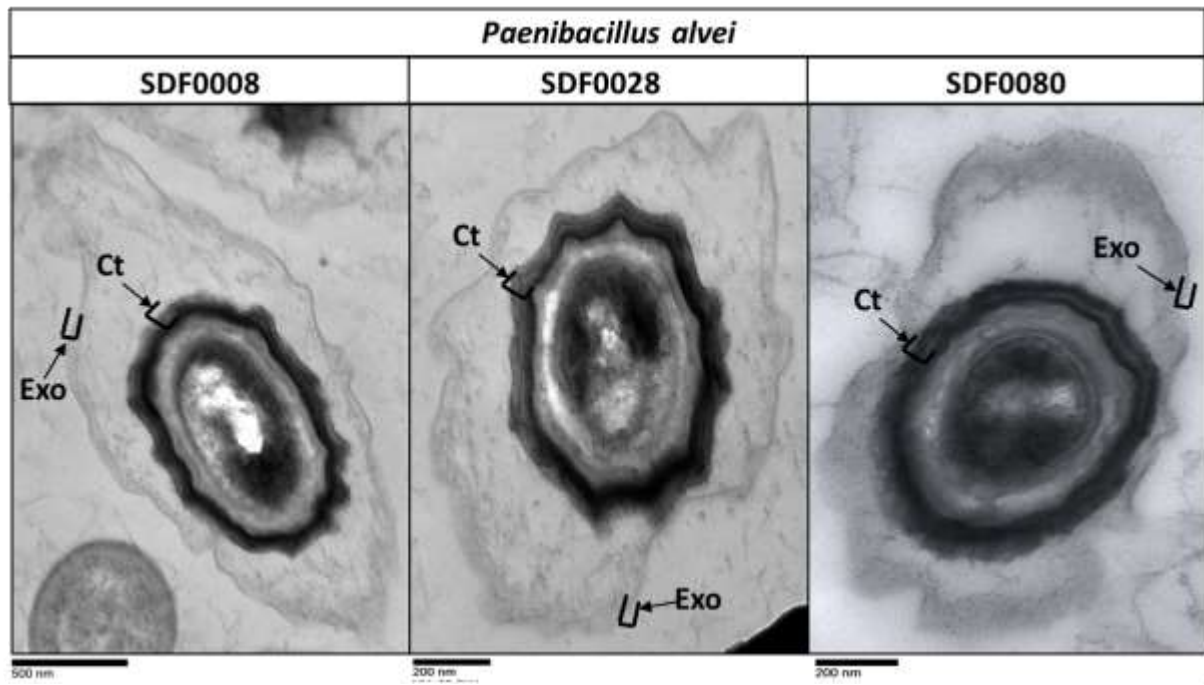
Figure 9. Thin-section TEM analysis of *Lysinibacillus sphaericus* SDF0037. Spores were harvested at the times (t_n) indicated in the upper left of each panel, after the culture entered stationary phase (or in the panel to the immediate left where no time is indicated). Arrows point to spore structures as they become detectable during development, and are labelled as follows: (A) Septum formation. (B) Engulfment. (C) Coat deposition. (D), and (E) The beginning of exosporium formation. (F) Exosporium maturation and a possible second layer being formed. The images are meant to suggest plausible steps in assembly, since they were selected to represent the most predominant morphology found at each time period. SDF strain numbers, species, 200 nm, and 500 nm bars are indicated.

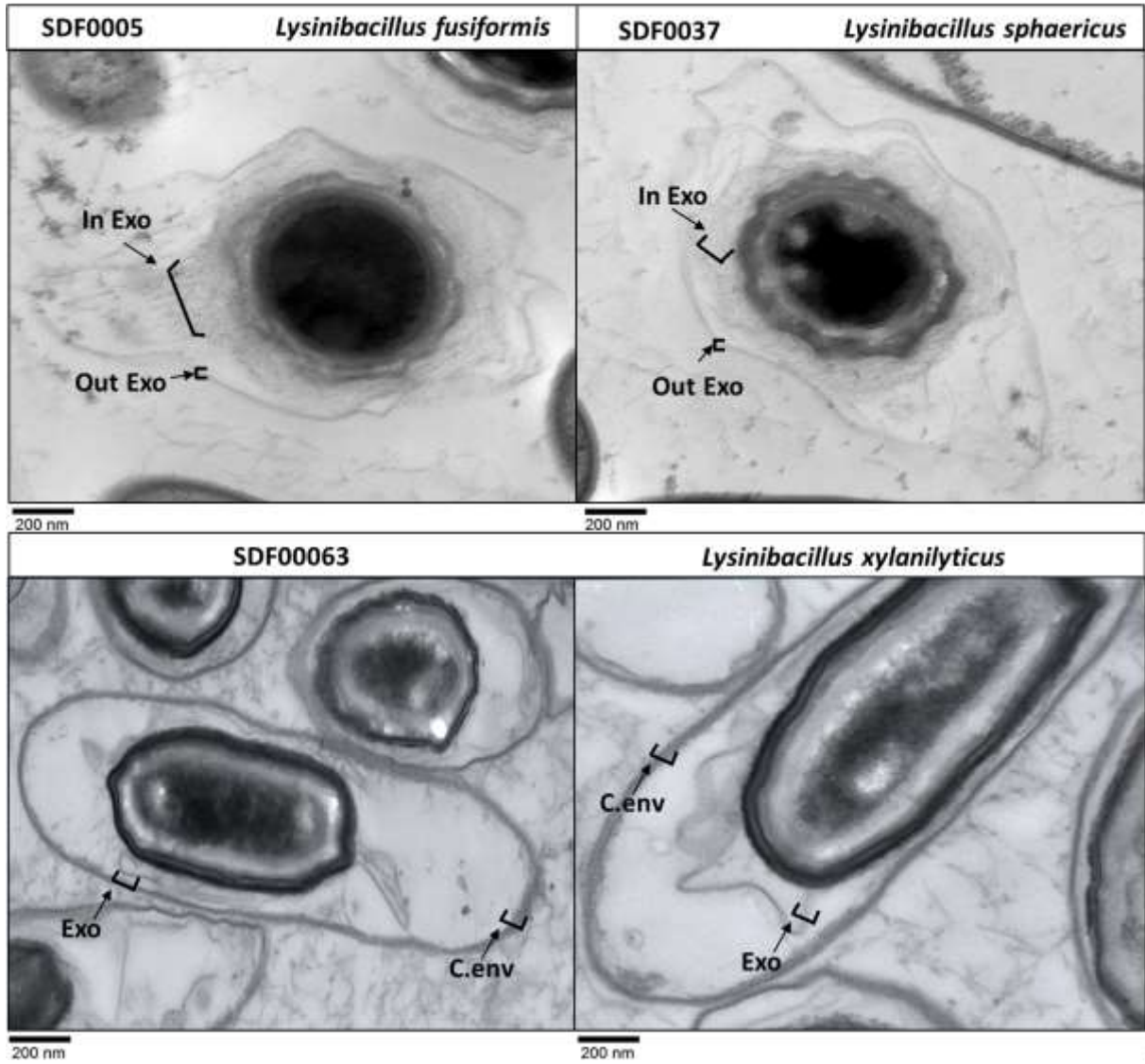
Figure 10. Thin-section TEM analysis of *B. megaterium* and *B. aryabbathay* SDF strain spores. Brackets indicate the exosporium. SDF strain numbers, species, and 500 nm bars are indicated.

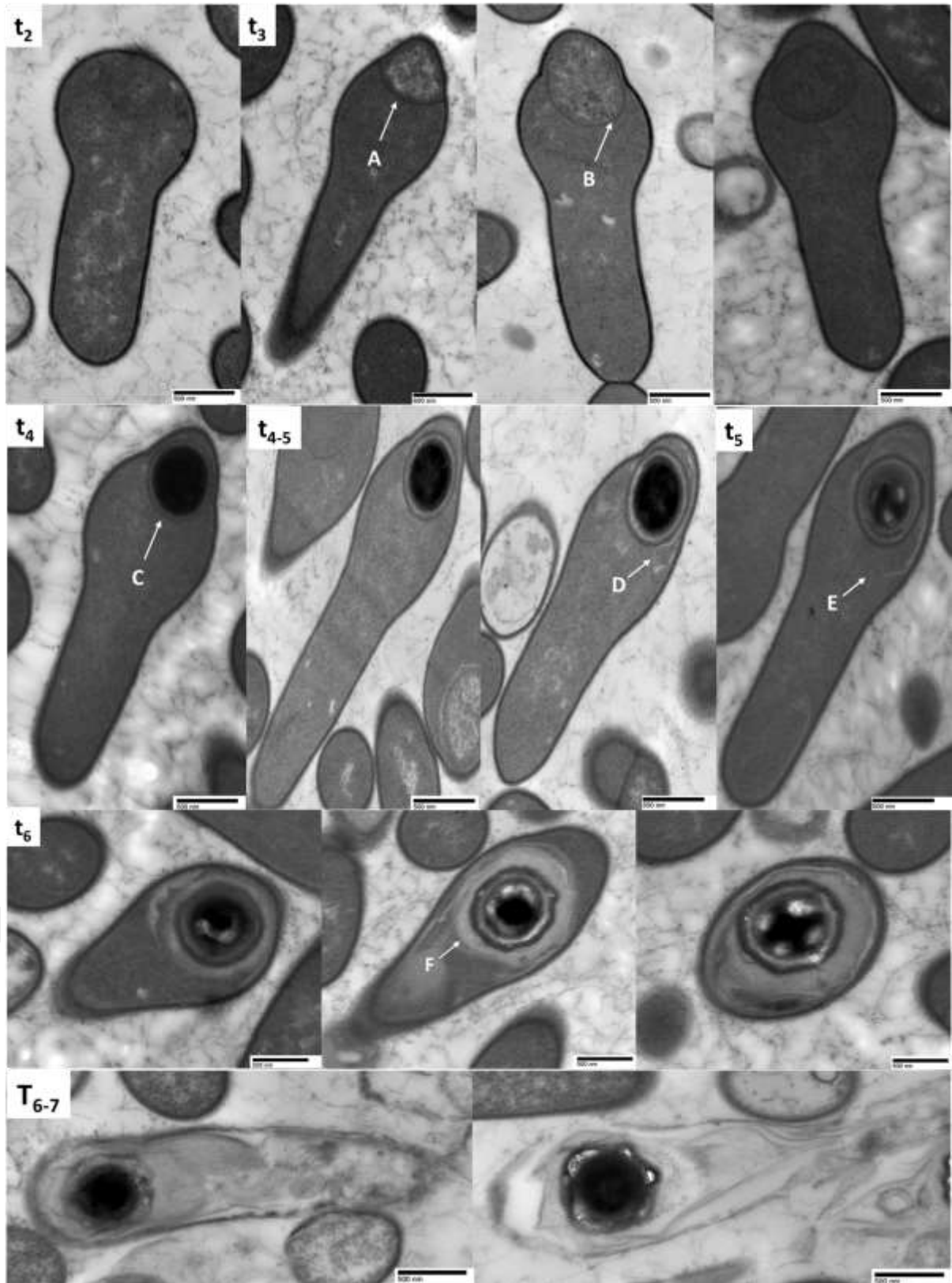












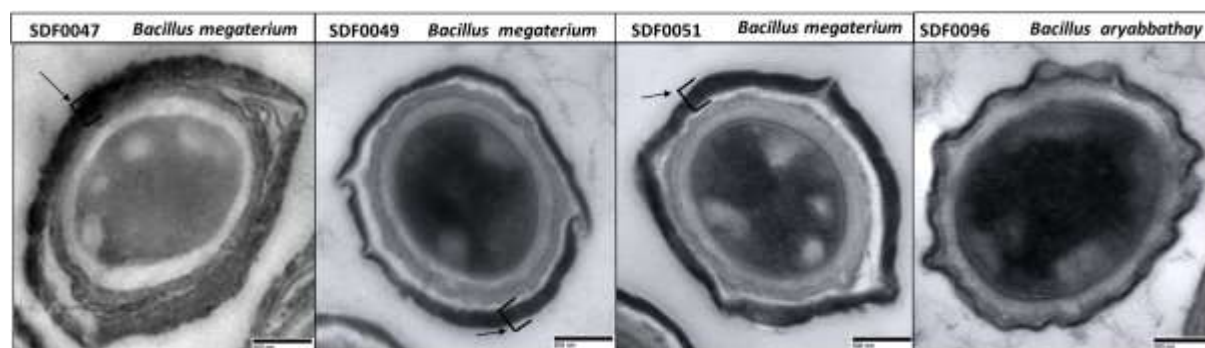


Table I. SDF strains selected for this work

Strain	Species (ID%)*	Accession number**
SDF0001	<i>Bacillus pumilus</i> (99%)	MH356287
SDF0002	<i>Bacillus safensis</i> (99%)	MH356288
SDF0005	<i>Lysinibacillus fusiformis</i> (98%)	MH356291
SDF0008	<i>Paenibacillus alvei</i> (99%)	MH356294
SDF0009	<i>Bacillus simplex</i> (99%)	MH356295
SDF0010	<i>Bacillus clausii</i> (99%)	MH356296
SDF0011	<i>Bacillus pumilus</i> (100%)	MH356297
SDF0012	<i>Bacillus clausii</i> (99%)	MH569343
SDF0013	<i>Bacillus safensis</i> (99%) ^a	MH356298
SDF0018	<i>Bacillus clausii</i> (100%)	MH356303
SDF0020	<i>Brevibacillus agri</i> (100%)	MH356305
SDF0027	<i>Bacillus safensis</i> (100%)	MH356308
SDF0028	<i>Paenibacillus alvei</i> (100%)	MH356309
SDF0037	<i>Lysinibacillus sphaericus</i> (99%)	MH356316
SDF0047	<i>Bacillus megaterium</i> (98%)	MH356320
SDF0049	<i>Bacillus megaterium</i> (99%)	MH356321

SDF0051	<i>Bacillus megaterium</i> (99%)	MH356323
SDF0063	<i>Lysinibacillus xylanilyticus</i> (99%)	MH356333
SDF0080	<i>Paenibacillus alvei</i> (99%)	MH356346
SDF0096	<i>Bacillus aryabhatay</i> (100%) ^b	MH356357
SDF0141	<i>Bacillus amyloliquefaciens</i> (99%)	MH356389
SDF0151	<i>Bacillus amyloliquefaciens</i> (99%)	MH356399

*As determined by partial 16S rDNA sequences. ** NCBI GenBank.
Alternative identity: ^a*B. pumilus* or ^b*B. megaterium*.

III. Capítulo 2. Inactivation of SpoVID protein gene in *Lysinibacillus spp.*

I. Introduction

Lysinibacillus spp. are ubiquitous Gram-positive, aerobic or facultative bacteria that, when facing starvation, forms a swollen sporangium and a spherical terminal endospore (Fekete *et al.*, 2010; Wenzler *et al.*, 2015). Organisms in this genus were previously regarded as members of the rRNA group 2 of the genus *Bacillus* (Neide, 1904), but the taxonomic status of these microorganisms was subsequently re-named as genus *Lysinibacillus* (Ahmed *et al.*, 2007) based on the distinctive peptidoglycan composition of the cell wall. Compared with *Bacillus*, *Lysinibacillus* contains lysine and aspartate in the peptidoglycan as diagnostic amino acids, in contrast to meso-diaminopimelic acid typically found in the genus *Bacillus* (Miwa *et al.*, 2009). These findings were corroborated along with further physiological analyses using standard phenotypic tests for *Bacillus* identification, that revealed the lack of carbohydrate fermentation, except N-acetylglucosamine (Russel *et al.*, 1989), and instead, the use of organic and amino acids as carbon sources (Silva *et al.*, 2014).

Lysinibacillus is commonly found in soil and aquatic environments, being also isolated from plant tissues (Melnick *et al.*, 2011), from fermented plant seed products (Parkouda *et al.*, 2010) and even from puffer fish liver specimens (Wang *et al.*, 2010). Species of this genus are rarely isolated from human specimens and often regarded as environmental contaminants when isolated in the clinical microbiology laboratory. Despite this perception, their potential to cause human disease has been documented (Wenzler *et al.*, 2015).

Certain species from the genus *Lysinibacillus* also show outstanding potential for environmental and industrial applications beyond biological control, especially in bioremediation of toxic metals (Lozano *et al.* 2013; Rahman *et al.*, 2015; Peña *et al.* 2015), phosphorous solubilization (He *et al.* 2014), among others. Some strains exhibit high toxicity against mosquito larvae and have been widely used in insect control programs to reduce the populations of vector species that transmit tropical diseases, such as malaria, filariasis and arboviral diseases (e.g. yellow fever and dengue) (Berry *et al.*, 2012).

At the time of writing, the genus contains the following species with validly published names: *Lysinibacillus boronitolerans*, *L. fusiformis*, *L. sphaericus* (Ahmed *et al.*, 2007), *L. parviboronicapiens* (Miwa *et al.*, 2009), *L. xylanilyticus* (Lee *et al.*, 2010), *L. macroides* (Coorevits *et al.*, 2012), *L. mangiferahumii* (Yang *et al.*, 2012), *L. sinduriensis*, *L.*

massiliensis, *L. odysseyi* (Jung *et al.*, 2012), *L. tabacifolii* (Duan *et al.*, 2013) and *L. chungkukjangi* (Kim *et al.*, 2013).

Apart from being considered a relevant genus for many fields of study and its many applications mentioned above, little is known about the mechanisms used on *Lysinibacillus* spore assembly. Most or all we know about sporulation in this genus is over extrapolated from the model strains *B. subtilis* and *B. anthracis* (Holt and Leadbeater, 1969; Santo and Doi, 1974; Aronson and Fitz-James, 1976; Driks, 1999; Driks, 2009; McKenney *et al.*, 2013; Bozue *et al.*, 2015; Stewart, 2015; Driks and Eichenberger 2016).

The morphological stages of sporulation in *Lysinibacillus* have been well documented by transmission electron microscopy (TEM) that demonstrated the architectural complexity of the spore layers (Holt *et al.*, 1975; Kalfon *et al.*, 1984). The sequence of sporulation events in is fairly typical to what is seen on model strains such as *B. subtilis* and *B. anthracis*, except for production of endospores in ellipsoidal or spherical forms which lie terminally in a swollen sporangium.

Endospore formation, or sporulation, is a complex and dynamic process. A series of concentric shells that act as protective barriers (Knaysi and Hillier, 1949; Pandey and Aronson 1979; Driks, 1999; Driks, 2004; Priest *et al.*, 2004; Ghosh *et al.*, 2008; McKenney and Eichenberger 2012; McKenney, 2013) is assembled surrounding the core (the inner most compartment, housing the spore chromosome): an inner membrane, a thin peptidoglycan layer called the germ cell wall, a thick peptidoglycan layer (the cortex) and additional outer layers that vary in number and structure among species (Driks and Eichenberger, 2016).

At a minimum, these outer layers include those of the coat, a multilayered-proteinaceous spore coat, composed of at least 70 different proteins, that provides protection to the spore and participates in germination, the process of breaking dormancy and returning to active metabolism (Aronson and Fitz-James, 1976; Setlow, 1995; Driks, 1999; Meador-Parton and Popham 2000; Henriques and Moran, 2007; Driks, 2007, McKenney *et al.*, 2013; Driks and Eichenberger, 2016). For many species, including *B. subtilis*, the coat is the outermost spore layer. In other species, however, including *B. anthracis* and *L. sphaericus*, there are two additional layers, an interspace and, surrounding that, an exosporium (Beaman *et al.*, 1972; Waller *et al.* 2004; Driks, 2007; Traag *et al.*, 2010; McKenney *et al.*, 2013; Bozue *et al.*, 2015; Stewart, 2015).

Spore coat formation in *B. subtilis* can be divided into two distinct stages (Zheng and Losick 1990; Webb *et al.*, 1995; Little and Driks, 2001; Ozin *et al.*, 2001; Costa *et al.*, 2006; Ramamurthi *et al.*, 2006; Costa *et al.*, 2007; Ramamurthi and Losick, 2008; Mullerova *et al.*,

2009; Ramamurthi *et al.*, 2009; Wang *et al.*, 2009; McKenney and Eichenberger, 2012). Both stages are classified by the presence of key-proteins for sporulation, or morphogenetic proteins. The first stage is the recruitment of proteins to the spore surface, dependent on the morphogenetic protein SpoIVA (Stevens *et al.*, 1992). The second stage, known as encasement, involves the migration of the coat proteins around the circumference of the spore in successive waves, a process dependent on the morphogenetic protein SpoVID and the transcriptional regulation of individual coat genes. (Wang *et al.*, 2009)

Genetic and biochemical evidence supports the hypothesis that SpoVID promotes encasement of the spore (Figure 1) by establishing direct protein-protein interactions with other coat morphogenetic proteins (Wang *et al.*, 2009; Francesco *et al.*, 2012). It was previously demonstrated that SpoVID directly interacts with SpoIVA, the inner coat morphogenetic protein, SafA (Ozin *et al.*, 2000; Ozin *et al.*, 2001), and SpoVID with the outer coat morphogenetic protein, CotE (Francesco *et al.*, 2012).

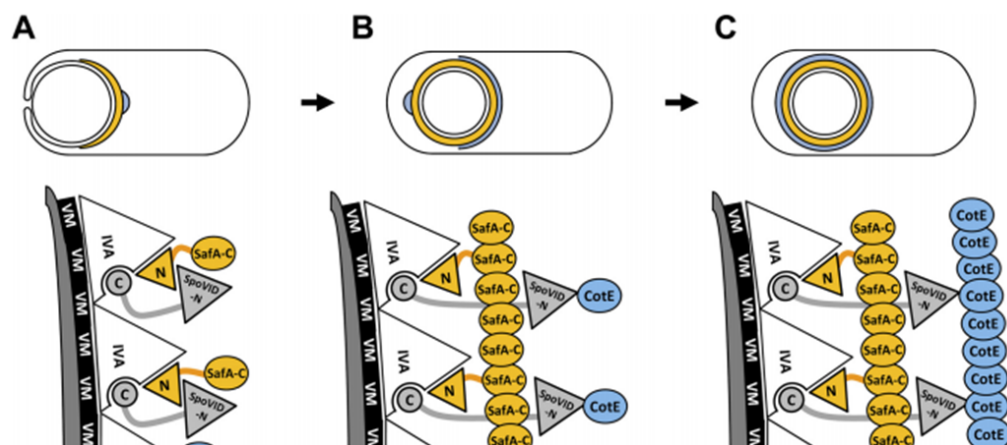


Figure 1. A model for spore encasement mediated by SpoVID. (A) Proteins of the basement layer of the spore coat localize to the surface of the spore coat, according to previously characterized interactions. The small peptide SpoVM (black) binds to the basement layer and interacts directly with SpoIVA (white triangles). SpoIVA interact with the C-terminal domain of SpoVID (gray circles). Additional interactions have been reported between the SpoVID N-terminal domain (gray triangles) and SafA N-terminal domain (yellow triangles), as well as between SpoIVA, SafA, and SpoVID. (B) Encasement is favored by the SpoVID N-terminal domain and its interactions with SafA and CotE. (C) Completion of encasement and multimerization of CotE. A possible increase in CotE levels in the late stages of sporulation (i.e., post-engulfment) has been suggested. Adapted from Francesco *et al.*, (2012)

The model of spore coat assembly and spore encasement incorporates several physical interactions between the principal coat morphogenetic proteins (Driks, 2002; Lai *et al.*, 2003; Kim *et al.*, 2006). This model is only limited to what is known in *B. subtilis* and, at some

degree in *B. anthracis*. As a consequence, specific functions of spore coat proteins, almost in its totality, remain unknown in other genus and *Bacillus* species. Here we propose the investigation to what degree this knowledge can be applied to non-model species from the genus *Lysinibacillus*.

II. Methods

Bacterial strains. Before selection for *Lysinibacillus* strains, 43 SDF strains (Table I) were randomly selected from SDF0001 to SDF0154 strains deposited at the CBafes, hosted at the University of Brasilia, Brazil (Cavalcante *et al.*, 2018). Strain CCGB 743 was selected from the Coleção de Culturas do Gênero *Bacillus* e Gêneros Correlatos, CCGB, hosted at FIOCRUZ, Rio de Janeiro, Brazil. *Escherichia coli* DH5 α was used for cloning and for triparental conjugation the recombinant strains *E. coli* DH5 α as donor strains, and *E. coli* SS1827 (Stibitz and Carbonetti, 1994), as helper strain, and SDF strains were used.

Table I. SDF strains selected to this study

Strain	Organism*	Accession number**	Strain	Organism*	Accession number**
SDF0001	<i>Bacillus pumilus</i>	MH356287	SDF0024	<i>Bacillus simplex</i>	MH569346
SDF0002	<i>Bacillus safensis</i>	MH356288	SDF0027	<i>Bacillus safensis</i>	MH356308
SDF0003	<i>Bacillus subtilis</i>	MH356289	SDF0028	<i>Paenibacillus alvei</i>	MH356309
SDF0005	<i>Lysinibacillus fusiformis</i>	MH356291	SDF0029	<i>Bacillus aryabathai</i>	MH356310
SDF0006	<i>Bacillus cereus</i>	MH356292	SDF0030	<i>Bacillus thuringiensis</i>	MH356311
SDF0007	<i>Bacillus circulans</i>	MH356293	SDF0032	<i>Bacillus cereus</i>	MH356312
SDF0008	<i>Paenibacillus alvei</i>	MH356294	SDF0037	<i>Lysinibacillus sphaericus</i>	MH356316
SDF0009	<i>Bacillus simplex</i>	MH356295	SDF0043	<i>Bacillus safensis</i>	MH356317
SDF0010	<i>Bacillus clausii</i>	MH356296	SDF0047	<i>Bacillus megaterium</i>	MH356320
SDF0011	<i>Bacillus pumilus</i>	MH356297	SDF0049	<i>Bacillus aryabhatai</i>	MH356321
SDF0012	<i>Bacillus clausii</i>	MH569343	SDF0062	ND	-----
SDF0013	<i>Bacillus safensis</i>	MH356298	SDF0063	<i>Lysinibacillus xylanilyticus</i>	MH356333
SDF0015	<i>Bacillus oleronius</i>	MH356300	SDF0068	<i>Bacillus simplex</i>	MH356337
SDF0016	<i>Bacillus simplex</i>	MH356301	SDF0080	<i>Paenibacillus alvei</i>	MH356346
SDF0017	<i>Bacillus altitudinis</i>	MH356302	SDF0086	<i>Bacillus aryabathai</i>	MH356349
SDF0018	<i>Bacillus clausii</i>	MH356303	SDF0089	<i>Bacillus anthracys</i>	MH356351
SDF0019	<i>Lysinibacillus sphaericus</i>	MH356304	SDF0094	<i>Bacillus megaterium</i>	MH356355
SDF0020	<i>Brevibacillus laterosporus</i>	MH356305	SDF0096	<i>Bacillus megaterium</i>	MH356357
SDF0021	<i>Bacillus pumilus</i>	MH569344	SDF00100	<i>Bacillus thuringiensis</i>	MH569353
SDF0023	<i>Paenibacillus alvei</i>	MH569345	SDF00141	<i>Bacillus pumilus</i>	MH356389

*Classification based on rDNA 16S sequences. ** NCBI database.

Plasmids. For conjugation events vectors pRP1028 (Figura 2; Plaut and Stibitz, 2015) and pBKJ236 (Janes and Stibitz, 2006) were used. Both plasmids are bifunctional and bear: i) a fragment corresponding to a functional origin of replication from *E. coli* derived from plasmid pSC101 (Armstrong *et al.*, 1984); ii) origin of replication that is temperature sensitive and derived from plasmid pWV01 (Maguin *et al.*, 1992), for conditional replication in *Bacillus*, and iii) *oriT* from RP4 (Trieu-Cuot *et al.*, 1991) and a site I-SceI (Colleaux *et al.*, 1998). A resistance gene for spectinomycin (adeniltransferase *aad9*) from the transposon *Tn554* of *Staphylococcus aureus* under control of the promotor *trc* has been included in pRP1028 (Figura 7) in substitution to the parental eritromycin resistance gene. pRP1028 also bears a coding sequence (*rfp*) for a red fluorescent protein TurboRFP (Merzlyak *et al.*, 2007), codons optimized for *B. anthracis* and inserted at the region of the promotor *rrnB* P2 from *B. subtilis*. For convenience, the site of cloning from pBKJ236 was modified and grouped. These two vectors are also described in table II.

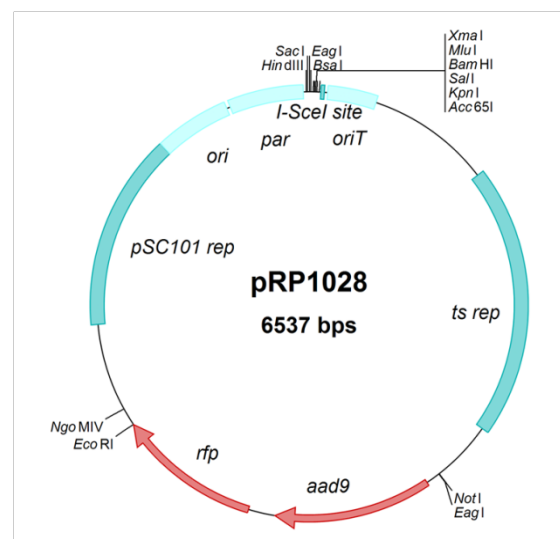


Figure 2. pRP1028 map. The bifunctional plasmid pRP1028 with 6.537 bp was built from (Plaut and Stibitz, 2015) pBKJ236 (Janes and Stibitz, 2006) using spectinomycin as selection maker for Gram positives. Even though plasmid pRP1028 has been significantly rearranged in relation to its parental, the components that allow allelic transfer as the origin of transference (*oriT*) were kept. The first is functional *E. coli* (*pSC101 rep*) and the second (*ts rep*) is temperature sensitive (replication is conditioned to growth on 37 °C) for replication in Gram-positives. This plasmid also bears a sequence for a red fluorescent protein gene (*rfp*). Arrows points the direction of transcription.

Table II. Plasmids used in this study

Plasmídeo	Descrição	Referência
pRP1028	Alelle exchange vector Tm ^S ; Sp ^r	Plaut and Stibitz, 2015
pBKJ236	Expression vector I-SceI; Tc ^r , Ap ^r	Janes and Stibitz, 2006

Culture media. Luria-Bertani (LB; Difco™). 0.5% Yeast extract (*p/v*); 1% Casein (*p/v*); 1% NaCl (*p/v*); pH 7.2. **Brain heart infusion (BHI; Hach).** 0.8% Brain heart infusion; 0.5% animal tissue hidrolised; 0.6% 0.5% Hidrolized casein; NaCl; 0.2% glucose; 0.25% Na₂HPO₄; pH 7.4. **Difco sporulation media (DSM; Difco™).** 3% Meat extract; 5% peptone; pH 6,8. **Sterile supplements** (added after autoclave): Ca(NO₃)₂ 1 M; MnCl₂ 0,01 M; FeSO₄ 0,001 M; filtered with cellulose 0.22 µm. **Solid media.** Obtained after inclusion of 1.8% ágar.

Cell growth and storage. Vegetative cells from the strains shown on table I were obtained after cells from single colonies were transferred to LB media, kept at 28 °C with aeration (220 rpm) for adequate time. Vegetative cells were kept in 15% glicerol aliquots and stored at -80 °C till the moment of use. Fore recombination experiments, cells from table I were grown on BHI media supplemented with either spectinomycin (100 µg/mL, or 250 µg/mL), or erythromycin (100 µg/mL or 250 µg/mL), except when indicated. When demanded, BHI media was supplemented with polymyxin B (60 U/mL) for inhibition of Gram-negative growth. Strains from *E. coli* were grown on solid LB media supplemented with spectinomycin (100 µg/mL) when necessary.

Cultivation conditions for phase contrast microscopic analysis. The SDF strains (Table I) were grown on solid LB (1% tryptone; 0.5% yeast extract; 1% NaCl, and 1.8% agar) at 30 °C, and sporulated on liquid DSM (Difco) at 30 °C, 150 rpm (for 48–96 h). Sporulation was assessed by phase contrast microscopy (Axiolab, Zeiss). Spores were washed twice with sterile distilled water (7,300 x g, 5 min), resuspended in sterile distilled water, and stored at 4 °C.

Table III. Primers used for the amplification of morphogenetic proteins and plasmids

Reference species/Plasmid	ID	Nucleotide sequence 5' →3'	Size (nt)	Annealing temperature (T _m , in °C)
<i>L. sphaericus</i> C3-41	<i>LyspoVID_E</i> (Fw)	AAAAAAgagctcATTGTTCAAAAGGGAGACACATTGTGG	39	62,9
	<i>LyspoVID_F</i> (Rv)	TTTTTTGGTACCGGCCACCACATTTGATGATAAATTGGTT	40	60,8
	<i>LyspoIVA</i> (Fw)	AAAAAAgagctcGCAGAGCGAACAAATGGCGATG	22	59,4
	<i>LyspoIVA</i> (Rv)	TTTTTTGGTACCGCCTCTTGTAATAATACTGAATATCCGCTTCTCTC	36	59,4
	<i>LycotE</i> (Fw)	AAAAAAgagctcCGACAAATCGTGACGAAAGCAGTAG	25	58
	<i>LycotE</i> (Rv)	TTTTTTGGTACCCACAACCACTTCACGTTCCACTAC	25	59,7
<i>P. polymyxa</i> M1	<i>PbspVID</i> (Fw)	AAAAAAgagctcAGTCAGAGGATGTGCGGAGGCTG	35	60,2
	<i>PbspVID</i> (Rv)	TTTTTTGGTACCGCGCTGCTACTGTGTATGAAGTTTCCG	39	61,4
	<i>PbspIVA</i> (Fw)	AAAAAAgagctcGACATTGCCGAACGCACCGGA	21	62,9
	<i>PbspIVA</i> (Rv)	TTTTTTGGTACCCGCGCTGAGTGTCATGACTGG	21	60,7
	<i>PbcotE</i> (Fw)	AAAAAAgagctcGAGGTCGGGGTCGAGCTCCTC	21	63,6
	<i>PbcotE</i> (Rv)	TTTTTTGGTACCGGCATTGAGGTCATCGGGACG	21	60,5
<i>Br.s brevis</i> NBRC 100599	<i>BrspoVID</i> (Fw)	AAAAAAgagctcTTGCCATCAAGGAGACCATTTTCCT	37	58,8
	<i>BrspoVID</i> (Rv)	TTTTTTGGTACCCGAAGGTGTATTCCCATGCTTCTTGG	38	59,5
	<i>BrspoIVA</i> (Fw)	AAAAAAgagctcGACATTGCCGAGCGGACGGG	20	63,6
	<i>BrspoIVA</i> (Rv)	TTTTTTGGTACCCAACCCGCTCCTCTGCATCGATG	23	62,6
	<i>BrcotE</i> (Fw)	AAAAAAgagctcCTACAGTGCCGGGAACATCATCG	22	59,6
	<i>BrcotE</i> (Rv)	TTTTTTGGTACCCCTGACTGTAATGGTGCCTCC	22	59,7
pRP1028	pRP1_D(Fw)	CGGTGAGTGGCTCAGGGGTG	20	62,8
	pRP1_C(Rv)	CCACGCGTCCCGGGGTGAC	19	63,5
SDF0037ΩpRP1028LysVID	LysVIDpRP_G(Fw)	TTGCGTATTCATATTGTTCAAAAGGGAGACACA	30	60
	LysVIDpRP_H(Rv)	CCTACTGATGACGGGCATGGCG	22	62,3

Fw: Forward Primer. Rv: Reverse primer Nt.: nucleotides. Tm: Melting temperature. For cloning ends we introduced bases corresponding to the restriction sites Sac I (gagctc), in bold, and lowercase *Kpn* I (ggtacc).

Statistical analysis of morphogenetic protein genes. All genomes from reference strains are deposited on the NCBI database (Benson *et al.*, 2013) and were analyzed for the presence or absence of sequences from the five morphogenetic protein genes from *B. subtilis*: SpoIVA, SPoVID, SafA, CotE e CotO. After identification of the sequences, BLAST (Altschul *et al.*, 1990) and Clustal Omega (Goujon *et al.*, 2010) optimized for DNA, were used for alignment. The molecular relations inter-genus and intra-species were considered. The statistical analysis consisted on the calculus of medium values among the percentage of identity shared.

Primers. Genomic sequences used as reference for primer design were taken from the identification and analysis of the NCBI database (Benson *et al.*, 2013). In order to compare the genetic relatedness from model and non-model species, searches for morphogenetic sequences from the genus *Bacillus*, *Paenibacillus*, *Brevibacillus* e *Lysinibacillus*, as well as for the model species *B. subtilis* and *B. anthracis* were performed. For primer design, around 500 pb from the gene sequences of morphogenetic proteins of interest deposited at the NCBI (Benson *et al.*, 2013) database were inserted on the program GENTLE (www.gentle.magnusmanske.de/). The primer sequences are described at Table II. Restriction sites were introduced at 5' and 3' ends to allow cloning of PCR products on the linearized plasmid vectors shown on Table I. Preceding restriction sites, six nucleotides T were added to increase the restriction efficiency. Primers were synthesized by IDT (www.idtdna.com/calc/analyser) and are described on Table III.

DNA isolation and amplification. Bacterial cells were grown in LB medium supplemented with 20 mM L-threonine, at 28 °C and agitation (200 rpm) until A₆₀₀ between 5 and 6 U. Total DNA was extracted and purified using the Wizard genomic kit (Promega) according to the manufacturer's protocol and stored in nuclease free water at -20 °C.

Amplification of sequences from genes of interest. Target sequences were amplified on a thermocycler (Bio-Rad Dyad Disciple) using total DNA on a final volume of 25 µL reaction: buffer 1X; 1.5 mM MgCl₂; 200 µM dNTP (dATP, dCTP, dGTP, dTTP; Invitrogen); 0.1 µM Of each primer (Table III); 1.25 U/µL of Taq DNA Polymerase (Invitrogen) and <1,000 ng de DNA. The PCR program employed on the thermocycler was adjusted for the characteristics of each target sequence. The standard initial denaturation temperature was 94 °C for 2 minutes. Each reaction was adjusted for a total of 35 cycles as the settings described. Temperature of denaturation was 94 °C for 30 s. Annealing temperature was adjusted for each primer as described on column T_m from table III, for 30 s. Extension steps were performed at 64 °C and time adjusted to 1 min/kb from target sequence. PCR products were kept at 4 °C until analysis on 1% agarose gel.

Construction of donor strain and homologous recombination. For this work, the protocols described in Plaut and Stibitz (2015) were used. In order to disrupt the functional regions of

the target genes, the plasmid pRP1028 was linearized by double digestion with *Sac* I and *Kpn* I (Promega) as manufactures protocol. After double digestion of the PCR product of the target gene with the same enzymes, the plasmid and fragments restricted were analyzed in agarose gel (Figure 9), excised and purified (QIAquick PCR Purification kit, Qiagen). The concentration of both DNA fragments was determined by spectrophotometry (NanoDrop 2000 UV-Vis Thermo Scientific). For cloning of *spoVID* gene, 1 µg of the PCR product was ligated to pRP1028 using *T4 DNA ligase* (Invitrogen) as manufacturer specifications and using insert:vector ration at 3:1 based on the formula:

$$\frac{\text{Vector (ng)} \times \text{Insert size (kb)}}{\text{Vector size (kb)}} = \text{Insert (ng)}$$

The reactions of ligation were performed on a final volume of 10 µL bearing 10.3 ng of the vector; insert at the adjusted concentration according to the formula mentioned above and 1 U/µL of T4 DNA ligase and buffer 1X (Invitrogen). One µg of the recombinant plasmid (pRP1028ΩLysVID) was used for transforming competent cells using *E. coli* DH5α competent cells kit by CaCl₂(ThermoFisher scientific), as manufacturer specifications. Positive and negative controls were, respectively: pRP1028 intact and linearized. *E. coli* DH5α clones obtained were inoculated in selective media as described above. Recombinant and parental plasmids were extracted by alkaline lysis and purified by affinity chromatography using the kit *GeneJET plasmid miniprep* (ThermoFisher scientific), double digested (*Sac* I and *Kpn* I) and analyzed on 1% agarose gel. For pRP1028 transference and derivatives of triparental conjugation, the selected SDF and CCGB strains were inoculated on BHI media. Donor strains *E. coli* DH5αΩpRP1028LysVID and helper *E. coli* SS1827 were inoculated on LB media, all containing appropriate antibiotics at appropriate concentrations. With a sterile swab, colonies of interest obtained after an overnight incubation were transferred to fresh BHI media, mixed, and incubated overnight at room temperature. Using a sterile swab, the content of the plate used for conjugation was removed, re-inoculated on fresh BHI media bearing spectinomycin and polymysin (BHI-SpcPmx) and incubated at room temperature until it was possible to distinguish colonies resembling wild-type (WT), on a time frame of usually above 24 h. Isolated colonies were transferred to new BHI-SpcPmx plates and incubated at 37 °C for a period not superior to 24 h and growth evaluated. This last step was repeated at least 6 times. The presence or the lack of a phenotype resultant from pRP1028 (the resistance to spectinomycin and red pigmentation) were used as selection marks to recombinants of interest, named SDF0037ΩpRP1028LysVID and CCGB743ΩpRP1028LysVID for PCR analysis using the kit *Taq DNA polymerase, recombinant e PlatinumTaq DNA polymerase, high fidelity* (Invitrogen), as

manufacturers specifications, and primers described on the table III. Resulting PCR products were analyzed on 1% agarose gel, excised, purified using the kit *Wizard SV PCR Clean-Up System* (Promega) and sequenced using the services of GenScript (www.genscript.com).

Transmission electron microscopy. TEM was performed essentially as described in Margolis *et al.* (1991).

III. Results and Discussion

In the present work, we considered our previous the images published by Cavalcante *et al.* (2018) where, to gain insight into the formation of the *L. sphaericus* spore, we used TEM to analyze sporulating *L. sphaericus* SDF0037 cells at several time points during sporulation. Consistent with previous work (Kalfon *et. al.*, 1984), we found that the forespore-pole of the cell is swollen before septation, and that forespore septation and engulfment, and coat formation occur at roughly the times as in other species (Figure 3). We did not detect discreet stages within coat assembly. We visualized a single exosporium layer at hour 6 (t_6), which is, at least, several hours prior to the time we would expect the release of the spore from the mother cell.

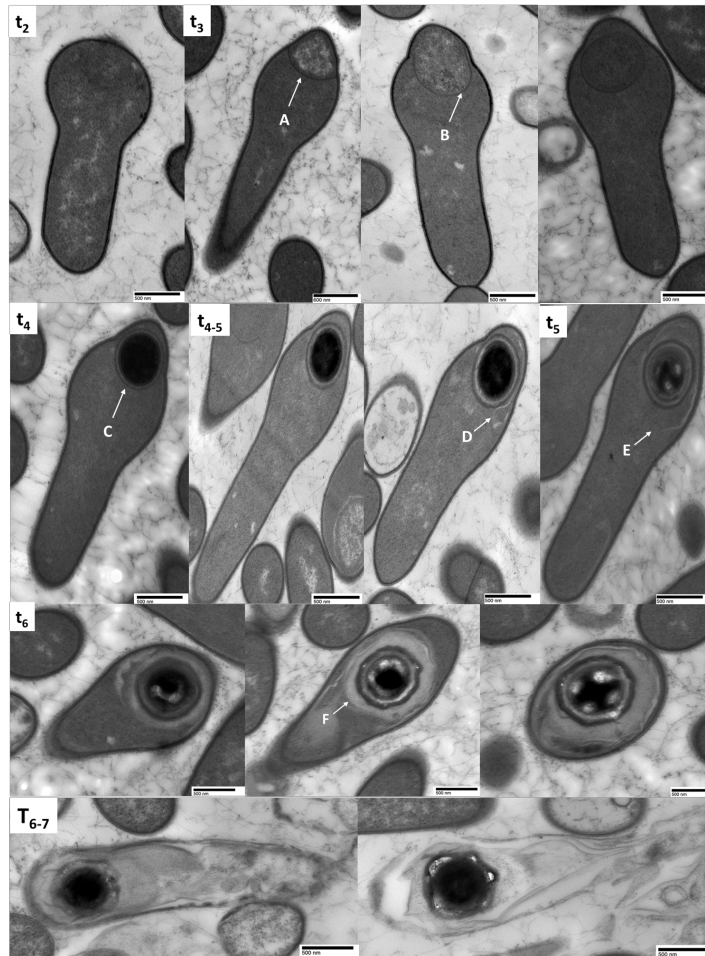


Figure 3. Thin-section TEM analysis of *Lysinibacillus sphaericus* SDF0037. Spores were harvested at the times (tn) indicated in the upper left of each panel, after the culture entered stationary phase (or in the panel to the immediate left where no time is indicated). Arrows point to spore structures as they become detectable during development and are labelled as follows: (A) Septum formation. (B) Engulfment. (C) Coat deposition. (D), and (E) The beginning of exosporium formation. (F) Exosporium maturation and a possible second layer being formed. The images are meant to suggest plausible steps in assembly, since they were selected to represent the most predominant morphology found at each time period, SDF strain numbers, species, 200 nm, and 500 nm bars are indicated. Adapted from Cavalcante *et al.*, 2018.

The analysis of the spore ultrastructure represents an important first step to understand the way these species assemble their structure and provides significant taxonomic information (Driks, 2009; McKenney, 2013). Thanks to the detailed knowledge of spore ultrastructure described above, we can point out that even though many similarities among these species and the model species *B. subtilis* and *B. anthracis* can be observed, other fundamental architecture features are present. Little is known about these structures and the knowledge about the composition, assembly, and function lacks important data to even begin with.

Aiming to better understand the composition of the spore coat in *Lysinibacillus spp.*, we selected 5 morphogenetic protein gene sequences as targets to be amplified and further inactivated. The selection was based on the relevance of morphogenetic proteins for the model species, which therefore would present a higher probability of resulting in clearer phenotypes when the corresponding genes are inactivated.

We used the strategy of disrupting the functional sequences of the genes coding morphogenetic proteins and further analyzing the resulting phenotype as described in Plaut and Stibitz (2015). It is important to point out that optimizing protocols for WT strains, added to the current absence of genomic data on SDF strains lead us to make eventual modifications on the protocol. The steps for genetic manipulation protocol described in Plaut and Stibitz (2015) consists in amplify a fragment of DNA containing the target gene to be inactivated, to clone this fragment on a bifunctional plasmid and to transfer this recombinant plasmid hosting the fragment corresponding to the gene of interest to a WT strain by triparental conjugation. After sequential inoculations of the recombinant cells in fresh selective media, we used PCR to analyze the incidence of a single integration of the resistance cassette and further verify the phenotype resultant of the disruption of the genomic sequence and consequent prevention of the gene expression. The event of homologous recombination is briefly described on Figure 4.

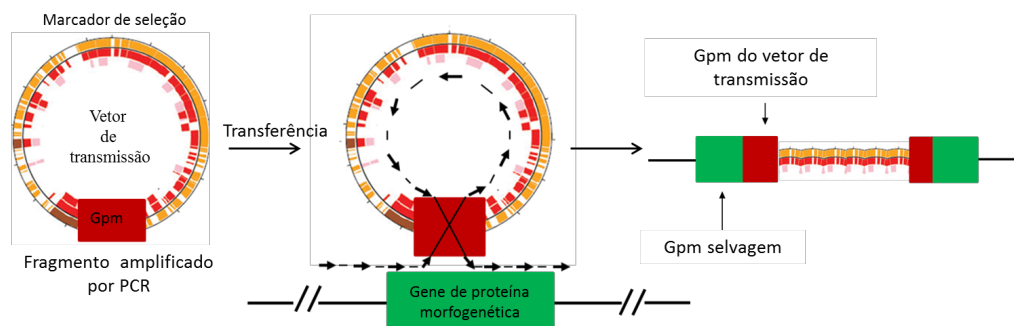


Figure 4. Representation of the strategy used to disruption of the functional structure of morphogenetic protein genes. The event of homologous recombination employed in this work consists in amplify, by PCR, a fragment of the target gene (Red), ligate it to a plasmid bearing a resistance cassette (pRP1028), so that the recombinant strain may be selected, and transfer it to a target strain. After series of events of cell replication, we expect that a single integration event has happened where the resistance cassette has been inserted in the middle of the target gene (Green), preventing transcription. Gpm: morphogenetic protein gene.

Because the plasmids used for cloning the genes of interest bear elements that provides resistance to the antibiotics spectinomycin, erythromycin, and kanamycin in *Bacillus spp.*, prior to initiating genomic transfer experiments, the selected *Lysinibacillus* strains, as other SDF strains, were pre-selected for resistance to these markers. The eight SDF strains that

presented resistance to, at least one, of the antibiotics are described on table III and were not used in this experiment.

Following the process of choice for *Lysinibacillus spp.* and other SDF strains that are suitable for the chosen methodology, 35 strains that were sensitive to the selective antibiotics were tested for the recombination protocol optimized for *B. anthracis* (Plaut e Stibitz, 2015).

Table IV. Resistance to antibiotics in SDF strains used in this study

Strain	Organism*	Antibiotic**
SDF0003	<i>B. subtilis</i>	spectinomycin
SDF0007	<i>B. circulans</i>	spectinomycin
SDF0008	<i>P. alvei</i>	kanamycin
SDF0019	<i>L. sphaericus</i>	spectinomycin
SDF0028	<i>P. alvei</i>	kanamycin
SDF0029	<i>B. megaterium</i>	spectinomycin
SDF0030	<i>B. thuringiensis</i>	spectinomycin
SDF0063	<i>L. xylanilyticus</i>	kanamycin

*As rDNA 16S phylogeny. **100 µL/mL.

Initially, many systems for disrupting the functional structure of the genes were considered, as well as three plasmid vectors for gene transference. The protocols for gene manipulation in *B. anthracis* described in Plaut and Stibitz (2015) and Janes and Stibitz (2006) encompass two plasmids, pRP1028 and pBKJ236 that represented the obvious choice for this initial attempt. Due to most of the efficient recombinant plasmid results emerging from the parental pRP1028, we decided on keeping this vector as the choice for conjugation experiments.

The triparental conjugation protocol consisted in using the *E. coli* strains *E. coli* SS1827 and *E. coli* DH5αΩpRP1028, as helper and donor strains, respectively. After growth on appropriate culture media, both strains and a *Lysinibacillus spp.* strain or an SDF strain were transferred to agar BHI and mixed together. After mixing, the plate was incubated at room temperature overnight and then transferred to selective media BHI-SpcPmx bearing antibiotics on a proper concentration for selection in *Bacillus spp.*

Plates with selective media, resulting from the last transference were inspected for the presence of colonies that were distinct from helper or donor *E. coli* colonies. Colonies that were similar to *Lysinibacillus spp.* or SDF strains were re-inoculated in fresh media bearing antibiotics on appropriate concentration and, after overnight incubation, evaluated for growth and colonies presenting red pigmentation, provided by the expression of the *rfp* gene from pRP1028.

SDF strains, classified by rRNA 16S gene sequences (Table III), presented positive results for triparental conjugation experiment: SDF0005, SDF0019 and SDF0037 (*Lysinibacillus spp.*); SDF0008 and SDF0028 (*Paenibacillus spp.*); SDF0020 (*Brevibacillus spp.*) and SDF0018 (*Bacillus clausii*); CCGB 743 (*Lysinibacillus fusiformis*). Strains SDF0003, SDF0015, SDF0021, SDF0029, SDF0030, SDF0032, SDF0043, SDF0047, SDF0049, SDF0100 and SDF0141 were tested but the experiments were discontinued since they belong to species phylogenetically close to model strains *B. subtilis* and *B. anthracis*, representing little or no effectivity to demonstrate diversity on the mechanisms of spore structure assembly. These strains were stored for further experiments. Strains SDF0006, SDF0007, SDF0010, SDF0012, SDF0023, SDF0024, SDF0062, SDF0089 e SDF0094 (Table I) were tested but the experiments were discontinued since classification based on rRNA 16S were not available at the time the experiments were performed. These strains were stored for further experiments.

Strains that revealed the capacity of receiving the plasmid pRP1028 by conjugation were put to two additional tests to confirm the efficiency of the transference. The first test was to verify the ability of these strains to form spores, aiming to exclude the possibility of the colonies belonging to *E. coli* strains and to exclude the possibility of mutations preventing the entire sporulation cycle. All recombinant mutant candidates kept their ability to form spores in the sporulation media DSM (Difco) at 37 °C. Heat-shocking treatment was performed for spore activation (65 °C for 10 min), followed by serial dilution and inoculation in solid media. Sporulation efficiency was reduced when compared to parental WT strains but all recombinant strains present growth at the conditions evaluated.

The second test for gene transfer efficiency evaluation was the confirmation of the presence of the plasmid pRP1028 by PCR. The primers used for this test are described on table III. Plasmid DNA from mutant candidate strains was extracted and purification via alkaline lysis and affinity chromatography, respectively. The plasmid DNA was used as a template for amplification of the gene of interest. PCR products were analyzed in 1% agarose gel (Figure 5). A fragment of 3,874 pb compatible to the size of the vector pRP1028, can be verified at the lanes corresponding to the strain SDF0037 Ω pRP1028, even though it presented less intensity when compared to the positive control, the donor strain *E. coli* DH5 α Ω pRP1028. This difference can be explained by the plasmid copy numbers found in the different hosting cells. Possibly, the fact that we were not using a *B. anthracis* strain did not allow specific amplification and many additional bands can be observed on the gel. The protocol was further optimized for the systems of interest.

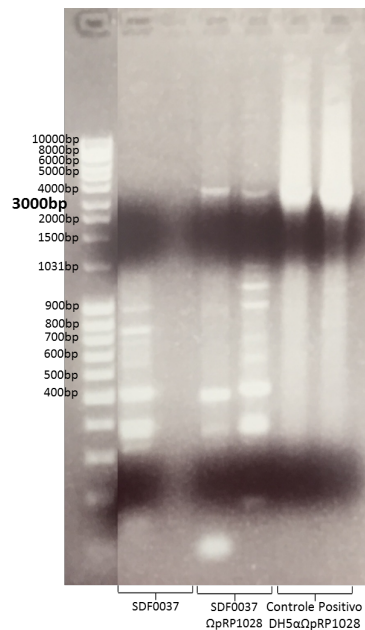


Figure 5. Analysis of transformation of strain SDF0037. The efficiency of the transformation of the strain SDF0037 was verified by PCR. A fragment with approximate 3,874 bp from plasmid pRP1028 was amplified and analyzed in 1,8% agarose gel. The fragment can be observed on lanes SDF0037ΩpRP1028, with less intensity than plasmid from donor strain (positive control *E. coli* DH5αΩpRP1028).

These same results were found on strains (Table I) *L. fusiformis* SDF0005; *L. sphaericus* SDF0037; *L. xylanilyticus* SDF0063, and, *L. fusiformis* CCGB 743 (results not shown). Also *P. alvei* SDF0008 and *P. alvei* SDF0028 and *Brevibacillus agrii* SDF0020 (results not shown).

At this point, it is important to mention that, until the moment these experiments were done, none of the mutant candidate strains presented the phenotype red pigmented colonies resulting from the expression of the *rfp* gene from plasmid pRP1028. Roger Plaut (2009), describes that in species other than *E. coli*, including those from the genus *Bacillus*, the occurrence of variants *rfp* negatives (*rpf*) it is extremely common, and for that reason, the lack of colonies presenting red pigmentation is not a factor determining a fail of the insertion of the gene of interest in the genome of the hosting cell.




After the methodology of plasmid insertion was tested, it was necessary to build the tools for the homologous recombination. It was required that the fragment of the target gene could be amplified by PCR so that it would be cloned on the chosen vector (pRP1028). Because, at the time these experiments were performed, information regarding the genomic

sequences of the strains selected for this work was not available, such as precise sequences for the target genes and flanking regions, an alternative solution was developed.

As reported previously, even though the phylum *Firmicutes* is highly diverse, it is of general consensus that species on this phylum, either spore-formers or asporogenous, share a common set of core genes and respective gene products that are well preserved (Gupta, 2000; Lake *et al.*, 2009; Galperin, 2013). Analysis of genomic sequences suggests that around half of the coat protein genes in *B. subtilis* strains share orthologues detectable in other *Bacillus spp.*, while the other half doesn't appear to be conserved at all (McKenney *et al.*, 2012).

Having that in mind, a brief analysis of the NCBI (Benson *et al.*, 2013) database was performed, using species with available genomic sequences (table V) and related to the selected strains of *L. sphaericus* (SDF0005, SDF0037, SDF0063, and CCGB 743), *P. alvei* SDF0008 and SDF0028, and *Br. agrii* SDF0020, considered mutant candidates strains, in pursuit of the rates of conservation of the genes from the five morphogenetic proteins SpoIVA, SPoVID, SafA, CotE, and CotO. These genes were tested with the tool BLAST (Altschul *et al.*, 1990) as the percentage of sequence conservation in relation to model species *B. subtilis*, *B. cereus* and *B. anthracis* as in relation to indices intra-genus and intra-species.

Table V. Number of genomes present on NCBI database

Species	Genomes	 Complete	 Scaffold	 Contig
<i>L. sphaericus</i>	14	4	6	4
<i>P. alvei</i>	3	0	0	3
<i>P. polymixa</i>	19	6	4	9
<i>Br. Agri</i>	2	0	0	2
<i>Br. laterosporus</i>	5	1	2	2
<i>B. cereus</i>	266	32	154	51
<i>B. anthracis</i>	138	44	41	43
<i>B. subtilis</i>	155	46	21	48

For the selection of reference-strains we used as criteria the availability of complete genome data present on the database NCBI (Table V). *L. sphaericus* C3-41, *P. polymyxa* M1 and *Br. laterosporus* LMG 15441 were used as reference strains for primer design, complementary to the

sequence of genes of interest (Table III) on the selected strains of *L. sphaericus*. (SDF0005, SDF0037, SDF0063 and CCGB 743) and of *P. alvei* (SDF0008, and SDF0028;) and *Br.agri* SDF0020 mutant candidate strains.

Using as an example, the reference strain *L. sphaericus* C3-41 and the respective gene for the morphogenetic protein SpoVID, the BLAST (Altschul *et al.*, 1990) tool was incapable of recognizing orthologue genes in strains belonging to *B. subtilis* and *B. anthracis*. However, this same tool revealed an average conservation percentage of 83% intra-genus while intra-species was 100%. We realized that, in theory, the high conservation levels of *spoVID* intra-species in *Lysinibacillus spp.* would be enough so that the sequence of the reference strain *L. sphaericus* C3-41 could be used as reference for primer design without loss of vital information on SDF strains belonging to the genus *Lysinibacillus* with no readily available genome information. The same was found to be, in theory, true for the strains of genera *Paenibacillus* and *Brevibacillus*. Also, for other morphogenetic proteins such as CotE that presents orthologues in *B. anthracis* detectable by BLAST (Altschul *et al.*, 1990) and share identity of 64%. The levels of intra-genus conservation however are 86% while intra-species are 96%. A graphic representation of the statistical analysis performed for the genera *Paenibacillus*, *Lysinibacillus*, and *Brevibacillus* is shown on figure 6.

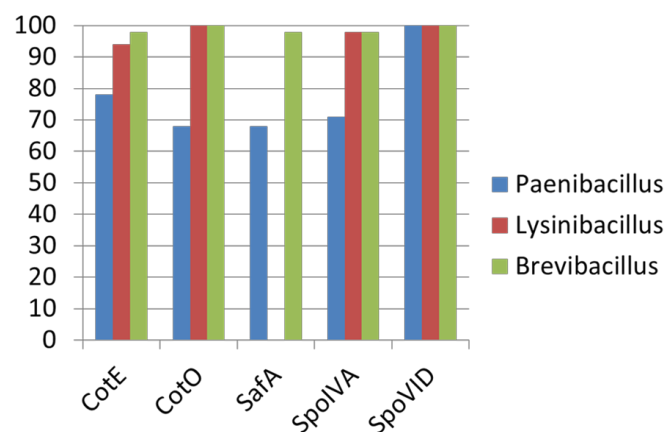


Figure 6. Conservation of morphogenetic protein genes intra-genus. Percentage of genetic identity shared among sequences of genes of morphogenetic proteins in different species of the same genus. Y axis represents the percentages of average conservation.

The level of molecular relatedness or levels of conservation among the orthologues found in strains with genomes available on NCBI (Benson *et al.*, 2013) database was considered enough so

that these would be used as mold for genetic manipulation of SDF and CCGB strains with no available sequenced genomes.

The gene coding the morphogenetic protein SpoVID was considered to be the obvious choice to begin this work with, because, among all sequences analyzed, it was the one that presented highest levels of conservation. *Lysinibacillus sphaericus* SDF0037 and *Lysinibacillus fusiformis* CCGB 743 were considered as examples for this work because these two strains presented the most promising results among the strains genetically manipulated by homologous recombination events. It is important to mention that the results presented from here, were also performed on other selected *L. sphaericus* (SDF0005, SDF0063) and *Paenibacillus alvei* SDF0008, SDF0028; and *Br. laterosporus* SDF0020 as well as other morphogenetic protein genes than *spoVID* (*cotE* and *spoIVA*) while with inconclusive results.

Following the original protocol described in Plaut and Stibitz (2015), it was established that the fragment to be amplified for homologous recombination should be above the minimum size of 500 bp and that the forward primer used for amplification should be complementary to the first 15 nucleotides of the gene sequence following the 5' extremity of the target gene. These measures are done aiming to keep the resistance cassette from plasmid pRP1028 inserted on an efficient way on a stable intern region of the target gene. First, we amplified a fragment sizing 593 bp from the DNA of the strain *L. sphaericus* SDF0037 using complementary primers drawn from the sequence of the orthologue gene from *L. sphaericus* C3-41. A graphic representation of primers named LysSpoVID E (forward) and F (reverse) used to amplify the fragment of the gene *spoVID* is shown on figure 7.

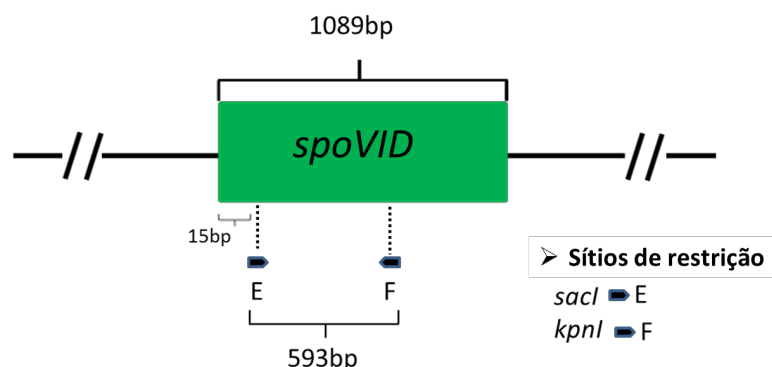


Figure 7. Representative model of the target fragment to be amplified by PCR. To increase efficiency and stability of the integration of the plasmid bearing the fragment of the gene *spoVID*, primers annealed 15 nt after the beginning of the coding sequence. Primers forward LysSpoVID_E and reverse LysSpoVID_F; bearing restriction sites *Sac* I and *Kpn* I, respectively.

The final product obtained by PCR amplification was inspected on 1% agarose gel with duplicate samples (Figure 8) where fragments of around 600 bp could be observed. These fragments were extracted, purified (QIAquick PCR Purification kit, Qiagen), and sequenced using the services of the company Genscript (www.genscript.com). The sequence obtained was analyzed with the tool BLAST (Altschul *et al.*, 1990) where we verified an identity of 82-86% shared with *spoVID* gene sequences from other *Lysinibacillus spp.* (Figure 8). It is important to mention that these values may not represent the real percentage because the coverage obtained was under 100%.

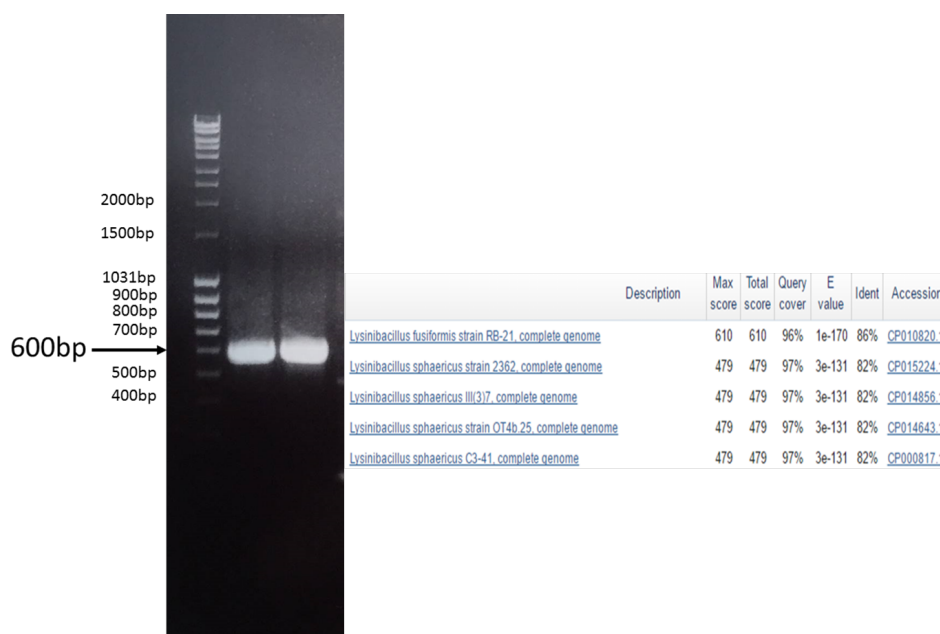


Figure 8. *spoVID* gene from *Lysinibacillus sphaericus* SDF0037. After PCR amplification using DNA from *L. sphaericus* SDF0037, fragments of approximately 600 bp were obtained. Sequences of these PCR products revealed identity between 82 and 86% with genes *spoVID* from strains of the genus *Lysinibacillus* deposited on NCBI.

As we mentioned before, the same strategy was employed for genes *spoIVA* and *cotE* and for the selected strains of *L. shericus*. (SDF0005, SDF0063) and *P. alvei* strains SDF0008, and SDF0028, besides *Br. agrii* SDF0020. A similar fragment corresponding to the gene of interest by using complementary primers designed from reference strains was obtained. The gene *spoVID* was amplified from strains SDF0005, SDF0008, SDF0028, and SDF0063. The gene *cotE* was amplified from strains SDF0008, SDF0028, and SDF0037 and the gene *spoIVA* from strains SDF0008 and SDF0028. All products obtained were inspected on 1% agarose gel in duplicate, excised, purified, and sequenced using the services of Genscript (results not shown). The sequences obtained were analyzed using the tool BLAST (Altschul *et al.*, 1990). An identity of at least 75% shared with their

respective sequences of references from different reference strains were identified (results not shown).

The methodology chosen did not allow the amplification of any gene from the strain SDF0020, identified using 16S rRNA gene sequence as *Br. agri*. We hypothesize that strains belonging to the genus *Brevibacillus* may not present a high conservation of morphogenetic protein genes sequences as the other genera analyzed. The protocol for genetic manipulation of *Brevibacillus* should be adapted.

Once we properly identified *spoVID* gene fragment amplified from total DNA from *L. sphaericus* SDF0037, we restricted the fragment with the enzymes *Kpn I* and *Sac I* and ligated to the plasmid pRP1028 linearized by the same double digestion. The resultant recombinant plasmid was designated pRP1028 Ω LysVID and used for transformation of *E. coli* DH5 α competent cells via CaCl₂ (ThermoFisher scientific), resulting on the recombinant strain *E. coli* DH5 α Ω pRP1028LysVID.

Aiming to verify the cloning a partial sequence of *spoVID* gene on the recombinant plasmid from the strain *E. coli* DH5 α Ω pRP1028LysVID, plasmid DNA was extracted and digested with the enzymes *Kpn I* and *Sac I*. The products of the double digestion from four different recombinant clones were analyzed in agarose gel in duplicate. Figure 9 shows the presence of two fragments around the expected size of 6,000 bp and 600 bp, for plasmid and insert, respectively.

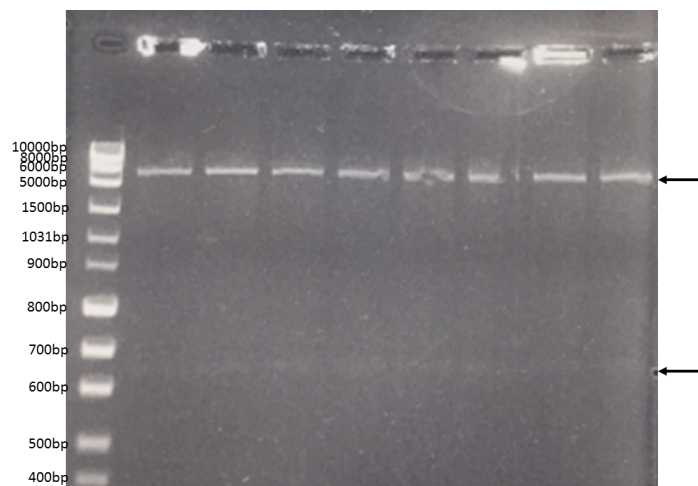


Figure 9. Analysis of restricted plasmid pRP1028 Ω LysVID. To verify cloning of the gene *spoVID*, recombinant plasmid was digested with the enzymes *Kpn I* and *Sac I* and analyzed for the presence of two fragments corresponding to the plasmid pRP1028 (approximately 6,000 bp) and around 600 bp, corresponding to part of the sequence of the gene *spoVID*.

III.1 – Construction of the mutant candidate *Lysinibacillus sphaericus* SDF0037 Ω pRP1028LysVID

The standard protocol for triparental conjugation was performed using *E. coli* DH5 α Ω pRP1028LysVID as donor strain, *E. coli* SS1827, as helper strain along with *L. sphaericus* SDF0037. After inducing conjugation, cells were transferred to a plate bearing fresh BHI-SpcPmx. Colonies presenting close characteristics to WT *Lysinibacillus* were selected and transferred in fourth sequential mode to fresh solid media and, in the last round, selected for spectinomycin resistance.

Because there was the possibility of the resistance phenotype being due to the resistance cassette from plasmid pRP1028LysVID being incorporated on chromosomal sites other than the target gene *spoVID*, or the remote possibility of replication of free plasmid on the cell cytoplasm on host cells, it was necessary to evaluate and validate the single integration and the correct insertion of the plasmid on the site of interest. To this end, the standard strategy described in Plaut and Stibitz (2015) is to amplify a fragment encompassing 100 bp flanking the extremities 5' (Figure 10, primer A) and 3' (Figure 10, primer B), respectively from the WT *spoVID* gene in pairs with primers designed from the plasmid pRP1028 (Figure 10, primers C and D).

As mentioned before, the genomic sequences of SDF strains used in this work were not available at the time this experiment was performed. For this reason, modifications on the standard protocol had to be made. Using the tool BLAST (Altschul *et al.*, 1990), an analysis of the identity shared between the flanking sequences of the regions 5' and 3' of the *spoVID* gene from *L. sphaericus* strains available on NCBI (Benson *et al.*, 2013) revealed that, besides the high levels of conservation of *spoVID* gene sequence, there was no guarantee that the identity of the flanking regions would be enough. Thus, the reference strains would be used for complementary primer design as done previously. The strategy used was to design a forward primer (Figure 10, G) complementary to the region of 15 bp skipped while amplifying the WT *spoVID* sequence fragment and a reverse (Figure 10, H) primer located on a region after nucleotide 593 used to amplify the WT *spoVID* fragment. A representation of the complementary primers regions is shown on figure 10.

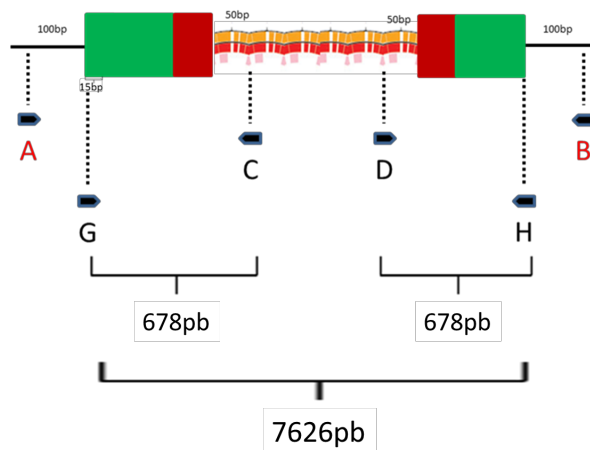


Figure 10. Homologous recombination event in SDF0037 Ω pRP1028LysVID. The standard protocol for verifying the insertion site (primers **A** and **B**) could not be used to verify if the integration happened at the target site, because the target does not share enough identity with other species from the genus *Lysinibacillus* with sequences available on databases. In order to overcome this limitation, we designed primers **G** and **H**, complementary to the 15 bp of the extremities 5' and 3', respectively, from the gene *spoVID*. The expected PCR results should present fragments with 678 bp amplified by the pairs of primers GC and DH, or a fragment with the equivalent size of 7.626 bp amplified by primers GH.

In case of success on the insertion of the sequence from plasmid pRP1028, PCR products sizing 678 bp from primers GC or DH were expected to be found, in addition to a product sizing 7,626 bp from primers GH (this value is due to the addition of base pairs from WT *spoVID* gene plus pRP1028 Ω LysVID). The PCR products obtained, however, revealed two sets of intriguing fragments (Figure 11).

PCR amplifications from primers G and C resulted on a fragment with approximately 700 bp (Figure 11. lanes corresponding to primers G and C). This fragment was excised, purified (QIAquick PCR Purification kit Qiagen) and sequenced. BLAST (Altschul *et al.*, 1990) analysis revealed an identity of 86% with *spoVID* gene sequence from *L. sphaericus* strains. This result suggests that a single integration happened on the expected site and that the functional *spoVID* sequence would have been disrupted.

Added to the data mentioned above, it was not possible to amplify any fragment from primers D and H. This result, however, does not invalidate necessarily the hypothesis that the insertion did not happen at the correct site. The sequences of the morphogenetic protein genes were amplified from reference strains. Therefore, we must consider the possibility that the complementary region amplified from primer H may not share enough identity with the corresponding region on the WT strain SDF0037. In other words, there was no guarantee that primers D and H would amplify any fragment even with the correct integration on the target site. It is necessary to validate the insertion

on this extremity with different primer designs or with a different methodology such as western blotting.

Other factor that prevented a solid interpretation of the results regarding the homologous recombination at the target site, was the amplification of a fragment with approximate 1,031 bp, amplified from primers G and H (Figure 11, lanes indicated by primers G and H). As previously mentioned, the amplification from primers G and H, a fragment with the expected size of 7,626 bp (resulting from the amplification of WT *spoVID* gene and plasmid pRP1028 Ω LysVID) would be obtained in case the insertion had happened at the correct site. The amplification of such a long fragment from primer H at the conditions described above is certainly difficult to achieve and it was revealed to be inadequate at the conditions mentioned above. On the opposite from what we expected, a fragment with the approximate size of 1,031 bp was obtained, which is the expected size for a PCR product using WT *spoVID* gene sequence as template.

This fragment was excised, purified (QIAquick PCR purification kit, Qiagen) and sequenced. The sequence obtained was analyzed by BLAST (Altschul *et al.*, 1990), revealing an identity of 88% with the sequence of *spoVID* gene from the reference strain *L. sphaericus* C3-41. The sequence of this fragment was also aligned to that of *spoVID* gene using the tool Clustal Omega (Goujon *et al.*, 2010), where we observed many regions shared by the two sequences.

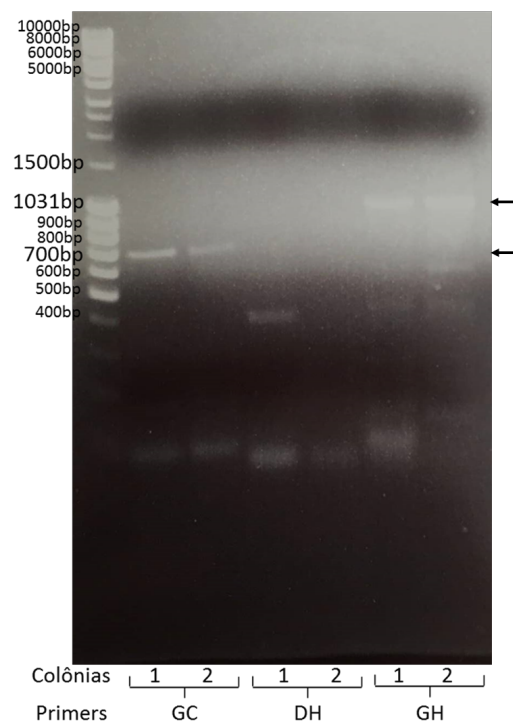


Figure 11. Analysis of recombinant strain of *L. sphaericus* SDF0037 Ω pRP1028LysVID. PCR from cells from the fourth re-inoculum of *L. sphaericus* SDF0037 Ω pRP1028LysVID should result in fragment of 678 bp, initiated by the complementary primers GC and DH. This was verified in gel, where two colonies from distinct plates presented fragment amplified with the expected size. (lanes GC), which, after sequencing, revealed as the correct fragment from recombination pRP1028 Ω LysVID. However, an additional fragment of approximately 1,031 bp was initiated by primers GH (lanes GH) complementary to a region very close to the expected for the WT *spoVID* gene. Sequencing of this fragment confirmed that this corresponded to WT *spoVID* without the presence of plasmid pRP1028 Ω LysVID.

The presence of a PCR product with the corresponding size for the WT gene paired with a fragment indicating the correct event of single integration at the expected site of insertion is suggestive of many possibilities. Although the genomic sequence for *L. sphaericus* SDF0037 was not available, we assumed that, this organism might present two copies of *spoVID* gene. This affirmation, however, is not supported by the present literature, because there are no reports of *Lysinibacillus* spp. genomes bearing more than one copy for this gene. A different possibility is that the colonies were formed from cells where the integration event happened at the correct site of insertion, while others where the phenotype of antibiotic resistance to spectinomycin was due the expression of the resistance gene from the parental plasmid pRP1028.

As an attempt to obtain a pure culture, we decided to increase the number of re-isolations, and verify again which would be the results from a new PCR amplification. From the transference of recombinant cells to a sixth plate containing selective media, it was possible to verify the presence of both white colonies, and typical pink colonies from WT *Lysinibacillus* spp., phenotype resultant from the acquisition of genetic information from the plasmid pRP1028. Both phenotypes are shown on figure 12.

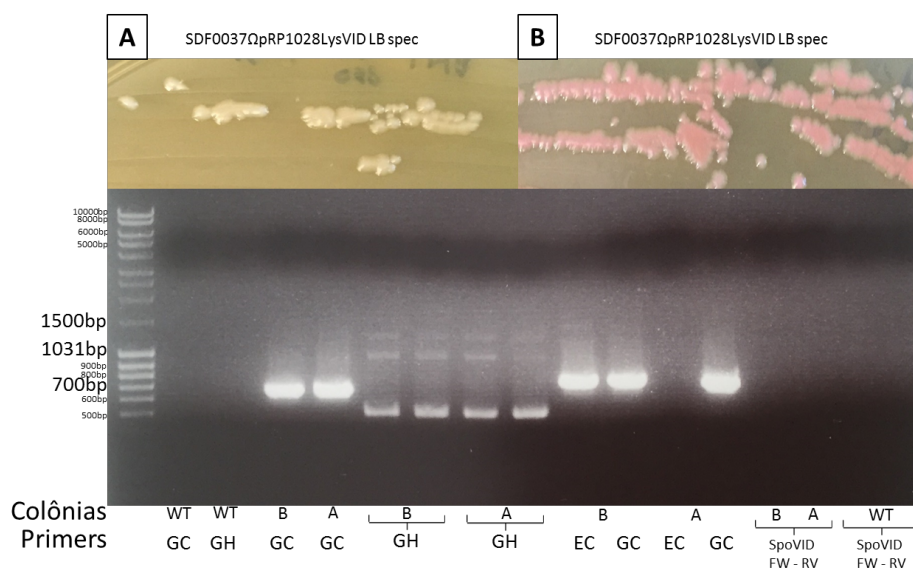


Figure 12. Phenotypes and PCR results of the recombinant strain *L. sphaericus* SDF0037ΩpRP1028LysVID. The presence of heterogeneous colonies could be the reason why PCR products related to mutant and WT genes are being obtained. Colonies with the phenotype for red pigmentation production (*rpf* B) started to differentiate from the usual *Lysinibacillus* sp. colonies (*rpf* A) from the sixth re-inoculums. However, the PCR products from the colonies revealed that, still yet, both would present products corresponding to mutant gene (lanes GC) and WT gene (lanes GH). The reaction used complimentary primers EC and GC suggests the presence of free plasmid inserted to the genomes in colonies with red pigment production phenotype. It is importante to mention that positive controls for the amplification of the WT fragment from the gene *spoVID* (SpoVID Fw-Rv) were not well succeeded in this experiment.

Aiming to confirm the correct single integration and to verify the purity of the colonies, new sets of PCR were performed. The resultant PCR products, however, revealed that, even with the emergency of new phenotypes, both plates featured colonies that generated the same expected results for both mutant and WT PCR amplifications with pairs of primers GC and GH. Reactions using primers EC and GC (the primer E was used to amplify the initial fragment used to build the plasmid pRP1028 Ω LSVID) is suggestive of the presence of free plasmid and inserted to the genome of the colonies with red pigment phenotype. It is important to mention that positive controls for amplification of the WT *spoVID* gene (*spoVID* Fw-Rv) were not successful on this experiment. Therefore, new sets of PCR were performed with different colonies from this recombinant where the WT *spoVID* gene was not observed (results not shown). These results, however, need to be confirmed with new sets of reactions.

Because the confirmation of recombination were inconclusive at the moment, we decided to choose a second mutant attempt from the other selected *Lysinibacillus* strains, the *L. sphaericus* SDF0005 and SDF0063, and *L. fusiformis* CCGB 743. Strains SDF0005 and CCGB 743 were considered to be sensitive to spectinomycin, presenting no sign of growth after one-week incubation at both 28 and 37 °C. *L. sphaericus* SDF0063 was considered to be sensitive to spectinomycin, but presented reduced growth at 37 °C and, therefore, was stored for further experiments.

Due to the *spoVID* gene sequence analysis by BLAST (Altschul *et al.*, 1990) revealed high level of sequence conservation, we decided on using the same plasmid pRP1028LysVID, designed from *L. sphaericus* C3-41 reference strain to attempt a homologous recombination event, even though the strains in which we would apply the protocol were identified as a different species (*L. fusiformis* and *L. sphaericus*).

The standard protocol for triparental conjugation was performed using *E. coli* DH5 α pRP1028LysVID as donor strain, *E. coli* SS1827 as helper strain along with *L. fusiformis* CCGB 743 or *L. fusiformis* SDF0005. After inducing conjugation, cells were transferred to a plate bearing fresh BHI-SpcPmx. Colonies that resembled WT *Lysinibacillus* colonies were selected and re-inoculated and after the fourth sequential re-inoculation it was possible to select for colonies with spectinomycin resistance. Recombinant *L. fusiformis* SDF0005 presented serious growth defects demonstrated by highly reduced growth rates after serial inoculations and, therefore, it was stored for further experiments. *L. fusiformis* CCGB 743 presented regular growth rates, similar to what was observed on the WT strain (Figure 13 A). Consequently, this strain was selected as the best suitable candidate for recombination evaluation. Again, it was necessary to evaluate and validate the single integration and the correct insertion of the plasmid on the site of interest in *L. fusiformis* CCGB 743.

PCR amplifications from primers G and C resulted on a fragment with approximately 700 bp (Figure 13 B; lanes corresponding to primers GC), being the expected fragment of 678 bp. This fragment was excised, purified (QIAquick PCR Purification kit Qiagen) and sequenced. After BLAST (Altschul *et al.*, 1990) analysis, it was revealed that product from primer G (Fw) shared an identity of 96% with *spoVID* gene sequence from the reference *L. fusiformis* RB-21 and other *Lysinibacillus* strains while sequence product from primer C (Rv) shared 98% identity with pRP1028 sequence. This result suggests that a single integration happened on the expected site and that the functional *spoVID* gene sequence would have been disrupted. The WT negative control also showed the expected result with no detectable reaction product. No detectable product was found on reactions using primer GH either. As previously mentioned, for this reaction with primers G and H, a fragment with the expected size of 7,626 bp (resulting from the amplification of WT *spoVID* gene and plasmid pRP1028 Ω LysVID) sequences would be obtained in case the insertion had happened at the correct site. The amplification of such a long fragment at the conditions described above is certainly difficult to achieve and it was revealed to be inadequate at the conditions mentioned above. This result indicates, but does not confirm alone, the absence of the WT gene sequence, and further investigation is necessary to confirm that recombinants *L. fusiformis* CCGB 743 Ω pRP1028LysVID are pure culture and host no WT cells.

A second set of reactions with primers D and H were performed. PCR amplifications from primers D and H resulted on a fragment with approximately 1,300 bp, being the expected fragment size 1,134 bp. This fragment was excised, purified (QIAquick PCR Purification kit Qiagen) and sequenced. BLAST (Altschul *et al.*, 1990) analysis revealed that product from primer D (Fw) shared an identity of 77% with *spoVID* gene sequence from the reference *L. fusiformis* RB-21 and other *Lysinibacillus* strains while sequence product from primer H (Rv) shared 98% identity with pRP1028 sequence. This result was verified only for one of the two colonies presented on Figure 13 B.

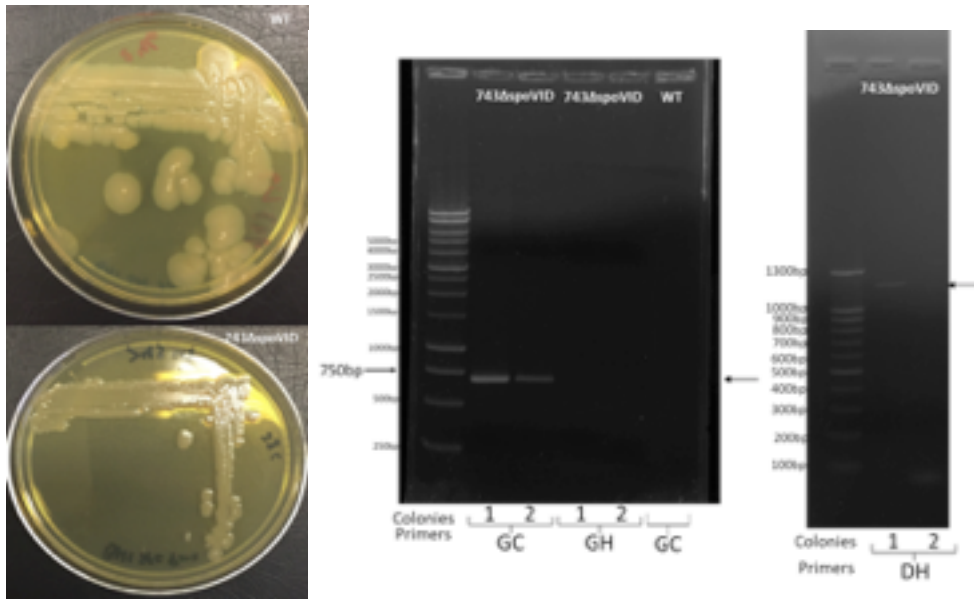


Figure 13. Phenotypes and PCR results of the recombinant strain *L. fusiformis* CCGB 743RpRP1028LysVID. Colonies of this mutant candidate did not present the the phenotype for red pigmentation production (*rpf*⁻) and presented similar morphology to the usual *Lysinibacillus sp.* colonies (A). However, the PCR products from the colonies (B) resulted on a fragment with approximately 700 bp (lanes GC) and no product amplification from neither WT gene nor plasmid (lanes GH). Negative control (WT colonies DNA with primers GC) was successful on this experiment. On the second set of PCR, the reaction using complimentary primers DH resulted on a fragment with approximately 1,300 bp, being the expected fragment size of 1,134 bp.

From a comparison of the sequences obtained, we can infer several important observations. The significant differences between *L. fusiformis* CCGB 743 mutant candidate *spoVID* gene sequences and the sequences in the NCBI (Benson *et al.*, 2013) databases include what appear to be bp substitutions, as well as regions of missing nucleotides (data not shown). We suggest that there are several potential sources of these differences, which include sequencing errors and strain-to-strain variation. A striking difference between *L. fusiformis* CCGB 743 mutant candidate and data base-derived *spoVID* gene sequences is the presence of gaps and inserts, perhaps as a consequence of the process of recombination in this species.

We note that the next step should take a step forward, and to properly obtain the *spoVID* gene sequence from the WT version of *L. fusiformis* CCGB 743. This will be required to access the real gene sequence prior to confirm the integration, but also to help resolving the issues mentioned above. To that end, we will design two new primers, in addition to the pair G and H, to sequence *L. fusiformis* CCGB 743 *spoVID* gene. These are, although, steps for a further work, and for the present work we proceeded with TEM analysis of both mutant candidates.

V.3 –The ultrastructure of spores produced by *L. sphaericus* SDF0037, *L. fusiformis* CCGB 743, and mutant candidates *L. sphaericus* SDF0037 Δ *spoVID* and *L. fusiformis* CCGB 743 Δ *spoVID*

Knowing that, in theory, clear phenotype changes would result from an event of knockout mutation in the *spoVID* gene, the spore ultrastructure was evaluated comparing WT and mutant candidate phenotypes.

On model species, *B. anthracis* and *B. subtilis*, the phenotype resulting of the inactivation of genes coding the protein SpoVID is the complete loss of the all coat layers, due to lack of anchoring sites for other structural proteins to attach to the basal layer. In *B. anthracis*, this phenotype is easier to be observed because of the presence of a single outermost and loosely attached layer, the exosporium, which surrounds the entire spore and is able to hold the disrupted fragments of the coat close to the free spore (Driks, 2007; McKenney 2013) (Figure 14).

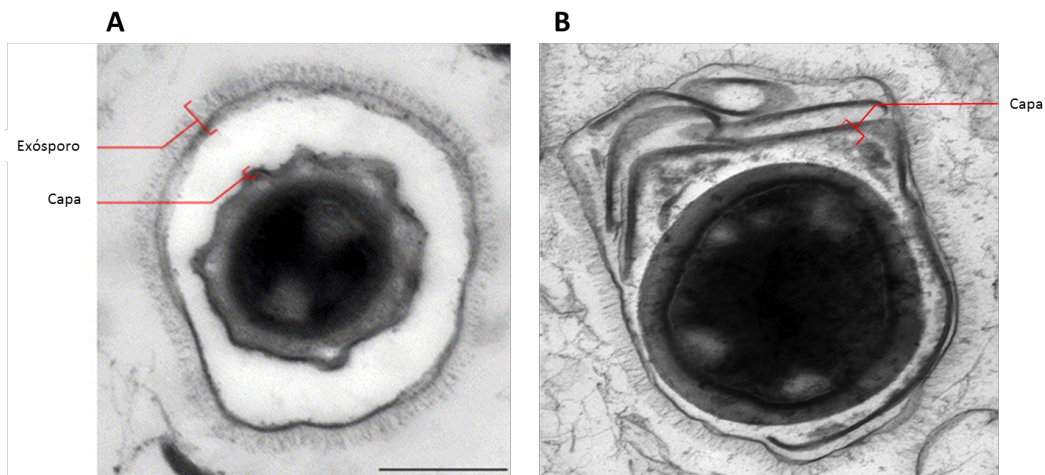


Figure 14. Resultant phenotype from the inactivation of *spoVID* in *B. anthracis*. The architecture of the *B. anthracis* spore (A; adapted from Driks, 2002) is changed drastically after deletion on the gene sequence that codes the morphogenetic protein SpoVID. The mutant produces the proteins from the layers corresponding to the coat but fails to assemble the spore around the basement layer (B; Courtesy of Tyler Boone).

Considering this information, it would be expected to see a clear phenotype of major changes on the spore architecture in regard to the coat layers attachment on strains *L. sphaericus* SDF0037 Δ *spoVID* and *L. fusiformis* CCGB 743 Δ *spoVID*. It is also important to remember that a typical spore from genus *Lysinibacillus* will present as a peculiar characteristic an additional layer of the exosporium (Holt *et al.*, 1975; Stewart, 2015), which is represented by an inner exosporium, smaller and electron denser when observed by TEM. This double-layered exosporium is not commonly found on spores from other genera described on the literature. Also, an outer

exosporium, which resembles much the typical exosporium observed in *B. anthracis* or, for example, *Paenibacillus* species (Driks, 2007; Stewart, 2015).

Interestingly, a double-layered exosporium was observed on TEM images from both strains *Lysinibacillus sphaericus* SDF0037 and *L. fusiformis* CCGB 743 Δ spoVID (Figure 15). On the recombinant strain, mutant candidate *Lysinibacillus sphaericus* SDF0037 Δ spoVID an alleged phenotype attributed to the lack of the protein SpoVID on the spore architecture could be observed, as shown on figure 15, and compared to that observed for the WT strain.

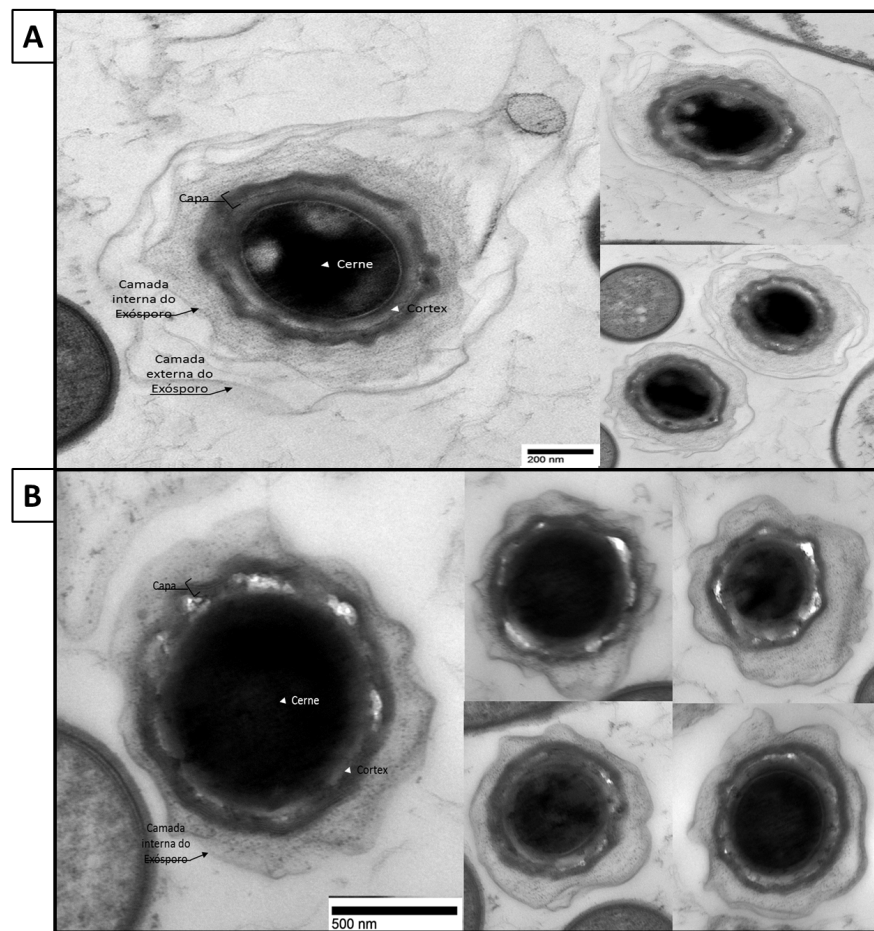


Figure 15. Ultrastructure of the spore produced by *L. sphaericus* SDF0037 and *L. sphaericus* SDF0037 Δ spoVID. The spore from *L. sphaericus* presents as a remarkable characteristic the presence of two layers of exosporium, or a lamellar exosporium. This peculiar structure encompasses an internal layer, more electron-dense, and an outer layer, bigger, looser and less electron-dense (A). The phenotype observed after the inactivation of the gene coding SpoVID on recombinant *L. sphaericus* SDF0037 Δ spoVID (B) was of the complete absence of the outer exosporium layer, without any other detectable change on the spore coat, as observed in model species *B. subtilis* and *B. anthracis*.

In contrast to the resulting phenotype from the inactivation of *spoVID* gene on model strains *B. subtilis* and *B. anthracis*, on mutant candidate *L. sphaericus*. SDF0037 Δ *spoVID*, we observed the lack of the second exosporium layer, or the outer exosporium, without any detectable changes on the overall coat morphology when TEM images were analyzed. From the images, however, it is not possible to determine if the phenotype is resultant from the complete absence of the layer assembly or if the layer is assembled on a defective way so that it loses or lacks attachment sites after the release of the spore on the environment. When analyzing TEM images of the mutant candidate *L. sphaericus*. SDF0037 Δ *spoVID*, we could also observe free spores presenting the WT morphology but on a much-reduced rate than those presenting a defective phenotype, possibly attributed to the recombination event.

Also, on the recombinant strain, mutant candidate *L. fusiformis* CCGB 743 Δ *spoVID* an alleged phenotype attributed to the lack of the protein SpoVID on the spore architecture could be observed, as shown on figure 16, and compared to that observed for the WT strain.

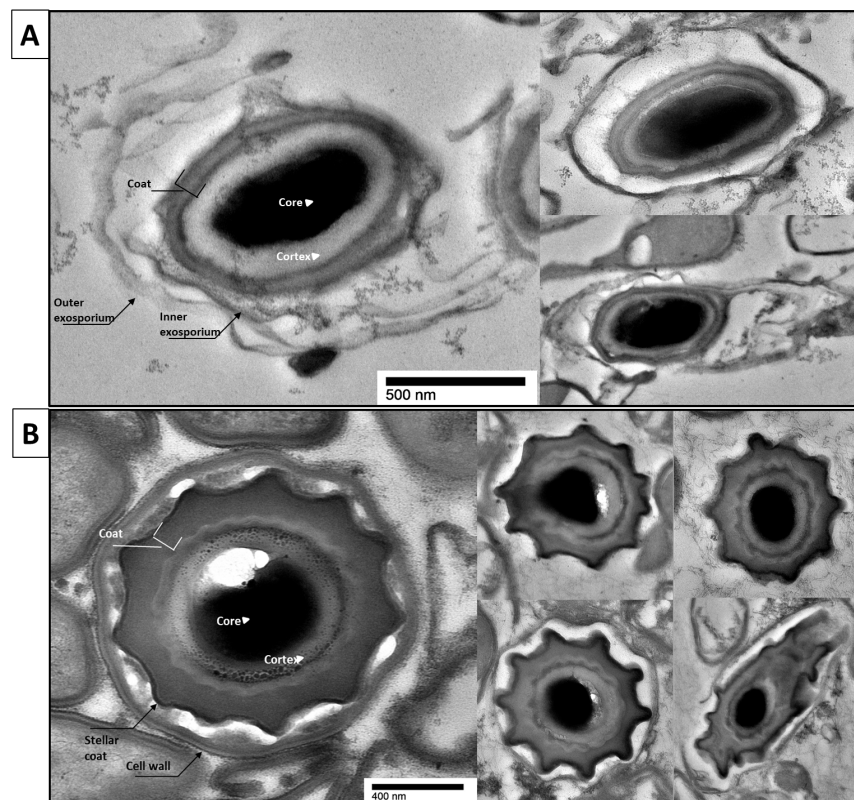


Figure 16. Ultrastructure of the spore produced by *L. fusiformis* CCGB 743 and *L. fusiformis* CCGB 743 Ω pRP1028LysVID. The spore from *L. fusiformis* also presents as a remarkable characteristic the presence of two layers of exosporium, or a lamellar exosporium the same way as *L. sphaericus* (A). The phenotype observed after the inactivation of the gene coding SpoVID on recombinant *L. fusiformis* CCGB 743 Ω pRP1028LysVID. (B) was similar to the observed in model species *B. subtilis* and *B. anthracis* in the sense that the coat seems to be affected by the lack of the protein, acquiring a stellar shape, much looser and with less definition than in the WT strain.

Similarly, the resulting phenotype from the inactivation of *spoVID* gene on model strains *B. subtilis* and *B. anthracis*, as well as, on mutant candidate *L. fusiformis* CCGB 743 Δ *spoVID*, we observed changes on the overall look of the coat morphology when TEM images were analyzed. What appears to be a stellar coat patten was formed, not detectable on WT strains. It is important to mention that none of the observed spores from Figure 16 are free spores. Therefore, due to the fact a spore is only considered to be complete (mature spore) when released to the environment, we cannot make solid conclusions about defects on spore formation other than speculative observations based on alterations on the ultratructure at the time of sporulation observed.

From the images, however, it is not possible to determine if the phenotype is resultant from the entire coat layer being built on a defective way so that it loses or lacks attachment or if there is a loose attachment of coat proteins making the scaffolds depending on SpoVID protein activity lose control of the assembly. When analyzing TEM images of the mutant candidate *L. fusiformis* CCGB 743 Δ *spoVID*, we could also observe the lack of any exosporium layers, absent even on its early stages of assembly. Again, we note that these are not free spores, so maybe the absence of an exosporium is due to the time in the process of sporulation in which these cells were observed.

Taken together, we argue that these are all preliminary observations and much more sampling is needed so that we can assure that there is an actual phenotype resulting from recombination events.

The confirmation of the results presented above, however, demands deep analysis or robust methods. New PCR analyses are necessary to confirm the insertion at the correct site and the absence of the WT gene. The analysis of the complete genome sequence on different SDF strains might provide the tools necessary for confirmation of the insertion as well as act as a tool for building new recombinant strains. Other techniques such as Southern blotting, might be employed to verify recombination, even if it is suggested that the confirmation by PCR is enough. Additional MET images analyses are necessary to avoid biases such as sample preparation, resin, and stain infiltration defects, that might result on undetectable features of the ultrastructure.

In addition, on the recombinant strain, complementing the target gene *spoVID* with a copy in plasmid and analyzing the potential to return to WT phenotype is a robust approach that, besides having to consider risks of bias such as gene hiper-expression, it could provide a clear answer regarding the phenotype caused by the deletion of the *spoVID* sequence.

Future experiments approaching phenotypical characteristics of the mutant candidates *Lysinibacillus sphaericus* SDF0037 and *L. fusiformis* CCGB 743 Δ *spoVID* will be conducted aiming to identify the main differences between the mutant strains and the WT. Coat protein profiling will be performed in order to identify conserved and labile proteins so that an initial network of structure

proteins dependent of SpoVID can be assembled. Other phenotypic characteristics will be tested, such as resistance properties to solvents and lysozyme, hydrophobicity, thermo-resistance, and adhesion to surfaces. The lack of a second exosporium layer phenotype might also be tested in field for the possible entomopathogenic activity, since the exosporium on *Lysinibacillus sphaericus* is the structure responsible for hosting a crystal protein with activity against Diptera larvae.

The high-level of conservation of genes identified for *Lysinibacillus spp.* and the possibility of protocol optimizations for species of this genus, opens the possibility that new mutants are developed.

Even if it is necessary more data to confirm the actual disruption of the gene *spoVID*, or that these preliminary results reveal that the recombination did not happen, our study corroborates the importance of expanding the knowledge on non-model strains. The morphogenetic proteins known from model species, *B. subtilis* and *B. anthracis*, could have the same importance to other species and genus of spore-formers, presenting the exact same function. But maybe, these proteins present different functions, or even no function at all, in non-model spore-former species. We hypothesize that the expansion of the knowledge about the events of sporulation in non-model species, especially those distantly related to the genus *Bacillus* on the phylogenetic tree, will certainly reveal how inadequate it is to assume that there are no gaps among the diversity of ways spore-formers species build spores.

IV .Referências bibliográficas

- Altschul, S.F., Gish, W., Miller, W., Myers, E.W., and Lipman, D.J. (1990) **Basic local alignment search tool**. J Mol Biol 215:403-410.
- Ahmed, Yokota, A., Yamazoe, A., and Fujiwara T. (2007). **Proposal of *Lysinibacillus boronitolerans* gen. nov.sp. nov., and transfer of *Bacillus fusiformis* to *Lysinibacillus fusiformis* comb. nov. and *Bacillus sphaericus* to *Lysinibacillus sphaericus*** Int Journal of Systematic and Evolutionary Microbiology.
- Armstrong K.A., Acosta R., Ledner E., Machida Y., Pancotto M., McCormick M.,(1984) **A 37 X 10(3) molecular weight plasmid-encoded protein is required for replication and copy number control in the plasmid pSC101 and its temperature-sensitive derivative pHS1**. J Mol Biol. 1984; 175(3):331–48.
- Aronson, A., 2002.**Sporulation and d-endotoxin synthesis by *Bacillus thuringiensis***.Cell. Mol. Life Sci. 59, 417–425.
- Aronson, A., and Fitz-James, P., (1976).**Structure and morphogenesis of the bacterial spore coat**. Bacteriol Rev 40,360–402.
- Beaman,T.C., Pankratz H.S., and Gerhardt P.,(1972) **Ultrastructure of the exosporium and underlying inclusions in spores of *Bacillus megaterium* strains**. J. Bacteriol. 109:1198–1209.
- Benson, D. A., Cavanaugh, M., Clark, K., Karsch-Mizrachi, I., Lipman, D. J., Ostell, J., & Sayers, E. W. (2013). **GenBank. Nucleic acids research**, 41(D1), D36-D42.
- Binnewies, T.T., Motro, Y., Hallin, P.F., Lund, O., Dunn, D., La, T., *et al.* (2006) **Ten years of bacterial genome sequencing: comparative-genomics-based discoveries**. *Funct Integr Genomics* 6: 165–185.
- Brillard, J. e Lereclus, D. (2004).**Comparison of cytotoxin *cytK* promoters from *Bacillus cereus* strain ATCC 14579 and from a *B. cereus* food-poisoning strain**.*Microbiology-Sgm* 150, 2699-2705.
- Cano, R.J., Borucki, M.K. (1995). **Revival and identification of bacterial spores in 25- to 40-million-year-old Dominican amber**. Science, 268(5213):1060-4.
- Colleaux L., D'Auriol L., Galibert F., Dujon B. (1988) **Recognition and cleavage site of the intron-encoded omega transposase**. Proc Natl Acad Sci U S A.; 85(16):6022–6.
- Davis, B.D., Dulbecco, R., Eisen, H. and Ginsberg, (1990).**Bacterial architecture**.In **Microbiology**, Eds., p. 47. Philadelphia, PA: J.B. Lippincott.
- de Vos, P. (2011).**Studying the Bacterial Diversity of the Soil by Culture-independent approaches**. Endospore forming soil bacteria. Vol 27 1-7
- de Vos, P.; Garrity, G.; Jones, D.; Krieg, N.R.; Ludwig, W.; Rainey, F.A.; Schleifer, K.-H.; Whitman, W.B. (Eds.). (2009). **Bergey's Manual of Systematic Bacteriology. Volume 3: The Firmicutes**. Second Ed.
- Driks A, Roels S, Beall B, Moran CP, Jr, Losick R. (1994). **Subcellular localization of proteins involved in the assembly of the spore coat of *Bacillus subtilis***. Genes Dev. 8:234–244
- Driks, A., (1999). **The *Bacillus subtilis* spore coat**. Microbiol Mol Biol Rev 63, 1–20.
- Driks, A., (2002). **Maximum shields:the assembly and function of the bacterial spore coat**. TRENDS in Microbiology Vol.10 No.6
- Driks, A., (2003). **The dynamic spore coat**.Proc Natl Acad Sci USA 100(6):3007–3009.
- Driks, A., (2007).**Surface appendages of bacterial spores**. Molecular Microbiology 63(3), 623–625.

- El-Bendary M., Priest F.G., Charles J.F., Mitchell W.J. (2005) **Crystal protein synthesis is dependent on early sporulation gene expression in *Bacillus sphaericus***. 51-56 First published online: 1 November
- Fritze, D. (2004). **Taxonomy of the Genus *Bacillus* and related genera: the aerobic endospore-forming bacteria**. *Phytopatology*, **94**(11).1245-1248.
- Galperin, M.Y. (2013). **Genome diversity of spore-forming *Firmicutes***. *Microbiology Spectrum*, **1**(2): 1-15.
- Garrity, G.M.; Bell, J.A.; Lilburn, T.G. (2003).**Taxonomic outline of the prokaryotes**. In: *Bergey's manual of systematic bacteriology*.
- Gibbons, N.E., and Murray, R.G.E., (1978). **Proposals concerning the higher taxa of bacteria**. *Int J Syst Bacteriol* **28**:1-6
- Giorno, R., Bozue. J., Cote, C., Wenzel, T., Sulayman, M., Krishna, M., Michael, R.M., Wang, R., Zielke, R.R., Maddock, J., Friedlander, A., Welkos, S., and Driks, A. (2007).**Morphogenesis of the *Bacillus anthracis* Spore**.*Journal of bacteriology*, p. 691–705 Vol. 189, No. 30021-9193.
- Goujon M., McWilliam H., Li W., Valentin F., Squizzato S., Paern J., Lopez R. (2010) **A new bioinformatics analysis tools framework at EMBL-EBI** *Nucleic acids research* **W695-9**
- Guinebrétiere, M.H., and Sanchis, V., (2003).***Bacillus cereus*sensu lato**. *Bull Soc Fr Microbiol* **18**:95-103.
- Hannay Cl.1957. **The parasporal body of *Bacillus laterosporus* Laubach**.*J Biophys Biochem Cytol*. Nov 25;3(6):1001-10.
- Henriques AO, Moran CP., Jr (2007). **Structure, assembly, and function of the spore surface layers**. *Annu. Rev. Microbiol.* **61**:555–588
- Henriques, A.O., and Moran, C.P.Jr., (2007). **Structure, assembly, and function of the spore surface layers**. *Annu. Rev. Microbiol.* **61**, 555–588. 16.
- Holt S.C., Gauthier J.J., Tipper D.J. (1975). **Ultrastructural studies of sporulation in *Bacillus sphaericus***. *J Bacteriol* **122**:1322–1338.
- Holt, J.G., (1986). **Bergey's Manual of Systematic Bacteriology** gram-positive bacteria other than actinomycetes. Williams & Williams, Baltimore, MD.
- Hoon M. J.L., Eichenberger P., and Vitkup D., (2010) **Hierarchical Evolution of the Bacterial Sporulation Network**.*Current Biology***20**, R735–R745
- Imamura D, Kuwana R, Takamatsu H, Watabe K. (2011). **Proteins involved in formation of the outermost layer of *Bacillus subtilis* spores**. *J. Bacteriol.* **193**:4075–4080
- Janes B.K. and Stibitz, S (2006).**Routine Markerless Gene Replacement in *Bacillus anthracis***. *Infect. Immun.* vol. 74 no. 3 1949-1953
- Joshi L.T., Phillips D.S., Williams C.F., Alyousef A., Baillie L. (2012). **Contribution of spores to the ability of *Clostridium difficile* to adhere to surfaces**. *Appl Environ Microbiol* Nov;**78**(21):7671-9.
- Kalfon A., Charles J.-F., Bourgin C. (1984) **Sporulation of *Bacillus sphaericus* 2297: an electron microscope study of crystal-like inclusion biogenesis and toxicity to mosquito larvae**. *J. Gen. Microbiol.* **130**, 893–900.
- Kim, K.K., Lee K.C., YuH., Ryoo S., Park Y. and LeeJ.S., (2009). ***Paenibacillus sputi* sp. nov., isolated from the sputum of a patient with pulmonary disease**.*International Journal of Systematic and Evolutionary Microbiology* vol. 60, part 10, pp. 2371 - 2376
- King, J. (1980). **Regulation of structural protein interactions as revealed in phage morphogenesis regulation and development**. vol. 2.Plenum Press, New York, N.Y.
- Knaysi, G. and Hillier, J., (1949). **Preliminary observations on the germination of the endospore in *Bacillus megatherium* and the structure of the spore coat**. *J Bacteriol* **57**, 23–29.

- La Duc, M.; Satomi, M.; Venkateswaran, K. (2004). ***Bacillusodysseyi* sp. nov., a round-spore-forming bacillus isolated from the Mars Odyssey spacecraft.** International Journal of Systematic and Evolutionary Microbiology, 54: 195-201.
- Lai E.M., Phadke N.D., Kachman M.T., Giorno R., Vazquez S., Vazquez J.A., Maddock J.R., Driks A., (2003). **Proteomic analysis of the spore coats of *Bacillus subtilis* and *Bacillus anthracis*.** J Bacteriol. Feb;185(4):1443-54.
- Logan N.A., Berge O., Bishop A.H., Busse H.J., De Vos P., Fritze D., Heyndrickx M., Kämpfer P., Salkinoja-Salonen M.S., Seldin L., Rabinovitch L., Ventosa A., (2009). **Proposed minimal standards for describing new taxa of aerobic, endospore-forming bacteria.** Int J Syst Evol Microbiol 59:2114–2121
- Logan, N.A. and De Vos, P. (2009). **Genus I. *Bacillus* Cohn 1872, Bergey's Manual of Systematic Bacteriology.** 174AL. Vol3. *The firmicutes* 2nd Edition.
- Losick, R., and P. Stragier.(1992). **Crisscross regulation of cell-type-specific gene expression during development in *Bacillus subtilis*.** Nature 355:601– 604.
- Maguin E., Duwat P., Hege T., Ehrlich D., Gruss A. (1992) **New thermosensitive plasmid for gram-positive bacteria.** J Bacteriol. 174(17):5633–8.
- Mandic-Mulec I., Prosser J.I.; 2011. **Diversity of Endospore forming Bacteria in soil: characterization and driving mechanisms.** Endospore forming soil bacteria. Vol 27 31-57
- McKenney P.T., Driks A., Eichenberger P. ,(2013). **The *Bacillus subtilis* endospore: assembly and functions of the multilayered coat.** Nat Rev Microbiol.33-44. December.
- McKenney PT, Eichenberger P. (2012). **Dynamics of spore coat morphogenesis in *Bacillus subtilis*.** Mol. Microbiol. 83:245–260
- McKenney PT, et al. (2010). **A distance-weighted interaction map reveals a previously uncharacterized layer of the *Bacillus subtilis* spore coat.** Curr. Biol. 20:934–938
- Meador-Parton, J. and Popham, D. (2000). **Structural analysis of *Bacillus subtilis* spore peptidoglycan during sporulation.** J Bacteriol 182, 4491–4499.
- Merzlyak EM, Goedhart J, Shcherbo D, Bulina ME, Shcheglov AS, Fradkov AF, (2007). **Bright monomeric red fluorescent protein with an extended fluorescence lifetime.** Nat Methods.; 4(7):555–7.
- Miller M.B. and Bassler B.L..(2001). **Quorum sensing in bacteria.** Annu Rev Microbiol.;55:165-99.
- Moberly, B.J., Shafa, F. and Gerhardt, P., (1966). **Structural details of *anthrax* spores during stages of transformation into vegetative cells.** J Bacteriol 92, 220–228.
- Montaldi F.A., Roth I.L. (1990) **Parasporal bodies of *Bacillus laterosporus* sporangia.** J. Bacteriol.;172:2168–2171.
- Narula J., Kuchina A., Dong-yeon D., Fujita M., Gurol M., Oleg A. (2015) **Chromosomal Arrangement of Phosphorelay Genes Couples Sporulation and DNA Replication,** Cell 162, 328–337 Elsevier Inc.
- Niall, A.L.,and Halket, G., (2011). **Developments in the taxonomy of aerobic, endospore forming Bacteria.** Endospore forming soil bacteria. Vol 27 1-7
- Nicholson, W.L., Munakata, N., Horneck, G., Melosh, H.J. and Setlow, P. (2000). **Resistance of *Bacillus* endospores to extreme terrestrial and extraterrestrial environments.** Microbiol Mol Biol Rev 64, 548–572.
- Ohba M, Mizuki E, and Uemori, A., (2009). **Parasporin, a New Anticancer Protein Group from *Bacillus thuringiensis*.** Anticancer Research, 29: 427-434,
- Ozin AJ, Henriques AO, Yi H, Moran CP., Jr (2000). **Morphogenetic proteins SpoVID and SafA form a complex during assembly of the *Bacillus subtilis* spore coat.** J. Bacteriol. 182:1828–1833

- Piggot, P.J., and Coote, J.G., (1976). **Genetic aspects of bacterial endospore formation.** *Bacteriol. Rev.* 40, 908–962.
- Piggot, P.J., and Losick, R., (2002). **Sporulation genes and intercompartmental regulation.** In *Bacillus subtilis and Its Closest Relatives: From Genes to Cells*, A.L. Sonenshein, J.A. Hoch, and R. Losick, eds. (Washington, DC: American Society for Microbiology), pp. 483–518.
- Pignatelli, M., Moya, A., Tamames, J., (2009). **EnvDB, a database for describing the environmental distribution of prokaryotic taxa.** *Environ. Microbiol. Rep.* 1, 191–197.
- Plaut R.D., Stibitz S. (2015) **Improvements to a Markerless Allelic Exchange System for Bacillus anthracis.** *PLoS ONE* 10(12): e0142758.
- Priest F. G., (1993). **Systematics and ecology of Bacillus.** In: *Bacillus subtilis and Other Gram-Positive Bacteria: Biochemistry, Physiology and Molecular genetics.* American Society for Microbiology. pp. 3–16.
- Ragkousi K, Setlow P. (2004). **Transglutaminase-mediated cross-linking of GerQ in the coats of Bacillus subtilis spores.** *J. Bacteriol.* 186:5567–5575
- Raiol, T., De-Souza, M. T., Oliveira, J. V. A., Silva, H. S. da I. L., Orem, J. C., Cavalcante, D. A., Moraes, L. M. P. (2014). **Draft Genome Sequence of FT9, a Novel Bacillus cereus Strain Isolated from a Brazilian Thermal Spring.** *Genome Announcements*, 2(5), e01027–14.
- Ramamurthi KS, Clapham KR, Losick R. (2006). **Peptide anchoring spore coat assembly to the outer forespore membrane in Bacillus subtilis.** *Mol. Microbiol.* 62:1547–1557
- Raymond B., Johnston P.R., Nielsen L.C., Lereclus D. and Crickmore N., (2010). *Bacillus thuringiensis: an impotent pathogen?*, Cell press.Elsevier Ltd.0966-842X, 2010.
- Redmond, C., Baillie, L.W., Hibbs, S., Moir, A.J. and Moir, A., (2004). **Identification of proteins in the exosporium of Bacillus anthracis.** *Microbiology* 150, 355–363.
- Roels S, Driks A, Losick R. (1992). **Characterization of spoIVA, a sporulation gene involved in coat morphogenesis in Bacillus subtilis.** *J. Bacteriol.* 174:575–585
- Ruiu L., (2013). *Brevibacillus laterosporus, a Pathogen of Invertebrates and a Broad-Spectrum Antimicrobial Species* *Insects.* Sep; 4(3): 476–492
- Russell, A., 1990. **Bacterial spores and chemical sporocidal agents.** *Clin Microbiol Rev* 3, 99–119.
- Schleifer, karl-heinz .(2009) **Phylum XIII.Firmicutes** Gibbons and Murray 1978, 5 (Firmacutes [sic] Gibbons and Murray 1978, 5) **Bergey's Manual of Systematic Bacteriology.** Vol3. *The firmicutes* 2nd Edition
- Setlow P. 2006. **Spores of Bacillus subtilis: Their resistance to and killing by radiation, heat and chemicals.** *J Appl Microbiol* 101(3):514– 525.
- Setlow P., 2003. **Spore germination.** *Curr Opin Microbiol* 6:550–556.
- Setlow, P. 1995. **Mechanisms for the prevention of damage to DNA in spores of Bacillus species.** *Ann Rev Microbiol* 49, 29–54.
- Sokolova, T.; Hanel, J.; Onyenwoke, R.U.; Reysenbach, A.L.; Banta, A.; Geyer, R.; Gonzalez, J.M.; Whitman, W.B.; Wiegel, J. (2007). **Novel chemolithotrophic, thermophilic, anaerobic bacteria Thermolithobacter ferrireducens gen. nov., sp. nov. and Thermolithobacter carboxydivorans sp. nov.** *Extremophiles.* 11 (1): 145–157.
- Stackebrandt, E., Murray, R.G.E and Trüper, H.G., (1988). **Proteobacteria classis nov., a name for the phylogenetic taxon that includes the "purple bacteria and their relatives.** *Int. J. Syst. Bacteriol* 38, 321–325.
- Stewart G.C. (2015). **The exosporium layer of bacterial spores: a connection to the environment and the infected host.** October. *Microbiol Mol Biol Rev*

- Stibitz, S. and Carbonetti, N.H. (1994) **Hfr mapping of mutations in *Bordetella pertussis* that define a genetic locus involved in virulence gene regulation.** J Bacteriol. Dec; 176(23): 7260–7266.
- Sundea E. P., Setlow P., Hederstedt L., and Hallea B. (2009) **The physical state of water in bacterial spores.** PNAS, November 17, vol. 106 no. 46 Edited by Richard M. Losick
- Traag B.A., Driks, A., Stragier, P., Bitter W., Broussard, G., Hatfull, G., Chu, F., Adams, K.N., Losick, R., (2010). **Do *mycobacteria* produce endospores?** Proc. Natl. Acad. Sci. U.S.A 107, 878-881.
- Trieu-Cuot P., Carlier C., Poyart-Salmeron C., Courvalin P. (1991) **Shuttle vectors containing a multiple cloning site and a lacZ alpha gene for conjugal transfer of DNA from *Escherichia coli* to gram-positive bacteria.** Gene.; 102(1):99–104.
- Verbaendert, I.; de Vos, P. (2011). **Studying Denitrification by Aerobic Endospore-forming Bacteria in Soil.** Em: **Endospore-Forming Soil Bacteria.** Springer, 1^a Ed.
- Villafane, R., Bechhofer, D.H. Narayanan, C.S., and Dubnau, D. (1987) **Replication control genes of plasmids pE194.** J Bacteriol 169: 4822-4829
- Vreeland, R.H., Rosenzweig, W.D., Powers, D.W. (2000). **Isolation of a 250 million-year-old halotolerant bacterium from a primary salt crystal.** Nature, 407(6806):897-900.
- Waller, L.N., Fox, N., Fox, K.F., Fox, A. and Price, R.L., (2004). **Ruthenium red staining for ultrastructural visualization of a glycoprotein layer surrounding the spore of *Bacillus anthracis* and *Bacillus subtilis*.** J Microbiol Methods 58, 23–30.
- Costa T, Isidro AL, Moran CP, Jr, Henriques AO. (2006). **Interaction between coat morphogenetic proteins SafA and SpoVID.** J. Bacteriol. 188:7731–7741
- Wang D-B, Yang R, Zhang Z-P, Bi L-J, You X-Y, Wei H-P, et al. (2009) **Detection of *B. anthracis* Spores and Vegetative Cells with the Same Monoclonal Antibodies.** PLoS ONE 4(11): e7810.
- Wang KH, et al. (2009). **The coat morphogenetic protein SpoVID is necessary for spore encasement in *Bacillus subtilis*.** Mol. Microbiol. 74:634–649
- Wang KH, et al. (2009). **The coat morphogenetic protein SpoVID is necessary for spore encasement in *Bacillus subtilis*.** Mol. Microbiol. 74:634–649
- Wenzler E., Kamboj K., Balada J. (2015) **Severe Sepsis Secondary to Persistent *Lysinibacillus sphaericus*, *Lysinibacillus fusiformis* and *Paenibacillus amylolyticus* Bacteremia** Int J of Infect Dise, Vol 35: 1201-9712,
- Yousten A.A., Davidson E.A. (1982) **Ultrastructural analysis of spores and parasporal crystals formed in *Bacillus sphaericus*.** Appl. Environ. Microbiol. 44, 1449–1455
- Zheng LB, Donovan WP, Fitz-James PC, Losick R. (1988). **Gene encoding a morphogenic protein required in the assembly of the outer coat of the *Bacillus subtilis* endospore.** Genes Dev. 2:1047–1054
- Zilhao R, et al. (2005). **Assembly and function of a spore coat-associated transglutaminase of *Bacillus subtilis*.** J. Bacteriol. 187:7753–7764

IV. Capítulo 3. Distribution of spore outer layer proteins on the order *Bacillales*

I. Introduction

I.1 – *B. subtilis* outer layer protein genes

A remarkable characteristic of two order within the phylum *Firmicutes* — the aerobic *Bacillales* and the anaerobic *Clostridiales*—is the ability to form spores via an evolutionarily conserved mechanism (de Hoon *et al.*, 2010; Galperin *et al.*, 2012). These bacteria include the model-species such as the pathogens *Bacillus anthracis* and *Clostridium difficile*, and the model organism for spore development, *Bacillus subtilis*, the first spore-forming bacteria for which the genome sequence was reported (Kunst *et al.*, 1997). The exact mechanism of spore persistence is unknown, and may be not attributed to a single characteristic, but rather, to a set of unique features. Spores of *Clostridiales* and *Bacillales* are encased in a complex series of concentric shells that provide protection of spores to extreme physical and chemical stresses, which include exposure to simulated extraterrestrial conditions (Nicholson *et al.*, 2000); facilitate germination (Nicholson, 2004; Henriques, 2004); and mediate interactions with the environment on structural and biochemical bases (Driks, 2003; Westphal, 2003).

It has long been assumed that the process of sporulation follows essentially the same morphological sequence as reported to *B. subtilis*, in addition to all endospore-forming organisms that have been examined, including extreme examples as the round-shaped *Sporosarcina spp.* (Mazanec *et al.*, 1965). However, interspecies and even intraspecies variation in the structure and composition of the spore surface layers exists and, likely, reflects the environmental conditions under which these spores are formed and persist (Zheng and Losick, 1990; Nicholson, 2004; Stewart, 2015).

Sporulation, or the formation of a spore, is a simple yet complicated example of differentiation, characterized in some depth on the model species *B. subtilis* and *B. anthracis* (Holt and Leadbeater, 1969; Santo and Doi, 1974; Aronson and Fitz-James, 1976; Driks, 1999; Driks, 2009; Mckenney *et al.*, 2013; Bozue *et al.*, 2015; Stewart, 2015; Driks and Eichenberger 2016). First, the cell replicates its DNA, divides asymmetrically and places copies of its genome in both compartments. Over the next steps, the smaller of the two compartments, the forespore (or prespore), develops into a mature spore capable of protecting the genome. A series of concentric shells is assembled surrounding the core (the inner most compartment, housing the spore chromosome): an inner membrane, a thin peptidoglycan layer called the germ cell wall, a thick peptidoglycan layer (the cortex), and additional outer layers that, at a minimum, those of the coat (Driks and Eichenberger, 2016).

The paradigm for coat architecture is provided by *B. subtilis*, which uses at least 80 different proteins to build this multilayered structure (Driks, 1999; Driks, 2009; Mckenney *et al.*, 2013.; Driks and Eichenberger, 2016). For many species, including *B. subtilis*, the coat is the outer-most spore layer. In other species, however, including *B. anthracis* and *B. megaterium*, there are two additional layers, an interspace and, surrounding that, an exosporium (Beaman *et al.*, 1972; Waller *et al.* 2004; Driks, 2007; Traag *et al.*, 2010; McKenney *et al.*, 2013; Bozue *et al.*, 2015; Stewart, 2015). Interestingly, over the past few decades, it has been observed that the number of coat layers and the presence or absence of appendages extending from the coat surface vary among species. The coat protein composition, however, has not yet been characterized in as much detail in other species, even though, in the past decade, several novel coat proteins have been identified in *B. anthracis* and *C. difficile* (Lai *et al.*, 2003; Díaz-González *et al.*, 2015).

In spite of the large percentage of conserved coat proteins, coat assembly differs significantly between *B. subtilis* and *B. anthracis* (Driks *et al.*, 2007). To a large degree, this is because important conserved morphogenetic proteins function in strikingly different ways in the two species. The morphogenetic protein CotE has a very important function in *B. anthracis* but not in *B. subtilis* spores: it guides the assembly of the exosporium. However, in contrast to the *B. subtilis*, CotE orthologue has only a modest role in coat protein assembly in *B. anthracis* and *B. subtilis*. SpoIVA has also a critical function in directing the assembly of the coat and exosporium to an area around the forespore in *B. anthracis*. This function is very similar to that of the *B. subtilis* orthologue, which directs the assembly of the coat to the forespore. CotH, directs coat protein deposition in both *B. subtilis* and *B. anthracis*. Additionally, however, in *B. anthracis*, CotH effects germination; in its absence, a higher number of spores germinates when compare to those of the wild-type strain.

With the expansion of the present understanding about the structure, composition, assembly, and functions of the spore-coat, new data about a small but growing number other spore-forming species is revealing that there is much to be learned beyond the relatively well-developed basis of knowledge in *B. subtilis*.

Because it has always been assumed that the pattern of spore proteins in *B. subtilis* would provide a template for all species, we asked ourselves which *B. subtilis* gene of outer spore layer tends to be in any genome of a spore-former. This represents the first step for any further research that aims to identify functions in any given outer spore -layer gene in non-model species.

Here, our goal is to analyse *in silico* the distribution of 78 *B. subtilis* and *B. anthracis* ultrastructure related protein genes among all spore-former species of *Bacillales* identified until the year of 2018. We used a comparative genomics computational analysis of databases to compare the

presence or the absence of genes from the coat of *B. subtilis* and the exosporium of *B. anthracis* with 193 complete genomes present on NCBI database.

II. Methods

***B. subtilis* and *B. anthracis* outer layer protein genes.** The NCBI references for the 78 outer layer genes presented on Table X were selected from two major reviews that list most, or at least the majority, of genes described for *B. subtilis* and *B. anthracis* at the present. Driks and Eichenberger, (2016) was used as reference for the 10 morphogenetic protein genes, 9 basement layer genes, 10 inner coat layer genes, 17 outer coat layer genes and 4 crust genes from *B. subtilis*. Driks and Mallozzi (2011), was used as reference for the 20 exosporium genes from *B. anthracis*. To this end, the corresponding amino acid sequences (.fna files) were downloaded from NCBI and used to build a BLAST database as described in BLAST[®] Command Line Applications User Manual (Camacho *et al.*, 2009), named Outer Layer AA.

***Bacillales* genomes.** We curated a list with a total of 193 NCBI accession numbers for species with sequenced genomes across the entire order of *Bacillales* (Table X). These genome sequences were used to build a database with protein predictions computationally generated by the NCBI database tools (www.ncbi.nlm.nih.gov/). This database was named *Bacillales* amino acid predictions or *Bacillales* AAP.

Comparative genomics. *Bacillales* AAP database was compared to Outer Layer AA database using automated BLASTp search. This analysis generated a list of matching sequences that revealed which *B. subtilis* or *B. anthracis* outer layer amino acid sequences presented similar orthologues to those from the protein predictions on the 193 *Bacillales* species from the list. These results were used to assemble an excel spreadsheet (Table X) fed with metadata represented by two colors. Boxes in green represent a positive match, or that the amino acid sequence from a determined protein related to the outer layers of the *B. subtilis* or *B. anthracis* spore that was similar to one or more amino acid prediction sequence from the genome. Boxes in red represent a negative match, or that the amino acid sequence from a determined protein related to the outer layers of the *B. subtilis* or *B. anthracis* spore that was not similar to any amino acid prediction sequence from the genome.

III. Results and Discussion

In the present work, the main objective was to determine which well-known outer layer spore proteins genes from *B. subtilis* and *B. anthracis* are likely to be present on every non-model spore-formers. It is important to mention that we do not over interpret the absence of a match on protein sequences of any given species as if the gene is not present on its genome. We hypothesize that a few outer layer genes tend to be relatively poorly conserved compared to other outer layer genes and, therefore, harder to detect bioinformatically. This is due to the fact that the methodology used was not optimized to identify differentiations on gene and amino acid sequences from the reference species *B. subtilis* and *B. anthracis*. Also, variations in these genes annotations such as different labels might mislead to a lack of identification. Although we note that these matches might appear if the detection criteria are relaxed.

To identify every spore-former genome present on the NCBI database, manual searches for the 11 families were performed. We selected for assembled genomes, either complete or incomplete in order to identify as many genomes as possible, excluding unassembled genomes (Table S1). First, we identified 5 genomes for *Alicyclobacillaceae* species; 68 genomes for *Bacillaceae* species; *Pasteuriaceae*; 29 genomes for *Paenibacillaceae* species; 3 genomes for *Sporolactobacillaceae* species; and 11 genomes for *Thermoactinomycetaceae* species. We also identified genomes for species of genera *Planococcaceae* (13), *Caryophanacea* (2), *Listeriaceae* (8), *Staphylococcaceae* (12), *Turicibacteraceae* (1), all families bearing well known asporogenous species.

After identifying and obtaining the files for each genome we divided the families in two groups based on the ability of forming a spore, resulting on a group with 157 reported spore-formersstrains and other with 36 asporogenous strains. We did this analysis by searching on data present on Bergey's manual *Firmicutes* (2009) and the in the List of approved prokaryote names (LPSN; Parte, 2013). Whenever the information regarding the ability to find a spore was absent on these two sources, we searched on the literature for papers that explicitly mentioned a visualization of a spore on any type of microscopy.

As described on the Methods section, all these genomes were used to build the *Bacillales* AAP database and contrast the amino acids predictions for these genome sequences against the Outer Layer AA database. The metadata resultant from this analysis was used to feed Tables S2, S3, and S4 with positive or negative matches between the sequences.

III.1 Frequently found proteins

Previously comparative genomic analyses have indicated that coat proteins are the most species-specific among all the sporulation proteins, suggesting that coat composition is highly influenced by the ecosystem in which a species resides (Driks and Eichenberger, 2016). This is not unexpected considering that coat composition may influence the surface properties that will mediate spore dispersal in the environment or attachment to specific hosts or surfaces.

Many proteins were identified to be conserved among all 157 spore-formers analysed. Four of the morphogenetic proteins were found in all species: CotE, SafA, SpoIVA, SpoVID. Basement layer: YhaX; inner coat proteins: YisY, YaaH, GerQ, YutH, ylbD, and outer coat: sspI, ytdA, yncD were also found distributed in at least 98% of the species. Galperin (*et al.*, 2012) stated that homologs of *B. subtilis* coat proteins are found primarily inside the family *Bacillaceae*, more rarely inside the family *Clostridia*, and, almost never, in asporogenic species. This statement seems to be true, since none of the morphogenetic proteins were found among all 57 asporogenous species analysed. Of the other proteins present in all spore-formers, only inner coat GerQ and YutH are absent in all asporogenous species analysed. This result suggests that maybe this core set of conserved proteins are necessary for other functions of the cell that maybe not related to sporulation.

The protein CotH was present in all *Bacillus* spp. except in *B. beveridgei*, *B. cellulosyliticus*, *B. coagulans*, *B. cohnii*, *B. endophyticus*, *B. shalodurans*, *B. horikoshii*, *B. infantis*, *B. krulwichiae*, *B. iehensis*, *B. muralis*, *B. oceanisediminis*, and *B. pseudofirmus*.

Basement layer proteins YheD and YcsK were found in many species being absent in only three species from genus *Bacillus*: *B. clausii*, *B. beveridgei*, and *B. pseudofirmus*.

Inner coat layers seem to be the structure with the higher number of conserved proteins identifiable by our methods. This suggests that there is an elevated chance of finding a core set of proteins related to the spore structure on the layers that works as a support for the

assembly of the outer structures such as outer layer and the exosporium. Also, it is possible that the diversity in the basement layer might be higher than the usually expected. This might suggest that adaptations driven by the environment affects the layer responsible to host most of the germination receptors.

III.2 Inconsistently found proteins

Many more protein sequences were found in only a few species and with no obvious pattern. Inner coat proteins Tgl, YjcQ, YsxE were found in most species. Inner coat proteins CwlJ, YjcQ were present in all *Bacillus* spp. except *B. beveridgei* and was not found in asporogenous species. Base layer protein YjzB was observed in only few species, being absent even from member of *B. cereus* group, except for *B. weihenstephanensis*. Inner coat proteins YyBI, YxeE, CotP were infrequently observed without any obvious pattern. Inner coat protein YsnD was found only in *B. gibsonii*. Outer coat protein YtxO was found only in *B. anthracis* and *B. gibsonii*, even though it is a protein described for *B. subtilis*.

The protein CotO was missing in a number of species with no obvious pattern. It is relevant that the analysis showed that this protein was not found in *B. anthracis* and some other *B. cereus* group species. However, it has been previously reported in *B. anthracis* (Driks and Eichenberger, 2016). As stated formerly, we are aware of the limitations of using only a *B. subtilis* reference for this type of analysis and the high probability of false negatives. Therefore, even though we need to point out absences, we consider here only the positive matches.

Outer coat protein CotG was found only in *B. amyloliquefaciens*, *B. gibsonii*, *B. vallismortis*, and *B. velezensis*. It was absent on all other *Bacillales* genome analysed.

III.3 Exosporium and crust proteins

Exosporium proteins ExsA and BclA were found in all *Bacillus* genomes analysed. Even though many species present an exosporium as it can be observed by TEM images commonly found in the literature (Stewart, 2015), the presence of these proteins has not yet been paired with a mandatory presence of an exosporium—there is no reported exosporium marker that we are aware of. Interestingly, even though ExsA is present in most *Bacillales* genomes outside the genus *Bacillus*, BclA was absent in all genomes belonging to other genera where BclB was more frequent. We suggest that BclB may be required for an outer

layer assembly in those species in the absence of BclA. Exosporium protein ExsFA was also found only in species inside the genus *Bacillus*: *B. atropheus*, *B. licheniformis*, *B. anthracis*, *B. cereus*, *B. cytotoxicus*, *B. mycoidis*, *B. thuringiensis*, *B. bombysepticus*, and *B. toyonensis*. Noteworthy, *B. atropheus* and *B. licheniformis* are both representatives of the *B. subtilis* group, formed only by well-known species with no exosporium. It appears that obtaining TEM images of at least some of the as yet unexamined species is important for further evaluation of the presence of these proteins. RocA and Sod15 were found among all species, but because these proteins are not exclusively found in the exosporium, these proteins were not considered as conserved exosporium proteins.

The crust is a structure described only for *B. subtilis* strains, discovered in 2008 with the advent of Ruthenium red as a stain for TEM. Even though, seven species have all the four crust proteins described so far: CgeA, CgeB, CotV, CotW. All these species are allocated in the genus *Bacillus*: *B. amyloliquefaciens*, *B. weihenstephanensis*, *B. gibsonii*, *B. sonorensis*, *B. vallismortis*, *B. velezensis*, and *B. xiamenensis*. Except for *B. weihenstephanensis* and *B. gibsonii*, all mentioned species are members of the *B. subtilis* group, which corroborates the possibility that the psicrotolerant *B. weihenstephanensis* may diverge from the other species of the *B. cereus* group as reported in the literature (Soufiane and Côté, 2013). CgeB was found on a small number of species outside the genus *Bacillus*, being present in almost all *Paenibacillus* spp..

III.4 Relevant absent proteins

Basement layer protein CmpA, inner coat proteins YeeK, CotT, YmaG, and outer coat proteins CotC, CotU were absent in all 193 genomes evaluated. Even though, our methods did not allow to significant statements regarding negative matching results, we hypothesize that, after analysis performed with a stronger methodology that allows the proper interpretation of negative results, a small subset of proteins that are useful for *B. subtilis* will not have any use on different species, and maybe not on different strains.

III.5 Core set of proteins and further experiments

Based on the levels of distribution of the proteins mentioned above we built a cartoon (Figure 1) with the most conserved proteins observed across genomes from the entire order *Bacillales*, split in layers. The most conserved proteins are represented by larger circles, while less conserved proteins are represented by smaller circles. This is the first report of an attempt to assemble

a set of conserved proteins across the order; most studies focus on species located on close branches to *B. subtilis* on the phylogenetic tree.

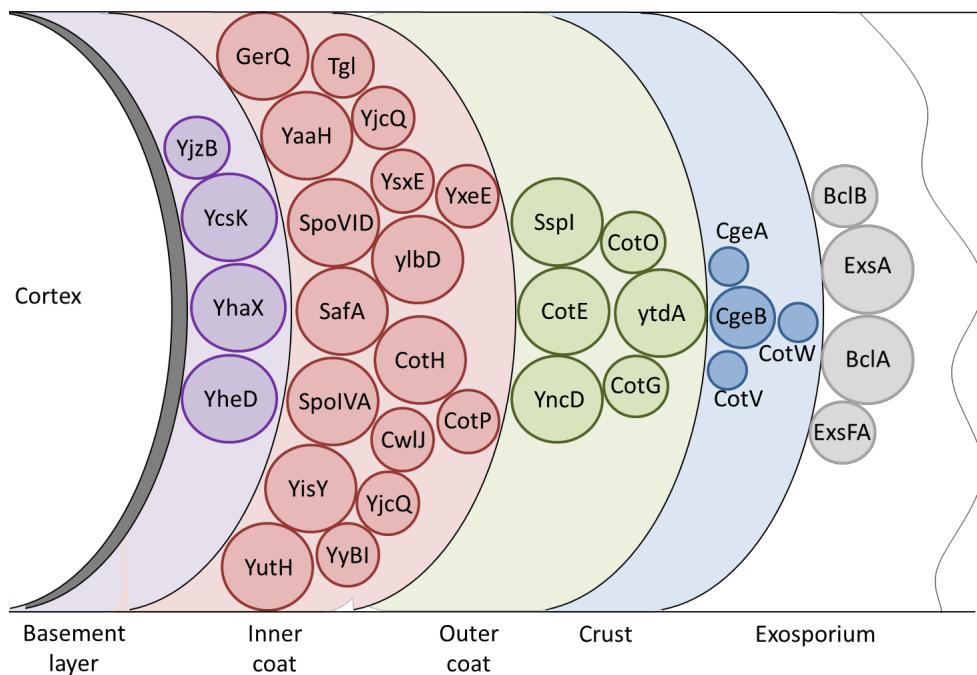


Figure 1. Core set of outer spore layer proteins across the order *Bacillales*. The outer spore layers are distributed from the left to the right. Basement layer is in purple, inner coat layer in red, outer coat layer in green, crust in blue and the exosporium and interspace in grey. The size of the circles indicates the relative level of conservation of a given protein among diverse species. If a protein was considered to be well distributed, or, present among at least 90% of positive matches, it received a large circle. If a given protein is well distributed, at least 60% of positive matches, but presented many negative matches, it received a medium circle. Small circles were given to proteins that were present in enough strains to be considered relevant, but not conserved among spore-formers. The inner coat was the layer with the higher rates of protein conservation, presenting more well conserved proteins than the other layers combined.

There is still limited knowledge regarding the function on the spore structure of these proteins that revealed to be inconsistent among the genomes analysed. Many, if not all, have little or no effect on the spore structure reported. In some cases, we are not aware of reports attempting to discover their function.

The next step should be to consider the data in light of each species; analysing which genes are present in, for example, *B. clausii* compared to *Brevibacillus laterosporus* or *Lysinibacillus sphaericus*, and, considering the morphological differences between the species, start to draw new experiments for genetic manipulation *in vivo* and proteomics.

Further, we will perform covariation analysis. The goal is to identify which, of the 78 outer layer protein genes identified so far, tend to be together in any given genome. After, we

intend to do a comparative analysis of the sequences of selected protein genes which have shown previously to be more relevant to *B. subtilis* layers; we aim to identify conserved and highly variable regions that could point us towards functional modules. Also, we intend to analyse variations of spore outer layer protein genes in the context of 16S rRNA gene variation, to see if we can learn anything about whether those spore proteins have evolved along with the core genome, or if there is any evidence for horizontal gene transfer.

IV. Referências bibliográficas

- Camacho C., Coulouris G., Avagyan V., Ma N., Papadopoulos J., Bealer K., Madden T.L., (2009) **BLAST+: architecture and applications.** *BMC Bioinformatics*, Vol10 -1,1
- de Hoon, M. J., Eichenberger, P. & Vitkup, D. (2010). **Hierarchical evolution of the bacterial sporulation network.** *Curr. Biol.* 20, R735–R745
- Díaz-González F, Milano M, Olguin-Araneda V, Pizarro-Cerda J, Castro-Córdova P, Tzeng SC, Maier CS, Sarker MR, Paredes-Sabja D. (2015). **Protein composition of the outermost exosporium-like layer of *Clostridium difficile* 630 spores.** *J Proteomics* 123:1–13.
- Donovan W, Zheng LB, Sandman K, Losick R. (1987). **Genes encoding spore coat polypeptides from *Bacillus subtilis*.** *J. Mol. Biol.* 196:1–10 32.
- Driks A. (1999). ***Bacillus subtilis* spore coat.** *Microbiol. Mol. Biol. Rev.* 63:1–20
- Driks A. (2003). **The dynamic spore.** *Proc. Natl. Acad. Sci. USA* 100:3007–9
- Galperin MY, Mekhedov SL, Puigbo P, Smirnov S, Wolf YI, Rigden DJ. (2012). **Genomic determinants of sporulation in Bacilli and Clostridia: towards the minimal set of sporulation-specific genes.** *Environ Microbiol* 14:2870–2890.
- Galperin, M. Y. *et al.* (2012) **Genomic determinants of sporulation in Bacilli and Clostridia: towards the minimal set of sporulation-specific genes.** *Environ. Microbiol.* 14, 2870–2890.
- Henriques AO, Costa T, Martins LO, Zilhao R. (2004). **Functional architecture and assembly of the spore coat.** See Ref. 129, pp. 34–52
- Kunst F, Ogasawara N, Moszer I, Albertini AM, Alloni G, *et al.* (1997). **The complete genome sequence of the gram-positive bacterium *Bacillus subtilis*.** *Nature* 390:249–56
- Lai EM, Phadke ND, Kachman MT, Giorno R, Vazquez S, Vazquez JA, Maddock JR, Driks A. (2003). **Proteomic analysis of the spore coats of *Bacillus subtilis* and *Bacillus anthracis*.** *J Bacteriol* 185:1443–1454.
- Mazanec K, Kocusr M, Martinec T. (1965). **Electron microscopy of ultrathin sections of *Sporosarcina urea*.** *J. Bacteriol.* 90:808–16
- Nicholson WL, Munakata N, Horneck G, Melosh HJ, Setlow P. (2000). **Resistance of *Bacillus* endospores to extreme terrestrial and extraterrestrial environments.** *Microbiol. Mol. Biol. Rev.* 64:548–72
- Nicholson WL. (2004). **Ubiquity, longevity, and ecological roles of *Bacillus* spores.** See Ref. 129, pp. 2–15 107.
- Parte A.C. (2013). **LPSN--list of prokaryotic names with standing in nomenclature.** *Nucleic acids research*, 42(Database issue), D613-6.
- Stewart G.C. (2015). **The Exosporium Layer of Bacterial Spores: a Connection to the Environment and the Infected Host** *Microbiol. Mol. Biol. Rev.* 79 (4) 437-457

- Soufiane B., Côté J.C. (2013) **Bacillus weihenstephanensis characteristics are present in Bacillus cereus and Bacillus mycoides strains.** FEMS Microbiol Lett 341(2):127-37.
- Westphal AJ, Price PB, Leighton TJ, Wheeler KE. (2003). **Kinetics of size changes of individual Bacillus thuringiensis spores in response to changes to relative humidity.** Proc. Natl. Acad. Sci. USA 100:3461–66
- Zheng L, Losick R. (1990). **Cascade regulation of spore coat gene expression in *Bacillus subtilis*.** J. Mol. Biol. 212:645–60

V. Supplementary information

Table S1. Assembled *Bacillales* genomes found on NCBI database and accession numbers.

Taxon	Accession number**	Taxon	Accession number**
Alicyclobacillaceae	Accession number**	Caryophanaceae (non-spore-former)	Accession number**
Alicyclobacillus acidocaldarius subsp. acidocaldarius DSM 446	NC_013205	Caryophanon latum DSM14151	NZ_MATO00000000
Alicyclobacillus acidocaldarius subsp. acidocaldarius Tc-4-1	NC_017167	Caryophanon tenue DSM14152	NZ_MASJ00000000
Kyrpidia tusciae DSM 2912	NC_014098	Listeriaceae (non-spore-former)/ Pasteuriaceae	
Tumebacillus algifaecis	NZ_CP022657	Brochothrix thermosphacta BI	NZ_CP023643
Tumebacillus sp. AR23208	NZ_CP021434	Brochothrix thermosphacta BII	NZ_CP023483
Bacillaceae		Listeria monocytogenes 08-5923	NC_013768
Aeribacillus pallidus KCTC3564	NZ_CP017703	Listeria monocytogenes EGD-e	NC_003210
Alkalibacillus haloalkaliphilus C5	NZ_AKIF00000000	Listeria monocytogenes HCC23	NC_011660
Amphibacillus marinus CGMCC 1.10434	NZ_FODJ00000000	Listeria monocytogenes serotype 4b str. F2365	NC_002973
Amphibacillus sediminis NBRC 103570	NZ_BCQW00000000	Listeria welshimeri serovar 6b str. SLCC5334	NC_008555
Amphibacillus xylanus NBRC 15112	NC_018704	Kurthia sp. 11kri321	NZ_CP013217
Anoxybacillus amylolyticus DSM15939	NZ_CP015438	Paenibacillaceae	Accession number**
Anoxybacillus gonensis G2	CP012152	Aneurinibacillus soli CB4	NZ_AP017312
Anoxybacillus tepidamans PS2	NZ_JHVN00000000	Aneurinibacillus sp. XH2	NZ_CP014140
Bacillus altitudinis SGAir0031 (CP022319)	CP022319	Brevibacillus brevis NBRC 100599	NC_012491
Bacillus amyloliquefasciens DSM7 (PRJEA41719)	FN597644	Brevibacillus formosus NF2	NZ_CP018145
Bacillus anthracis Ames Ancestor (PRJNA176033)	NC_007530	Brevibacillus laterosporus LMG 1544	NZ_CP007806
Bacillus aryabhata iK13 (PRJNA414277)	CP024035	Paenibacillus beijingensis DSM24997	NZ_CP011058
Bacillus atrophaeus SRCM101359 (PRJNA386751)	CP021500	Paenibacillus borealis DSM13188	NZ_CP009285
Bacillus Beveridgei MLTeJB (PRJNA261240)	CP012502	Paenibacillus bovis BD3526	NZ_CP013023
Bacillus bombysepticus wang (PRJNA242213)	CP007512	Paenibacillus donghaensis KCTC 13049	NZ_CP021780
Bacillus cellulosi lyticus DSM2522 (PRJNA38423)	CP002394	Paenibacillus durus DSM 1735	NZ_CP009288
Bacillus cereus ATCC14579 (PRJNA97797)	NC_004722	Paenibacillus larvae subsp. larvae ATCC 9545	NZ_CP019687
Bacillus clausii KSM-K16	AP006627	Paenibacillus mucilaginosus	NC_016935

(PRJNA13291)		3016	
Bacillus coagulans Dsm1 (PRJEB18146)	NZ_CP0097 09	Paenibacillus mucilaginosus K02	NC_017672
Bacillus cohnii DSM6307 (PRJNA357928)	CP018866	Paenibacillus mucilaginosus KNP414	NC_015690
Bacillus cytotoxicus NVH 391-98 (PRJNA13624)	CP000764	Paenibacillus naphthalenovorans 32OY	NZ_CP0136 52
Bacillus endophyticus Hbe603 (PRJNA280147)	CP011974	Paenibacillus odorifer DSM 15391	NZ_CP0094 28
Bacillus flexus KLbmp4941 (PRJNA331023)	CP016790	Paenibacillus polymyxa E681	NC_014483
Bacillus gibsonii FJAT10019 (PRJNA340205)	CP017070	Paenibacillus polymyxa M1	NC_017542
Bacillus glycinifermentans EVONIK (PRJNA407856)	NZ_LT6036 83	Paenibacillus polymyxa SC2	NC_014622
Bacillus halodurans C125 (PRJNA149331)	NC_002570	Paenibacillus sp. JDR-2	NC_012914
Bacillus horikoshii 20a (PRJNA377620)	CP020880	Paenibacillus sp. Y412MC10	NC_013406
Bacillus infantis NRRLB14911 (PRJNA212797)	CP006643	Paenibacillus stellifer DSM 14472	NZ_CP0092 86
Bacillus krulwichiae AM31D (PRJNA373882)	CP020814	Paenibacillus swuensis DY6	NZ_CP0113 88
Bacillus lehensis G1 (PRJNA178137)	CP003923	Paenibacillus terrae HPL-003	NC_016641
Bacillus licheniformis DSM13=ATCC14580 (PRJNA235989)	NC_006270	Paenibacillus yonginensis DCY84	NZ_CP0141 67
Bacillus megaterium NBRC15308=ATCC14581 (PRJNA238207)	CP009920	Saccharibacillus kuerlensis DSM 22868	NZ_ARJR0 0000000
Bacillus methanolicus MGA3 (PRJNA271081)	NZ_CP0077 39	Saccharibacillus sacchari DSM 19268	NZ_JFBU00 000000
Bacillus muralis G2568 (PRJNA283689)	CP017080	Thermicanus aegyptius DSM 12793	NZ_AZNU0 0000000
Bacillus mycoides ATCC6462 (PRJNA238211)	CP009692	Thermobacillus composti KWC4	NC_019897
Bacillus oceanisediminis 2691 (PRJNA167766)	CP015506		
Bacillus paralicheniformis ATCC9945a (PRJNA49115)	CP005965		
Bacillus pseudofirmus OF4 (PRJNA28811)	CP001878		
Bacillus pumilus SHB9 (PRJNA276289)	CP011007		
Bacillus simplex SHB26 (PRJNA276291)	CP011008		
Bacillus smithii DSM4216 (PRJNA258357)	CP012024		
Bacillus sonorensis SRCM101395 (PRJNA389958)	CP021920		
Bacillus thuringiensis konkukian str.97-27 (PRJNA58089)	NC_005957		
Bacillus toyonensis BCT7112	CP006863		
		Planococcaceae (non-spore- forming)	Accession number**
		Bhargavaea ginsengi CGMCC 1.6763	NZ_FNZF0 0000000
		Paenisporosarcina sp. HGH0030 (****sporeformer)	NZ_AGEQ0 0000000
		Planococcus kocurii ATCC 43650	NZ_CP0136 61
		Planococcus maritimus Y42	NZ_CP0196 40
		Planococcus rifietoensis M8	NZ_CP0136 59
		Planococcus sp. L10.15	NZ_CP0165 40
		Planococcus antarcticus DSM 14505	NZ_CP0165 34
		Planomicrobium glaciei CGMCC	NZ_FNDC0

(PRJNA225857)		1.6846	0000000
Bacillus vallismortis NBIF001 (PRJNA383078)	CP020893	Sporosarcina psychrophila DSM 6497 (****sporeformer)	NZ_CP0146 16
Bacillus velezensis FZB42 (PRJNA327241)	NC_009725	Sporosarcina sp. P33 (****sporeformer)	NZ_CP0150 27
Bacillus weihaiensis alg07 (PRJNA323409)	CP016020	Sporosarcina sp. P37 (****sporeformer)	NZ_CP0153 49
Bacillus weihenstephanensis KBAB4 (PRJNA13623)	CP000903	Sporosarcina ureae P8 (****sporeformer)	NZ_CP0152 07
Bacillus xiamenensis VV3 (PRJNA349777)	CP017786	Sporosarcina ureae P17a (****sporeformer)	NZ_CP0151 09
Caldalkalibacillus thermarum TA2.A1	NZ_AFCE0 0000000		
		Sporolactobacillaceae	Accession number**
Exiguobacterium antarcticum B7	NC_018665	Sporolactobacillus nakayamae ATCC 700379	NZ_FOOY0 0000000
Exiguobacterium aurantiacum DSM 6208	NZ_JNIQ00 000000	Sporolactobacillus vineae DSM 21990	NZ_ARJJ00 000000
Exiguobacterium sibiricum 255-15	NC_010556	Tuberibacillus calidus DSM17572	NZ_AUMM 00000000
		Staphylococcaceae (non-spore- former)	Accession number**
Exiguobacterium sp. AT1b	NC_012673		
Geobacillus genomsp. JF8	NC_022080	Staphylococcus aureus subsp. aureus NCTC 8325	NC_007795
Geobacillus kaustophilus HTA426	NC_006510	Staphylococcus epidermidis ATCC 12228	NC_004461
Geobacillus sp. C56-T3	NC_014206	Staphylococcus haemolyticus JCSC1435	NC_007168
Geobacillus stearothermophilus 10	NZ_CP0089 34	Gemella sp. oral taxon 928	NZ_CP0142 33
Geobacillus subterraneus KCTC3922	NZ_CP0143 42	Macrococcus canis KM45013	NZ_CP0210 59
Geobacillus thermoleovorans KCTC3570	NZ_CP0143 35	Macrococcus caseolyticus IMD0819	NZ_CP0210 58
Geobacillus thermoleovorans CCB_US3_UF5	NC_016593	Macrococcus caseolyticus JCSC5402	NC_011999
Gracilibacillus halophilus YIM- C55.5	NZ_APMLO 0000000	Macrococcus sp. IME1552	NZ_CP0171 56
Gracilibacillus kekensis CGMCC 1.10681	NZ_FRCZO 0000000	Salinicoccus halodurans H3B36	NZ_CP0113 66
Gracilibacillus lacisalsi DSM 19029	NZ_ARIY0 0000000	Nosocomiicoccus ampullae LUREC	NZ_MBFG0 0000000
Gracilibacillus massiliensis	NZ_CZRP0 0000000	Nosocomiicoccus sp. HMSC09A07	NZ_LWMX 01000000
Gracilibacillus orientalis CGMCC 1.4250	NZ_FOTR0 0000000	Nosocomiicoccus sp. HMSC059G07	NZ_LTSV0 0000000
		Thermoactinomycetaceae	Accession number**
Gracilibacillus timonensis P2481	NZ_FLKH0 0000000		
Gracilibacillus ureilyticus CGMCC 1.7727	NZ_FOGL0 0000000	Desmospora sp. 8437	AFHT00000 000
Halalkalibacillus halophilus DSM 18494	NZ_AUHI0 0000000	Kroppenstedtia eburnea DSM 45196	NZ_FTOD0 0000000
Halobacillus halophilus DSM 2266	NC_017668	Lihuaxuella thermophila DSM 46701	NZ_FOCQ0 0000000

Halobacillus halophilus HL2HP6	NZ_CP0221 06	Marininema halotolerans DSM45789	NZ_FPAA0 0000000
Halobacillus mangrovi KTB 131	NZ_CP0207 72	Marininema mesophilum DSM45610	NZ_FNNQ0 0000000
Halolactibacillus alkaliphilus CGMCC1.6843	NZ_FOWN 00000000	Melghirimyces thermohalophilus DSM 45514	NZ_FMZA0 0000000
Halolactibacillus halophilus DSM 17073	NZ_FOXC0 0000000	Planifilum fulgidum DSM 44945	NZ_FOOK0 0000000
Halolactibacillus miurensis DSM 17074	NZ_FPAI01 000000	Seinonella peptonophila DSM 44666	NZ_FQVL0 0000000
Halolactibacillus sp. JCM 19043	NZ_BAXD0 0000000	Shimazuella kribbensis DSM 45090	NZ_ATZF0 0000000
Jeotgalibacillus malaysiensis D5	NZ_CP0094 16	Thermoactinomyces sp. DSM45891	NZ_FPJZ0 000000
Jeotgalicoccus marinus DSM 19772	NZ_AUEE0 1000000	Thermoflavimicrobium dichotomicum DSM 44778	NZ_FORR0 0000000
Jeotgalicoccus saudimassiliensis 13MG44	NZ_CCSE0 1000000	Turicibacteraceae (non-spore- former)	Accession number**
Lentibacillus amyloliquefaciens LAM0015	NZ_CP0138 62	Turicibacter sp. H121	NZ_CP0134 76
Lysinibacillus fusiformis RB21	NZ_CP0108 20		
Lysinibacillus sphaericus 2362	NZ_CP0152 24		
Lysinibacillus sphaericus C3-41	CP000817		
Lysinibacillus sphaericus III37	NZ_CP0148 56		
Lysinibacillus sphaericus LMG22257	NZ_CP0175 60		
Lysinibacillus sphaericus DSM28	CP019980		
Lysinibacillus varians Gy32	NZ_CP0068 37		
Oceanobacillus iheyensis HTE831	NC_004193		
Ornithinibacillus halophilus IBRCM10683	NZ_FQVW 00000000		
Paraliobacillus ryukyuensis Marseille-P3391	NZ_FVZO0 0000000		
Paraliobacillus sp. PM-2	NZ_CTEI00 000000		
Paucisalibacillus globulus DSM 1884	NZ_AXVK0 0000000		
Paucisalibacillus globulus PG	NZ_FXXM0 1000000		
Piscibacillus halophilus DSM21633	NZ_FOES0 0000000		
Pontibacillus halophilus JSM 076056 = DSM 19796	NZ_AULI00 000000		
Pontibacillus marinus BH030004 = DSM 16465	NZ_AULJ0 0000000		
Salimicrobium jeotgali MJ3	NZ_CP0113 61		
Salsuginibacillus kocurii DSM 18087	NZ_ARIV0 0000000		

Tenuibacillus multivorans CGMCC 1.344	NZ_FNIG00 000000
Terribacillus halophilus T-h1	NZ_FUFU0 0000000
Thalassobacillus cyri CCM7597	NZ_FNQR0 0000000
Thalassobacillus devorans MSP14	NZ_AWXW 00000000
Ureibacillus thermosphaericus A1	NZ_AP0183 35
Virgibacillus halodenitrificans PDBF2	NZ_CP0179 62
Virgibacillus necropolis LMG19488	NZ_CP0224 37
Virgibacillus sp. 6R	NZ_CP0177 62
Virgibacillus sp. LM2416	NZ_CP0223 15
Virgibacillus sp. SK37	NZ_CP0071 61
Vulcanibacillus modesticaldus BR	NZ_MIJF00 000000

** NCBI database.

